

DETERMINATION OF HYDRATE FORMATION CONDITIONS OF
DRILLING FLUIDS

A THESIS SUBMITTED TO
THE GRADUATE SCHOOL OF NATURAL AND APPLIED SCIENCES
OF
MIDDLE EAST TECHNICAL UNIVERSITY

BY

ALIYA KUPEYEVA

IN PARTIAL FULFILLMENT OF THE REQUIREMENTS
FOR
THE DEGREE OF MASTER OF SCIENCE
IN
PETROLEUM AND NATURAL GAS ENGINEERING

AUGUST 2007

Approval of the thesis:

**DETERMINATION OF HYDRATE FORMATION CONDITIONS OF
DRILLING FLUIDS**

submitted by **Aliya KUPEYEVA** in partial fulfillment of the requirements for the
degree of **Master of Science in Petroleum and Natural Gas Engineering** by,

Prof. Dr. Canan Özgen _____
Dean, Graduate School of **Natural and Applied Sciences**

Prof. Dr. Mahmut Parlaktuna _____
Head of Department, **Petroleum and Natural Gas Engineering**

Prof. Dr. Mahmut Parlaktuna _____
Supervisor, **Petroleum and Natural Gas Engineering, METU**

Examining Committee Members:

Prof. Dr. Tanju Mehmetoğlu _____
Petroleum and Natural Gas Engineering, METU

Prof. Dr. Mahmut Parlaktuna _____
Petroleum and Natural Gas Engineering, METU

Doç. Dr. Serhat Akın _____
Petroleum and Natural Gas Engineering, METU

Asst. Prof. Dr. Evren Özbayoğlu _____
Petroleum and Natural Gas Engineering, METU

Petroleum Engineer Hüseyin Ali Doğan, M.Sc. _____
TPAO, Research Center

Date: _____

I hereby declare that all information in this document has been obtained and presented in accordance with academic rules and ethical conduct. I also declare that, as required by these rules and conduct, I have fully cited and referenced all material and results that are not original to this work.

Name, Last name: Aliya KUPEYEVA

Signature:

ABSTRACT

DETERMINATION OF HYDRATE FORMATION CONDITIONS OF DRILLING FLUIDS

Kupeyeva, Aliya

M.Sc., Department of Petroleum and Natural Gas Engineering

Supervisor: Prof. Dr. Mahmut Parlaktuna

August 2007, 92 pages

The objective of this study is to determine hydrate formation conditions of a multi-component polymer based drilling fluid. During the study, experimental work is carried out by using a system that contains a high-pressure hydrate formation cell and pressure-temperature data is recorded in each experiment.

Different concentrations of four components of drilling fluid, namely potassium chloride (KCl), partially hydrolyzed polyacrylamide (PHPA), xanthan gum (XCD) and polyalkylene glycol (poly.glycol) were used in the experiments, to study their effect on hydrate formation conditions.

Considering the pressure-temperature data obtained, hydrate equilibrium conditions are determined as well as the number of moles of free gas in the hydrate formation cell. The change in the number of moles of free gas in the hydrate formation cell with respect to time is considered as a way of determining rate of hydrate formation.

It is observed that KCl and XCD thermodynamically inhibit hydrate formation and an increase in the concentration of KCl and XCD shifts the hydrate equilibrium condition to lower equilibrium temperatures at a given pressure. On the contrary, poly.glycol and PHPA tend to promote the hydrate formation thermodynamically. On the other hand, the increase in polyglycol concentration has a kinetic inhibitive effect on the gas hydrate formation, and with the maximum concentrations of poly.

glycol in the given limits the rate of hydrate formation decreases almost twice from the initial values.

Keyword: Gas Hydrate, Hydrate Formation Conditions, Components of Drilling Fluid.

ÖZ

SONDAJ SIVILARININ HİDRAT OLUŞUM ŞARTLARININ BELİRLENMESİ

Kupeyeva, Aliya

Yüksek Lisans, Petrol ve Doğal Gaz Mühendisliği Bölümü

Tez Yöneticisi: Prof. Dr. Mahmut Parlaktuna

Ağustos 2007, 92 sayfa

Bu çalışmanın temel amacı çok bileşenli, polimer bazlı sondaj akışkanının hidrat oluşum şartlarının belirlenmesidir. Çalışma süresince yüksek basınçlı hidrat oluşum hücresi içeren bir deneysel düzeneğin kullanıldığı ve basınç-sıcaklık verisinin her deney için kaydedildiği deneysel bir çalışma yapılmıştır.

Deneylerde sondaj akışkanının dört bileşeninin farklı derişimleri kullanılmış ve derişimdeki değişikliklerin hidrat oluşum şartlarına etkisi çalışılmıştır.

Kaydedilen basınç-sıcaklık verisi kullanılarak sistemin hidrat denge koşulları ile hidrat oluşumu sırasında hücredeki serbest gaz mol sayıları saptanmıştır. Hücredeki serbest gaz mol sayısının zamanla değişimi hidrat oluşum hızının saptanmasının aracı olarak kullanılmıştır.

Yapılan gözlemlerde KCl ve XCD'nin termodinamik açıdan hidrat oluşumunu engellediği ve derişimlerinin artmasıyla verilen basınç değerindeki hidrat denge sıcaklığının daha düşük değerlere taşındığı saptanmıştır. Bunun aksine, poli-glikol ve PHPA'nın termodinamik açıdan hidrat oluşumunu kolaylaştırdığı gözlenmiştir. Öte yandan, poli-glikol derişiminin artmasıyla hidrat oluşumunun kinetik olarak engellendiği ve poli-glikolün denenen en yüksek derişiminde hidrat oluşum hızının yarı yarıya düştüğü saptanmıştır.

Anahtar kelimeler: Gaz Hidrat, Hidrat Oluşum Koşulları, Sondaj Akışkanı Bileşenleri

To My Family

ACKNOWLEDGEMENTS

I express my deep gratitude to Prof. Dr. Mahmut PARLAKTUNA for his patience, support, encouragement, advice and guidance throughout the study. Without his valuable support, it would not be possible to go so far, and his constructive suggestions are a valuable contribution to this project.

I would also like to express my sincere thanks to Naci DOĞRU and Emrah MANTAŞ for their help and contribution during the experiments and in the construction of the experimental set-up.

I would like to express my deepest gratitude to my family and friends for being always beside me with their love, support and guidance throughout all my life and also throughout this study. Especially I wish to thank my mother, Galiya Kupeyeva for her unconditional support and care, patience and understanding and explicit belief in me.

Finally, I would like to acknowledge the support provided by the Turkish Petroleum Corporation (TPAO) Research Center and its personnel, H. Ali Doğan, Selçuk Erkekol and Mehmet Uğur Aladut, in the preparing and providing drilling fluids used in this study.

TABLE OF CONTENTS

PLAGIARISM.....	iii
ABSTRACT.....	iv
ÖZ.....	vi
DEDICATION.....	vii
ACKNOWLEDGEMENTS.....	viii
TABLE OF CONTENTS.....	ix
LIST OF TABLES.....	xii
LIST OF FIGURES.....	xiv
CHAPTERS.....	1
1.INTRODUCTION.....	1
1 Properties of hydrates.....	2
1.2 Hydrates structure.....	3
1.3 Natural gas hydrate.....	5
1.4 Gas hydrates in pipelines.....	7
1.5 Utilization of gas hydrates.....	7
2. FORMATION AND PREVENTION OF GAS HYDRATES.....	9
2.1 Thermodynamic inhibitor.....	12
2.2 Low dosage inhibitors.....	15
2.2.2 Kinetic Inhibitors.....	15
2.2.2 Anti-Agglomerants.....	17
3. STATEMENT OF THE PROBLEM.....	21
4. EXPERIMENTAL SET-UP AND POCEDURE.....	22

4.1 Experimental Set-Up.....	22
4.2 Experimental Procedure.....	24
5. RESULTS AND DISCUSSION.....	26
5.1 Thermodynamic Analysis – Hydrate Hysteresis Curves.....	29
5.2 Kinetic Analysis – Number of Moles of Free Gas vs. Time.....	31
5.3 Group-1 Experiments: Comparison with Overall Increase In Concentration.....	35
5.4 Group -2: Experiments on Repeatability.....	40
5.5 Group-3: Effect of PHPA.....	42
5.6 Group-4: Effect of KCl.....	48
5.7 Group-5. Effect of XCD.....	53
5.8 Group-6. Effect of Poly. glycol.....	58
6.CONCLUSION.....	63
7. RECOMMENDATIONS.....	64
REFERENCES.....	65
APPENDICES	
A. REAGENTS.....	68
B. PRESSURE TEMPERATURE VS. TIME DIAGRAMS.....	72
C. PRESSURE VS. TEMPERATURE DIAGRAMS.....	79
D. NUMBER OF MOLES OF FREE GAS VS. TIME DIAGRAMS.....	86

LIST OF TABLES

Table 1.1. Achievements on different aspects of hydrates.....	2
Table 2.1 Comparison of two types of LDHI.....	18
Table 5.1. Components of drilling fluids and their minimum and maximum concentrations.....	27
Table 5.2. Groups of experiments.....	27
Table 5.3. Data obtained from hydrate hysteresis curve of Experiment-1.....	29
Table 5.4 Data obtained from Number of moles vs time diagram for Experiment-1.....	33
Table 5.5 Components concentration for Group-1 experiments.....	35
Table 5.6 .Data obtained from hydrate hysteresis curves for Experiments 1, 2 and 3.....	37
Table 5.7. Data for kinetic analysis for Group-1 experiments.....	39
Table 5.8. Data obtained from hydrate hysteresis curves from repeatability tests.....	40
Table 5.9 Components concentration for Group-3 experiments.....	42
Table 5.10 Data obtained from Hydrate hysteresis curves for Group-3 experiments.....	43
Table 5.11 Equations of straight line for each 1hour period for Group-3 experiments.....	46
Table 5.12 Reaction rates of Group-3 experiments.....	46
Table 5.13 Components concentration for Group-4 experiments.....	48
Table 5.14 Data obtained from Hydrate hysteresis curves for Group-4 experiments.....	49
Table 5.15 Data for kinetic analysis of Group-4 Experiments.....	51
Table-5.16 Components concentration for Group-5 experiments.....	53

Table -5.17 Data obtained from Hydrate hysteresis curves for Group-5 experiments.....	54
Table-5.18 Equations of straight line for each 1hour period for Group-5 experiments.....	55
Table- 5.19 Reaction rate for Group-5 Experiments.....	56
Table-5.20 Components concentration for Group-6 experiments.....	58
Table-5.21 Data obtained from Hydrate hysteresis curves for Group-6 experiments.....	59
Table-5.22 Equations of straight line for each 1hour period for Group-6 Experiments.....	61
Table-5.23 Reaction rate of Group-6 Experiments.....	62

LIST OF FIGURES

Figure 1.1. Hydrate structures (van Stackleberg, 1958).....	3
Figure 1.2. Crystalline structure of methane hydrate and ice (Sloan, 1990).....	4
Figure 2.1. Mechanism of hydrate formation (Lederhos et al (1996).....	10
Figure 4.1. Experimental set up (schematic view).....	23
Figure 4.2. High pressure reactor, pressure transducers and thermocouple.....	23
Figure 4.3. Constant temperature water bath and its accerrories	24
Figure 5.1. Temperature and pressure vs. time diagram (Experiment-1).....	28
Figure 5.2. Hydrate hysteresis curve (Experiment -1).....	30
Figure 5.3. Number of moles versus time diagram (Experiment 1).....	32
Figure-5.4 Detailed plot of Number of mole of free gas vs time diagram.....	33
Figure 5.5. Gas consumption rate for Experiment-1.....	34
Figure 5.6. Hydrate hysteresis curves for experiments-1, 2 and 3.....	36
Figure 5.7. Number of moles of free gas vs time diagrams of Group-1 experiments.....	37
Figure 5.8. Detailed plot of Number of mole of free gas vs time for Group-1.....	38
Figure 5.9. Gas consumption rate vs time diagram for Group-1 experiments.....	38
Figure 5.10. Hydrate hysteresis curves from repeatability tests	41
Figure 5.11. Number of moles of free gas comparison for repeatability tests.....	41
Figure 5.12. Hydrate hysteresis curves for Group-3 experiments.....	43
Figure 5.13. Number of moles of free gas vs. time diagram for Group-3 experiments.....	45
Figure 5.14. Detailed number of moles of free gas vs. time diagram for Group-3.....	45
Figure 5.15 Gas consumption rate vs. time histograms for Group-3 experiments.....	47
Figure 5.16 Hydrate hysteresis curves for Group-4 experiments.....	49
Figure 5.17 Number of moles of fee gas vs. time diagram for Group-4 experiments.....	50

Figure 5.18 Detailed number of moles of free gas vs. time diagrams for Group-4 experiments.....	51
Figure 5.19 Gas consumption rate of Group-4 experiments (except experiment-7).....	52
Figure 5.20 Hydrate hysteresis curves (Experiment 1-8-9).....	54
Figure 5.21 - Number of moles of free gas vs. time diagrams (experiment-1-8-9).....	55
Figure-5.22 Detailed number of moles of free gas vs. time diagram	56
Figure 5.23 Gas consumption rate for Group-5 experiments (experiments 1-8-9).....	57
Figure -5.24 Hydrate hysteresis curves (experiment 1-10-11).....	59
Figure-5.25 Number of moles of free gas vs. time diagram (experiment 1-10-11).....	60
Figure-5.26 Detailed number of moles of free gas vs. time diagram (experiment-1-10-11).....	61
Figure 5.27 Gas consumption rate for Group-6 experiments (experiment 1-10-11).....	62
Figure-B.1. Temperature and pressure vs. time diagram (Experiment-1).....	72
Figure-B.2. Temperature and pressure vs. time diagram (Experiment-1 repeatability test).....	73
Figure-B.3. Temperature and pressure vs. time diagram (Experiment-2).....	73
Figure-B.4. Temperature and pressure vs. time diagram (Experiment-3).....	74
Figure-B.5. Temperature and pressure vs. time diagram (Experiment-4).....	74
Figure-B.6. Temperature and pressure vs. time diagram (Experiment-5).....	75
Figure-B.7. Temperature and pressure vs. time diagram (Experiment-6).....	75
Figure-B.8. Temperature and pressure vs. time diagram (Experiment-7).....	76
Figure-B.9. Temperature and pressure vs. time diagram (Experiment-8).....	76
Figure-B.10. Temperature and pressure vs. time diagram (Experiment-9).....	77
Figure-B.11. Temperature and pressure vs. time diagram (Experiment-10).....	77
Figure-B.12. Temperature and pressure vs. time diagram (Experiment-11).....	78
Figure-C.1. Hydrate hysteresis curve (Experiment -1).....	79
Figure-C.2. Hydrate hysteresis curve (Experiment -1 repeatability test).....	80

Figure-C.3. Pressure vs. Temperature diagram (Experiment -2).....	80
Figure-C.4. Hydrate hysteresis curve (Experiment -3).....	81
Figure-C.5. Hydrate hysteresis curve (Experiment -4).....	81
Figure-C.6. Hydrate hysteresis curve (Experiment -5).....	82
Figure-C.7. Hydrate hysteresis curve (Experiment -6).....	82
Figure-C.8. Pressure vs. Temperature diagram (Experiment -7).....	83
Figure-C.9. Hydrate hysteresis curve (Experiment -8).....	83
Figure-C.10. Hydrate hysteresis curve (Experiment -9).....	84
Figure-C.11. Hydrate hysteresis curve (Experiment -10).....	84
Figure-C.12. Hydrate hysteresis curve (Experiment -11).....	85
Figure-D.1 Number of moles of free gas vs. time diagram (Experiment-1).....	86
Figure-D.2 Number of moles of free gas vs. time diagram (Experiment-1 repeatability test).....	87
Figure-D.3 Number of moles of free gas vs. time diagram (Experiment-2).....	87
Figure-D.4 Number of moles of free gas vs. time diagram (Experiment-3).....	88
Figure-D.5 Number of moles of free gas vs. time diagram (Experiment-4).....	88
Figure-D.6 Number of moles of free gas vs. time diagram (Experiment-5).....	89
Figure-D.7 Number of moles of free gas vs. time diagram (Experiment-6).....	89
Figure-D.8 Number of moles of free gas vs. time diagram (Experiment-7).....	90
Figure-D.9 Number of moles of free gas vs. time diagram (Experiment-8).....	90
Figure-D.10 Number of moles of free gas vs. time diagram (Experiment-9).....	91
Figure-D.11 Number of moles of free gas vs. time diagram (Experiment-10).....	91
Figure-D.12 Number of moles of free gas vs. time diagram (Experiment-11).....	92

CHAPTER 1

INTRODUCTION

Gas hydrates (clathrates) are crystal structures formed at certain thermobaric conditions from water and gas. Water forms a solid skeleton through hydrogen bonding and gas molecules are entrapped in the cavities of this skeleton due to the weak van der Waals forces. The name clathrate, from Latin «clathratus», that means "to cage", has been given by Powell in 1948. Hydrates of gas correspond to non stoichiometric, that is to variable compound structure. For the first time hydrates of gases (sulphurous gas and chlorine) observed at the end of 18th century by Jh. Priestley, B. Pelete and W. Karsten. First, who had described gas hydrates was Sir Henry Davy in 1810. By 1888 P. Villard synthesized hydrates of CH_4 , C_2H_6 , C_2H_4 , C_2H_2 , and N_2O . In 1940's the Soviet scientists stated the hypothesis about presence of deposits of gas hydrates in a zone of permafrost. In 1960's they found out the first gas hydrate deposits in the north of the USSR. Since that moment gas hydrates are considered as a potential source of energy. Later, it was found out by several researchers that gas hydrates are widely spread in the oceans and instable at increasing temperature. By some estimates, the energy locked up in methane hydrate deposits is more than twice the global reserves of all conventional gas, oil, and coal deposits combined. But no one has yet figured out how to recover the gas inexpensively, and no one knows how much is actually recoverable. Because methane is also a greenhouse gas, release of even a small percentage of total deposits could have a serious effect on Earth's atmosphere. Therefore, natural gas hydrates rivet special attention as a possible source of energy, and also as the main reason for

climate changes. Table 1.1 lists the achievements on gas the subject of hydrates with time. (J. Carrol, 2003)

Table 1.1. Achievements on different aspects of hydrates

Period	Achievements
1810	Sir Humphrey Davy discovers chlorine hydrate.
1888	Villard recognizes hydrates of CH ₄ , C ₂ H ₆ , C ₂ H ₄ , C ₂ H ₂ , and N ₂ O.
1930's	Hammerschmidt determines hydrates are blocking gas lines, and investigates hydrate inhibitors.
1940's	Soviets hypothesize the existence of natural methane hydrates in cold northern climates.
1960's	Molecular structure of hydrate is determined ("clathratus ~ to encage). Soviets recognize methane hydrate as a possible energy source, discover and produce the first major hydrate deposit in permafrost.
1970's	A bottom simulating reflector is drilled and is found to be associated with the base of hydrate stability.
1990's	Initial characterization and quantification of methane hydrate deposits in deep water.
2000's	Efforts to quantify location and abundance of hydrates begin. Large-scale efforts to exploit hydrates as fuel begin.

1.1 Properties of hydrates

Gas hydrates externally remind a compact snow. They often have characteristic smell of natural gas, and can burn. Due to clathrate structure the individual volume of gas hydrate can contain up to 160—180 volumes of pure gas. They easily break up to water and gas at increase in temperature. Clathrate hydrates are not chemical

compounds. The formation and decomposition of clathrate hydrates are first order phase transitions, not a chemical reaction

1.2 Hydrates Structures

Generally the structure of gas hydrates is described by formula $M \times n \times H_2O$, where

M — a molecule of gas,

n — number of molecules of the water in correspondence to one included molecule of gas, besides n — the variable number depending on type of hydrating gas, pressure and temperatures.

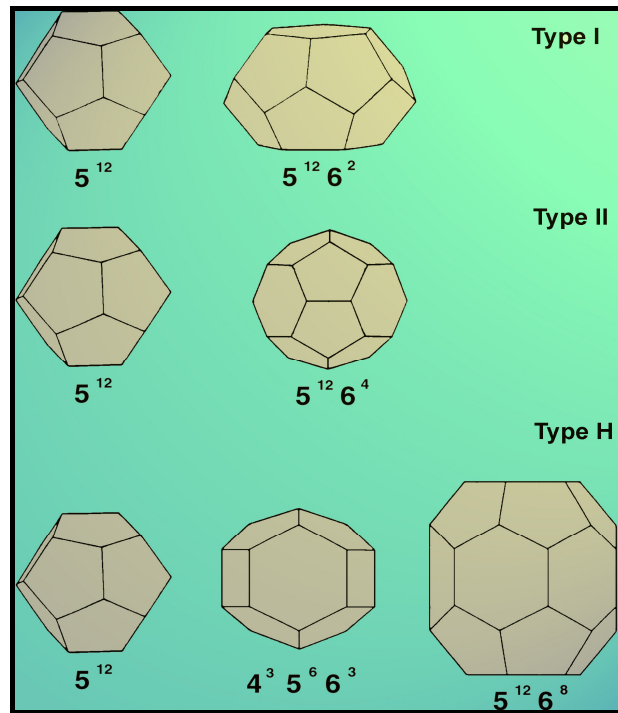


Figure 1.1. Hydrate structures (von Stackelberg 1958)

Gas hydrates usually form two crystallographic cubic structures – Structure (Type) I and Structure (Type) II. Rather seldom, a third hexagonal structure of space group may be observed (Type H) (Figure 1.1). The unit cell of Type I consists of 46 water molecules, forming two types of cages – small and large. The small cages in the unit

cell are two against six large ones. The small cage has the shape of pentagonal dodecahedron (5^{12}) and the large one that of tetrakaidecahedron ($5^{12}6^2$). Typical guests forming Type I hydrates are CO_2 and CH_4 . Figure 1.2 compares the structures of ice and methane hydrate.

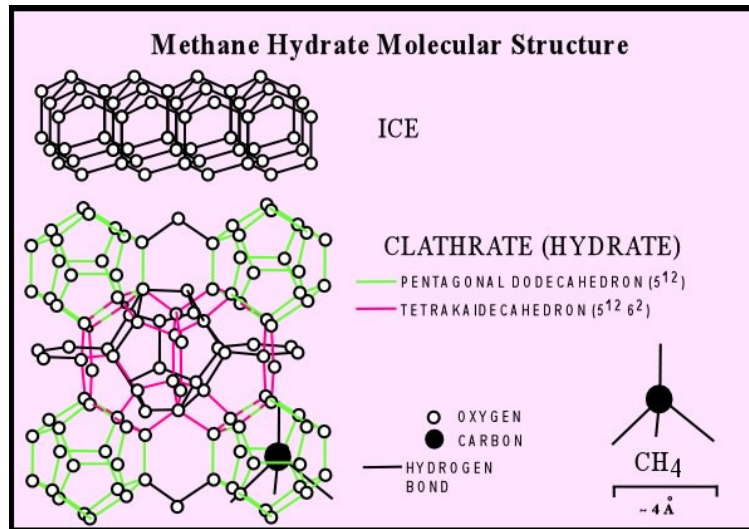


Figure 1.2. Crystalline structure of methane hydrate and ice (Sloan, 1990)

The unit cell of Type II consists of 136 water molecules, forming also two types of cages – small and large. In this case the small cages in the unit cell are sixteen against eight large ones. The small cage has again the shape of pentagonal dodecahedron (5^{12}) but the large one this time is hexakaidecahedron ($5^{12}6^4$). Type II hydrates are formed by gases like C_3H_8 , O_2 and N_2 .

The unit cell of Type H consists of 34 water molecules, forming three types of cages – two small of different type and one large. In this case, the unit cell consists of three small cages of type 5^{12} , twelve small ones of type $4^35^66^3$ and one large of type $5^{12}6^8$. The formation of Type H requires the cooperation of two guest gases (large and small) to be stable. It is the large cavity that allows structure H hydrates to fit in large molecules (e.g. butane, hydrocarbons), given the presence of other smaller help gases

to fill and support the remaining cavities. Structure H hydrates were suggested to exist in the Gulf of Mexico. There thermogenically-produced supplies of heavy hydrocarbons are common. (Sloan 1998)

1.2 Natural Gas Hydrates

Most of natural gases (CH_4 , C_2H_6 , C_3H_8 , CO_2 , N_2 , H_2S , isobutane, and etc.) form hydrates which exist at certain thermo baric conditions. The area of their existence is given as sea ground deposits and to areas permafrost rocks. Prevailing natural gas hydrates are hydrates of methane and carbon dioxide.

Methane clathrates are restricted to the shallow lithosphere (i.e. < 2000 m depth). Furthermore, necessary conditions are found only either in polar continental sedimentary rocks where surface temperatures are less than 0 °C; or in oceanic sediment at water depths greater than 300 m where the bottom water temperature is around 2 °C. Continental deposits have been located in Siberia and Alaska in sandstone and siltstone beds at less than 800 m depth. Oceanic deposits seem to be widespread in the continental shelf and can occur within the sediments at depth or close to the sediment-water interface. They may cap even larger deposits of gaseous methane (Kvenvolden, 1995).

There are two distinct types of oceanic deposits. The most common is dominated (> 99%) by methane contained in a structure I clathrate and generally found at depth in the sediment. Here, the methane is isotopically light ($^{13}\text{C} < -60\text{‰}$) which indicates that it is derived from the microbial reduction of CO_2 . The clathrates in these deep deposits are thought to have formed in-situ from the microbially-produced methane, as the ^{13}C values of clathrate and surrounding dissolved methane are similar (Milkov, 2004).

These deposits are located within a mid-depth zone around 300-500 m thick in the sediments (the Gas Hydrate Stability Zone, or GHSZ) where they coexist with methane dissolved in the pore-waters. Above this zone methane is only present in its dissolved form at concentrations that decrease towards the sediment surface. Below

it, methane is gaseous. At Blake Ridge on the Atlantic continental rise, the GHSZ started at 190 m depth and continued to 450 m, where it reached equilibrium with the gaseous phase. Measurements indicated that methane occupied 0-9% by volume in the GHSZ, and ~12% in the gaseous zone. (Dickens et. al., 1997)

In the less common second type found near the sediment surface some samples have a higher proportion of longer-chain hydrocarbons (<99% methane) contained in a structure II clathrate. Methane is isotopically heavier (^{13}C is -29 to -57 ‰) and is thought to have migrated upwards from deep sediments where methane was formed by thermal decomposition of organic matter. Examples of this type of deposit have been found in the Gulf of Mexico and the Caspian Sea. (Kvenvolden, 1995)

Some deposits have characteristics intermediate between the microbially- and thermally-sourced types and are considered to be formed from a mixture of the two.

The methane in gas hydrates is dominantly generated by bacterial degradation of organic matter in low oxygen environments. Organic matter in the uppermost few centimetres of sediments is first attacked by aerobic bacteria, generating CO_2 , which escapes from the sediments into the water column. In this region of aerobic bacterial activity sulfates are reduced to sulfides. If the sedimentation rate is low (<1 cm/kyr), the organic carbon content is low (<1%), and oxygen is abundant, aerobic bacteria use up all the organic matter in the sediments. But where sedimentation rates and the organic carbon content are high, the pore waters in the sediments are anoxic at depths of only a few cm, and methane is produced by anaerobic bacteria. This production of methane is a rather complicated process, requires the activity of several varieties of bacteria, a reducing environment (Eh -350 to -450 mV), and a pH between 6 and 8. In some regions (e.g., Gulf of Mexico) methane in clathrates may be at least partially derived from thermal degradation of organic matter, dominantly in petroleum. The methane in clathrates typically has a bacterial isotopic signature and highly variable ^{13}C (-40 to -100‰), with an approximate average of about -65‰. Below the zone of solid clathrates, large volumes of methane may occur as bubbles of free gas in the sediments. (Milkov, (2004))

1.4 Gas Hydrates in Pipelines

Thermodynamic conditions favouring hydrate formation are often found in pipelines. This is highly undesirable because the clathrate crystals might agglomerate and cause plugging of the flow-line, valves and instrumentation. The results can range from reduction of the flow to physical damages of the equipment. Hydrates have a strong tendency to agglomerate and to adhere to the pipe wall and thereby plug the pipeline. Once formed, they can be decomposed by increasing the temperature and/or decreasing the pressure. Even at these conditions, the clathrate dissociation is a slow process.

1.5 Utilization of Gas Hydrates

A number of laboratories in the world are actively seeking the solution to the problem of natural gas storage and transportation in a solid hydrate state. This method is based on a theoretical ratio of gas and water in a hydrate state (it is known that one volume of methane hydrate contains 164 volumes of gas and 0.8 volumes of water). Theoretically-wise it is very attractive to store or ship gas in a hydrate state, which is safer than in a liquefied or a compressed state.

However, the studies of kinetics of hydrate formation in static conditions indicate that producing monolith hydrate industrially is very costly and difficult. According to the researches the effective porosity of forming methane hydrate varies between 0 and 80% or more, depending on conditions. Therefore, the content of gas per unit volume will be variable, depending on density of forming hydrate. Hydrates formed in typical processes are highly porous with up to 80% porosity. Pores of the hydrate mass obtained in static conditions can be filled with free gas and water very slowly transforming into hydrate. Pores of the hydrate mass obtained in dynamic conditions are filled mainly with water. At a 20-25% hydrate content in actively stirred water the solution acts as a viscous low-mobility gel containing myriad of micro-crystals covered with strongly adsorbed layer of water. Diffusion of gas through such layer is

hindered. Transformation of a water-hydrate gel into a hydrate monolith proceeds very slowly. Microcrystals of hydrate have diameters, which are slightly greater than critical hydrate nuclei sizes. However, such a gel can be easily broken mechanically without decomposition of hydrate and it becomes fluid and mobile. New hydrate nuclei don't form even at significant supercooling on the surface of this gel, which is a multi-layer of bonded water molecules. At the base of these questions are two interrelated concepts – kinetics and morphology of hydrate crystals. It is impossible to develop effective technologies for preventing hydrate formation, for utilizing hydrates, and for surveying and developing hydrate deposits without discovering the laws of hydrate formation and decomposition kinetics in open volumes (wells, pipelines), closed volumes (hydrate-saturated rock), and without the knowledge of hydrate properties and their change with time. (Makogon et. al. 1999)

CHAPTER 2

FORMATION AND PREVENTION OF GAS HYDRATES

Gas hydrates form at gas/water boundary, with the most of the molecules coming from the molecules in the solution in the water phase. Since H₂S and CO₂ are more soluble in water compare to most other hydrocarbons, they tend to accelerate hydrate formation at higher temperatures. On the other hand, molecules larger than n-butane tend to inhibit hydrate formation. The n-butane does not form the hydrates itself but it participates in hydrate formation in association with lighter gases.

Kinetics of hydrate formation is still a current research topic. Since this process is not well understood, several theories have been developed explaining the mechanisms of hydrate formation. Lederhos *et al* (1996) proposed that gas hydrates form in an autocatalytic reaction mechanism, when water molecules cluster around natural gas molecules in structures similar to the ones shown in Figure 2.1.

This attraction between neighboring guest molecules is termed as "hydrophobic bonding", which can be described as the attraction between the apolar molecules inside the clusters [B]. Large and small clusters forming structures I and II are termed "labiles" because they are easy to break down, but relatively long-lived. Labiles can dissipate, or grow to become hydrate unit cells or agglomerations of unit cells forming what are known as "metastable nuclei" [C]. Then, growth can continue until crystals are stable, indicating the onset of secondary nucleation [D]. This theory implies reversibility of the process when the system is heated up.

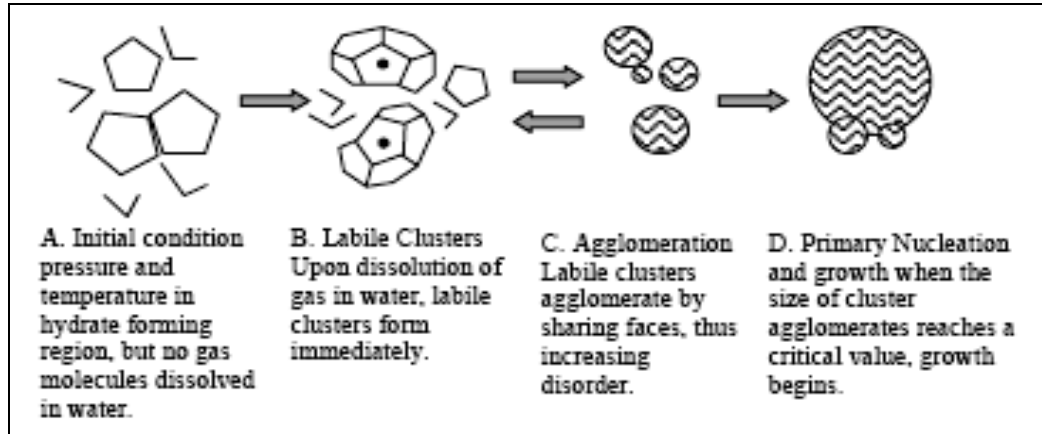


Figure 2.1. Mechanism of hydrate formation (Lederhos et .al.,1996).

Hydrates may form in the drilled wells if drilling utilizes the fresh water solutions in the low temperature and pressure intervals, during the drilling, while entering a pay zone, during mastering and testing of wells and during well shut in period. (Tahir, 2005).

In water based drilling mud, hydrates may cause problems in two ways. First, the hydrates may form a “plug” or solid mass within the wellbore. This plug could begin in areas of little or no circulation, such as chokelines, kill lines, or recess within the blow out preventers. Once formation has begun, growth may be quite rapid and then could spread to other parts of the system. Because of their mechanical strength, a large mass of hydrates may prevent drillstring rotation.

The second way in which hydrates may cause problems with drilling mud, results from their physical makeup. The water necessary for formation comes from the water based drilling mud itself. The loss of water from the mud causes flow properties to deteriorate severely. In the most extreme scenario, all solids will settle out, leaving little or no fluid in the well bore.(Kotkoskie et. al. 1992)

As for the gas well cases, the formation of gas hydrates in the flow string or in the reservoir will cause deterioration of gas well flow performance.

Therefore, preventing hydrates formation appears to be a key problem in a nowadays oil industry. The strategy of hydrate prevention comprises of activities, that are:

1. Avoiding of operational conditions that may cause hydrate formation;
2. Temporarily change of operational conditions in order to avoid formation of hydrates;
3. Prevention of hydrate formation by addition of chemicals that shift the hydrate equilibrium conditions towards lower temperature and pressure;
4. Addition of chemicals that increase hydrate formation time.

The last two methods correspond to adding of anti-hydrate inhibitor to the system, where the 3 methods is known to be the thermodynamic inhibiting and the last one stands to kinetic inhibiting.

The most common thermodynamic inhibitors are methanol, monoethylene glycol (MEG) and di-ethylene glycol (DEG) commonly referred to as glycol. All may be recovered and recirculated, but the economics of methanol recovery will not be favourable in most cases. MEG is preferred over DEG for applications where the temperature is expected to be $-10\text{ }^{\circ}\text{C}$ or lower due to high viscosity at low temperatures. TEG has too low vapour pressure to be suited as an inhibitor injected into a gas stream. More methanols will be lost in the gas phase when compared to MEG or DEG.

The use of kinetic inhibitors and anti-agglomerants in actual field operations is a new and evolving technology. It requires extensive tests and optimisation to the actual system. While kinetic inhibitors work by slowing down the kinetics of the nucleation, anti-agglomerants do not stop the nucleation, they rather stop the agglomeration (sticking together) of gas hydrate crystals. These two kind of inhibitors are also known as Low-Dosage-Hydrate-Inhibitors because they require much smaller concentrations than the conventional thermodynamic inhibitors. Kinetic inhibitors (which do not require water and hydrocarbon mixture to be effective) are usually polymers or copolymers and anti-agglomerants (requires water

and hydrocarbon mixture) are polymers or zwitterionic (usually ammonium and COOH) surfactants being both attracted to hydrates and hydrocarbons.

2.1 Thermodynamic Inhibitors

Thermodynamic inhibitors are added at high concentrations (10-60 wt.%) and alter the chemical potential of the aqueous or hydrate phase so that the hydrate dissociation curve is displaced to lower temperatures or higher pressures (Kelland et.al. 1995)

Historically, the most common hydrate inhibitors have been alcohols such as methanol (MeOH) and glycols. Classified as thermodynamic inhibitors, these additives function just as antifreeze in an automotive radiator. A thermodynamic inhibitor shifts the hydrate formation curve to the left so that the system can tolerate lower temperatures and higher pressures.

The higher the subcooling, the higher the amount of thermodynamic inhibitor that is needed. If sufficient thermodynamic hydrate inhibitor is present in the water phase, no hydrates will ever form.

Thermodynamic hydrate inhibitors are also capable of dissolving hydrate deposits that have already formed in systems. The required water phase concentration for thermodynamic hydrate inhibitors to work effectively can be extremely high (25-50% based on the volume of water in the system). In addition, some thermodynamic hydrate inhibitors, particularly methanol, partition significantly to the hydrocarbon phases; this must be accounted for in determining the required injection rates. (Baker Petrolite, 2006)

Methanol is still used at the oil/gas complex as hydrate formation inhibitor, it is used by relative cheapness and availability of this compound. However, it does not mean, that this chemical compound is the best one in use. Simply low cost and availability of methanol and the guaranteed effect from its application are sometimes

determining factor at a choice of inhibitors. Methanol is thoroughly investigated as inhibitor of hydrate formation and it is easily possible to find in the special literature any characteristics and initial data for calculation of technological processes with participation of methanol. Nevertheless, methanol possesses one extremely negative property: very high toxicity at similarity to ethyl spirit. Besides, due to its high toxicity, the other problem results in recycling of the fulfilled water solutions of methanol. This circumstance demands unprecedented security measures at purchase, transportation storage and use of methanol, expenses that are comparable to the cost of product itself (Istomin V. et. al., 2004).

In deepwater systems, it is not unusual to need 0.25 – 1 bbl methanol per bbl water produced. These types of product requirements can produce logistical problems of the highest magnitude. Besides maintaining large volumes of hazardous materials on offshore facilities where space is at a premium, the thermodynamic inhibitors have to be pumped under high pressure and in sufficient quantities to work effectively. On occasion, a production facility reaches a rate limit of methanol treatment, forcing the operator to curtail production or risk a hydrate plug. Another disadvantage is that the large volumes of inhibitor needed may severely impact on the capital costs for new asset design and construction. In particular, the inhibitor injection system (storage tank, chemical pump, and chemical umbilical / capillary) contributes significantly to the cost of a deepwater facility. Besides methanol possesses significant volatility, that alongside with technological losses, causes complexities at deep chemical processing of the hydrocarbon gas. These disadvantages of methanol as the thermodynamic inhibitor are defining under the certain circumstances and do expedient its replacement by other compounds possessing similar inhibiting qualities but less hazardous and toxic in use. Ethylene glycols such as mono-ethylene glycol (MEG) are less flammable, and reduce losses, but are more expensive and less available than methanol (Baker Petrolite, 2006).

According to Fadnes et. al. (1998), salts also can act as the thermodynamic inhibitors. They ionize the solution and interact with water molecules by bonds, resulting with cluster. Those bonds are stronger than van der Waals forces. So they

form clustering around the polar solute molecule and the potential hydrate formation molecule diminish in water. This process is called “salting out”. Thus the temperature of the hydrate formation will decrease.

At the beginning of 1990's studies were made in search of alternative thermodynamic inhibitors, Hale and Dewan (1990), reported of successful use of salts in combination with glycerol to prevent the hydrate formation, then Kotkoskie et. al. (1992) conducted a series of experiments involving 16 drilling fluids, and 3 different salts acting as thermodynamic inhibitors. According to the results salts like NaCl, and NaBr present significant inhibiting properties and could considerably shift the hydrate equilibria. CaCl₂ in spite the fact that it also positively affected the hydrate formation, was not the recommended choice among hydrate inhibitors, because of high corrosive effect. However, it did provide the maximum protection among pure salts. The highest hydrate temperature depression they measured in their tests was 69.6 °F for NaCl-saturated drilling fluid.

Ebeltoft et.al.(1997) had tested the salt/polymer system, by comparing of 25 drilling fluids in terms of hydrate inhibiting effect. In addition to previous 3 salts KCl was examined. The effect of glycol as a thermodynamic inhibitor, also was under consideration. According to the results the best composition of salt and glycols occurred to be 10%(Ethylene glycol)+15% (NaCl)+5%(KCl).

Quigley and Hubbar (1990) tested high concentrations of salts, alcohol, diols, surfactants, and their mixtures as hydrate inhibitors. Their measurements indicated that to drill at 3,100 ft water depth and 41 °F sea floor temperature, any combination of inhibitors equivalent to the inhibition capacity of 26 wt % NaCl would be safe to use. However, only 50 wt % methanol provided enough inhibition for safe drilling at 7,500 ft water depth and 39 °F. Even a mixture of 26 wt % NaCl and 20 wt % glycerol did not provide a sufficient safety margin at these conditions. Besides salt solutions are more corrosive and less effective than methanol or glycols, and could cause scale deposits in the process equipment.

Thermodynamic inhibition is still the widest method used worldwide, but its associated costs, environmental concerns and operational complexity have made researchers look for a different approach to the problem.

2.3 Low Dosage Inhibitors

This class of inhibitors as opposed to thermodynamic ones require lower dosage of chemical compounds to inhibit hydrates. Two classes of low dosage inhibitor are under research in today's oil industry: kinetic inhibitors and anti-agglomerants.

2.3.1 Kinetic Inhibitors

Kinetic inhibition of gas hydrates generally refers to the process by which the nucleation and growth of hydrate crystals are altered (modified) by using a low concentration of mostly polymeric- and surfactant-based chemicals. The inhibitors may cause one or more of the following effects:

- delay the appearance of the critical nuclei;
- slow the rate of hydrate formation; and/or
- prevent the agglomeration process (crystal modifier).

These chemicals do not disrupt the thermodynamic equilibrium of the hydrates.

Due to the similarity in composition of water and gas hydrates, kinetic ice inhibitors have helped inspire the development of kinetic hydrate inhibitors. For example, poly(N-vinyl pyrrolidone) (PVP) has been known for many years as a cryoprotectant for ice formation (Kelland, et.al. 1995). However, since gas hydrates forms primarily at the water/oil, water/gas interface, it was necessary to design the inhibitors which could exist in this interfacial region, unlike to kinetic ice inhibitors which can act in the bulk water phase. Sloan (1990) distinguished polymers time dependence from the

permanent time independence of the thermodynamic inhibition and were the first to use the term "kinetic inhibition". These chemicals can be effective at very low concentrations (< 1wt. %). They do not alter the thermodynamic conditions of hydrate formation. Kinetic inhibitors delay hydrate nucleation and subsequent crystal growth. These water-soluble compounds are inspired by antifreeze proteins (AFPs) secreted by some animal species to enable them to survive in sub-zero climates. Kinetic inhibitors are assumed to retard crystal growth by binding to the surface of hydrate particles in the early stages of nucleation and preventing the particle from reaching its critical size (the size at which particle growth becomes thermodynamically favourable). The duration of kinetic inhibition can be from several hours to days, which may exceed the residence time of fluids in process flowlines. Kelland et. al. (1995) studied the kinetic effect of different inhibitors in comparison with PVP. They tested butylated PVP (AgrimerP-904) and a terpolymer of N-vinyl pyrrolidone, N-vinyl caprolactam and dimethylaminomethacrylate (Gaffii VC-713). They had tested these polymers and observed greater kinetic inhibition activity than with any PVP sample. Besides in that research they developed a curve that shows the theoretical pressure-temperature limitations for use of hydrate inhibitors. In this curve, a safe pressure/temperature region is delineated for low-dosage inhibitors known at the time the curve was constructed. The diagram also includes predicted curves for theoretical future discoveries. Later again Kelland proposed a new class of kinetic inhibitors. The new kinetic inhibitor class is based on polymers of alkylacrylamides, plus blends of these with other synergists. They had concentrated on two polymers in particular, those based on the monomers acryloyl pyrrolidine (AP) and isopropylacrylamide (IP), and found that polymers of these monomers show high performance as kinetic hydrate inhibitors. These polymers inhibit hydrate formation in a similar way as the vinyl lactam polymers, by interaction of the pendant alkylamides groups with the hydrate surface. Besides, for practical applications the kinetic inhibitors appeared to be able to handle a subcooling of 10-12 °C, and even higher subcoolings if the residence time is short (Kelland et.al. 1999).

2.3.2 Anti-Agglomerants

These chemicals are polymers and surfactants, which are also added at low concentrations (<1wt.%). They allow hydrate formation, but work by preventing agglomeration of hydrates so that the hydrate crystals do not grow large enough to plug flowlines, but are transportable as a slurry. Anti-agglomerants only work in the presence of both water and liquid hydrocarbon phases but the mechanism of inhibition is not well understood. For some classes of anti-agglomerants, the chemicals seem to act on the newly-formed hydrate nuclei as an emulsifying agent (Paez, et.al. 2001).

The first article about surfactants as hydrate inhibitors appeared in 1972 by Yuliev. In early 1990's I.F.P. (Institute Francais du Petrole) has tested some chemical compounds, namely ethoxylated sorbitan monolaurate [$R = (CH_2CH_2O)_nH$], ethylene diamine-based block PO-EO copolymers, polymers of isobutylene succinate diester of monomethylpolyethylene glycol, which could act as anti agglomerants. Shell also had patented some surfactants as anti-agglomerants, these compounds include alkyl aromatic suiphonates and alkyl polyglycosides. Besides StatOil, SINTEF and NTH had researches on some surfactants including alkylphenylethoxylates. One of these, Berol 26, gave reasonable results in the high pressure wheel, but the concentrations used were very high (up to 7 wt.%). Other tests on sodium dodecyl sulphate (SDS), some polyacrylamides and tyrosine gave poor results (Kelland et. al. 1995).

Recently lot of researches were made on low dosage inhibitors application. Frostman (2000) had performed a laboratory and field test of Anti agglomerants LDHI. A Deepwater Gulf of Mexico system was chosen for the first field test of a new anti-agglomerant LDHI. The platform, located in 1980 ft of water, supported 10 dry tree wells and 2 subsea wells. In the experimental part of the research, two types of test were suggested, standard screening test and high pressure test. According to the laboratory results, 0.72 gal/bbl water was an optimum performance for the chosen system conditions. When performing the field test at first LDHI was injected via the

existing methanol injection system, at an estimated 1000 – 1300 gal/day, to displace methanol from the umbilical. This high injection rate was continued until 330 gal of LDHI had been pumped, which was sufficient to displace the methanol from the umbilical and slug the system with approximately 100 gal of the inhibitor. Then the LDHI was switched to a smaller pump and the rate decreased to 15 gal/day. After the LDHI concentration in the system leveled out, the injection rate was further reduced to 10 gal/day. Grindout of the oil suggested that the well was producing about 2 bbl water per day. At that point, the LDHI injection was slowed to 2.5 gal/day. This was the lowest injection rate attainable with the chemical injection pump. For the period of LDHI injection no hydrate problems were detected, even during shut-in period. There was some evidence that the LDHI reduced solids deposition in the flowline. The LDHI did not adversely affect overboard water quality: both oil and grease counts and aquatic toxicity tests remained within the normal operating range of this platform. The LDHI did not cause any emulsion problems.

Swanson (2005) also studied successful implementation of LDHI in Gulf of Mexico, in that case all three types of inhibitors were used, methanol injection from the beginning, which were substituted with two different anti agglomerants which were successfully used till the water cut increased to 50% and there was a necessity to use kinetic inhibitors. On the basis of field data they made a comparative analysis of anti agglomerants and kinetic inhibitors as follow:

Table 2.1 Comparison of two types of LDHI

KI advantages.	KI disadvantages	AAs advantages	AAs disadvantages
More compatible with changing Water cut	Sensitive to brine salinity with respect to solubility	Longer shut in times	Must have hydrocarbon liquid present
		Higher subcooling	
Reduced emulsion	Higher dose rate than AAs	Better solubility in highly saline brines	Typically limited to water cuts of 50% or less
Acceptable environmental impact	Limited subcooling possible	Lower dosage rates than KI	Environmental concerns
		Theor-y subcooling is not limited	

Frostman et. al. (2003) in recent paper made cost analysis. According to this paper application of LDHI can:

1. Lower Chemical costs: as far as treatment rate of LDHI is tens times lower than standard methanol injection;
2. Lower Transportation costs;
3. Lower Manpower cost;
4. No MeOH in Topside and Downstream operation;
5. Lower Pump Maintenance;
6. No Intervention during Shut-in;
7. Lower HS&E Risk.

In spite the fact that LDHI can significantly lower operational costs there still exist conditions at which their application is impossible.

The hope for low-dosage inhibitors has been that they would replace traditional thermodynamic inhibitors, but their action does not yet cover extreme conditions. Reservoirs in environments with temperatures below 0 °C would require antifreeze addition for controlling ice formation even if hydrate formation was not a threat. Under these conditions, extreme temperatures and pressures cause operators to use combined thermodynamic and low-dosage inhibitors. The topography of the pipeline also plays an important role in the performance of low-dosage inhibitors. In locations where the local residence time of the fluids is longer than the induction time of the low-dosage inhibitor used, gas hydrate plugging can occur. Gas pipelines represent a special case, because if the liquid phase is vaporized there is no solvent to carry the inhibitor and consequently, the inhibition effect could be lost. Shutdown conditions are different from normal operating conditions since the residence time of the fluids is extended and temperatures can drop (Paez et.al. 2001).

The other point of consideration when dealing with hydrate inhibitors is the influence of mud additives to gas liquid equilibria. Cha et.al. (1988) had reported of some

drilling mud components affect on gas hydrate formation. Ouar et.al. (1992) had tested fluids contained variable amounts of bentonite, thinner, caustic, barite, salt, xanthan gum, partially hydrolyzed polyacrylamide (PHPA), oil, drill solids, and methanol. It was suggested, that compounds such as PHPA and bentonite are thermodynamic promoters because they keep hydrates stable at higher temperatures relative to pure water. Another laboratory study also indicated a promotion of 2.0 to 3.0 °F in hydrate-equilibrium temperature for a fluid formulated from a mixture of bentonite, lignosulfonate, and sodium hydroxide. These observations require further verification as they imply that water activity is greater than 1.0 for aqueous solution of these compounds. The same compounds were also called kinetic promoters because they were found to enhance the rate and amount of hydrate formation relative to pure water.

Kotkoskie et.al. (1992) had also tested namely PHPA polymers and XCD influence on hydrate inhibition process. According to the report, they had tested fluids with the presence of PHPA and XCD and when both components were removed. The results showed that PHPA were a slight thermodynamic promoter of hydrate formation. This result was consistent with the previous researches in this direction. In case of XCD in spite the fact that previously it was reported as a slight thermodynamic inhibitor, their results were vice verse, and the mud samples with removed XCD showed better thermodynamic capacities.

CHAPTER 3

STATEMENT OF PROBLEM

Increase in energy demand and decrease in continental oil reserve force oil companies to exploit deeper ocean reservoirs. Drilling and/or production in deeper oceans will cause more frequent hydrate problems. Deeper ocean reservoirs commonly are under high pressure and low temperature conditions which in their term result in high possibility of hydrate formation, especially if a gas bearing formation is drilled. It is known that formation of hydrate in a pipe will reduce the pipe diameter eventually cause a permanent plugging. Besides formation of hydrates in water based drilling fluid may change its characteristics as far as water in gas hydrate structure is directly sorbed from drilling fluid. That reasons may complicate the drilling of deeper ocean reservoirs and result in higher economic costs. To prevent gas hydrate formation different inhibitors are usually added to drilling fluid.

Chemical hydrate inhibitors are classified as thermodynamic inhibitors and low dosage inhibitors (kinetic inhibitors and antiagglomerants). Respectively, they either shift the thermodynamic equilibrium, in other words, inhibitors change the hydrate formation conditions to lower temperature and pressure, or they directly affect to the rate of hydrate formation and slow down the hydration reaction time during drilling, as for the third type of inhibitors they do not prevent hydrates from forming but keep them in more dispersed form, so that hydrates would not stuck the pipe. The aim of this experimental study is to determine the hydrate formation conditions (formation, dissociation, inhibition) of a multi-component, polymer based drilling fluid by varying the concentrations of components, and to investigate hydrate inhibition capacities of these components in terms of thermodynamic and kinetic analysis.

CHAPTER 4

EXPERIMENTAL SET-UP AND PROCEDURE

4.1 Experimental Set-Up

The scheme of experimental set-up which were used while conducting the experiments is shown in Figure 4.1. The main equipment in which the drilling fluid was placed and hydrates were formed and dissociated is a cylindrical high-pressure reactor (Figure 4.2) with dimensions of 7.5 cm of inner diameter and 13.5 cm of inner length. It has the volume of 600 ml. It is made of stainless-steel and can stand up to 600 bar pressure. The high-pressure reactor is placed into a constant temperature water bath with volume of 125 liters. The temperature of the bath is controlled by means of a temperature controller/circulator and a refrigerated chiller both are immersed into the water bath (Figure 4.3). Besides, a thermocouple with an accuracy of ± 0.2 °C is placed inside the bath to control/record the temperature. The high pressure reactor is equipped with a thermocouple as well (with an accuracy of ± 0.2 °C) and pressure transducers to measure cell temperature and pressure. All these measuring devices are connected to a data-logger and a personal computer to record the temperature and pressure as the functions of time. The bath is equipped with a motor of 14.25 rpm. It is used during the experiments to provide the rocking of the reactor. Besides, there is a propeller that is fitted inside the bath. It provides mixing of water inside the bath, which provides a thorough full scaled cooling and heating of the system. Two glass balls are placed into the cell to provide better mixing of the fluid content in the reactor. Temperature and pressure are recorded every 5 seconds

throughout the experiments, by personal computer to which the thermocouples and pressure transducers are connected.

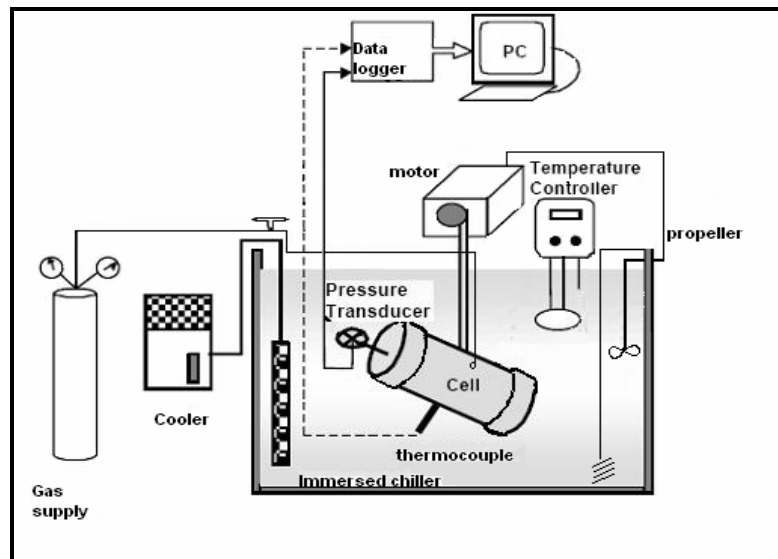


Figure 4.1. Experimental set up (schematic view)

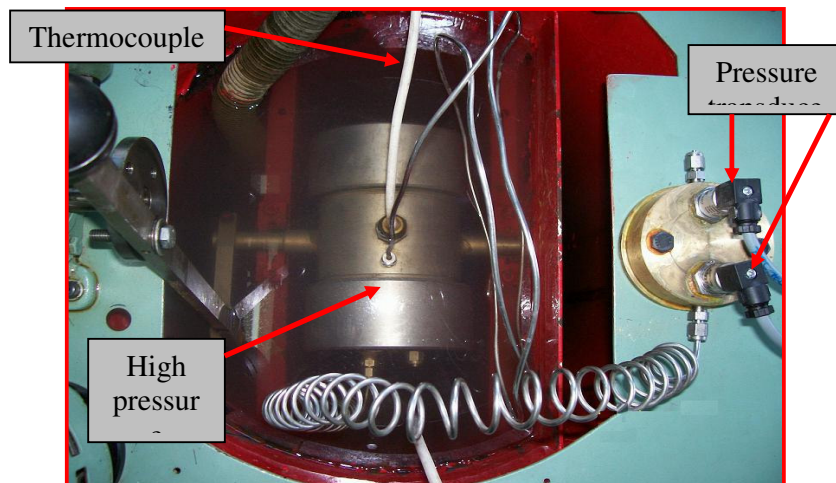


Figure 4.2. High pressure reactor, pressure transducers and thermocouple

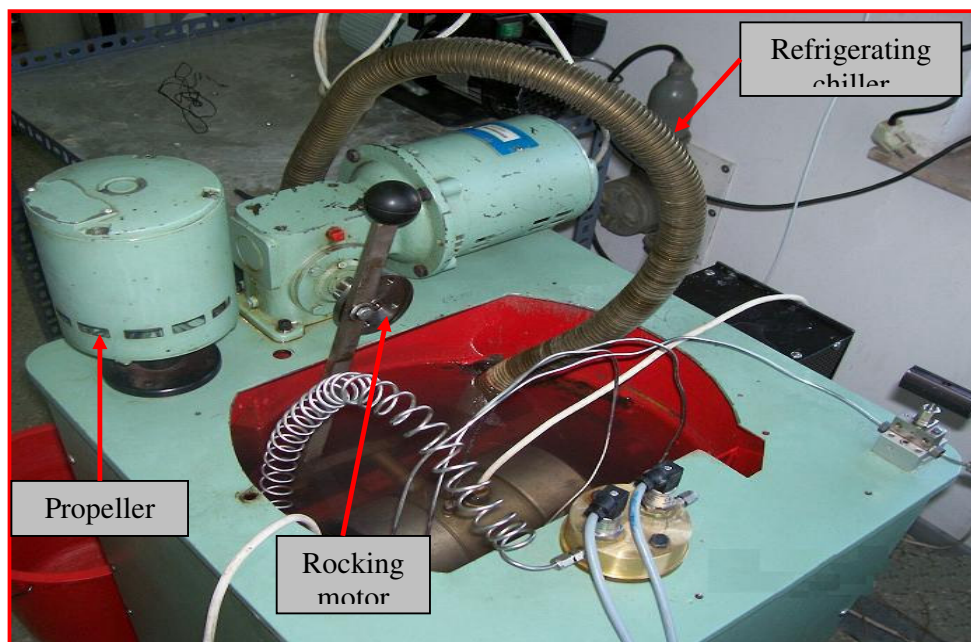


Figure 4.3. Constant temperature water bath and its accessories

4.2 Experimental Procedure

The following steps were followed while running a hydrate formation-dissociation test:

1. 300 ml of drilling fluid is placed into the high-pressure reactor
2. The temperature of the cell is adjusted to 15°C and the high-pressure cell is pressurized to the pressure of 57.2 bar by methane.
3. The cell is rocked for a while at constant temperature to dissolve the methane in water. After having a constant-stabilized pressure condition in the cell, cooling is started.
4. Cooling of the system causes a slight but continuous drop of cell pressure. This gradual pressure drop in the cell is due to the increase in solubility of gas in drilling fluid as well as pressure-temperature relationship through gas law. On the other hand, a sharp change in the pressure drop trend indicates the start of hydrate formation.

5. The cooling and the rocking of the cell continue for a certain period of time after the start of hydrate formation.
6. At the end of hydrate formation process, rocking and cooling of the cell is stopped and the system is allowed to heat with the aid of ambient temperature.
7. Increase in temperature results with dissociation of hydrate.

CHAPTER 5

RESULTS AND DISCUSSION

Twelve experiments in total were carried out during this study. Eleven of those experiments had different drilling fluid composition from each other to study the effect of chemical composition on the hydrate formation / inhibition conditions. On the other hand, two experiments with the same chemical composition were run to check the repeatability of experiments. The drilling fluids prepared by Drilling Technology Directorate of Research Center of Turkish Petroleum Corporation (TPAO Research center) were used during experiments. The concentrations of different components of drilling fluids were also set by TPAO Research center according to their necessity. The name of the components of drilling fluids with their minimum and maximum concentrations are given in Table 5.1. The specification of each component is indicated in Appendix A. Pure methane was used as the hydrate forming gas throughout the study.

As was mentioned in Chapter 3 (Statement of Problem), the purpose of these experiments was to determine the hydrate formation conditions (formation, dissociation, inhibition) of a multi-component, polymer based drilling fluid by varying the concentrations of components. Experiments (and consequently the analysis of data) were grouped into six groups (Table 5.2).

Table 5.1. Components of drilling fluids and their minimum and maximum concentrations

Component	Minimum	Maximum
KCl, (weight %)	7	12
PHPA, (lb/bbl)	0.75	1.25
Pac-LV, (lb/bbl)	2	4
Starch, (lb/bbl)	4	6
XCD, (lb/bbl)	0.5	1.0
Poly. glycol, (volume %)	3	5

Table 5.2. Groups of experiments

Group #	Experiment #	Variables	Purpose
1	1	PHPA, XCD, KCl, poly. glycol	To see the overall effect of all components with their increasing concentrations
	2		
	3		
2	1	No variables, all components at minimum level	To check the repeatability of tests, and see if the drilling fluid keeps its characteristics as time passes
	1-repeat		
3	1	PHPA	To see the effect of PHPA concentration on hydrate forming / inhibiting characteristics of drilling fluid
	4		
	5		
4	1	KCl	To observe the hydrate forming / inhibiting properties of drilling fluid with different concentration of KCl
	6		
	7		
5	1	XCD	To analyze the effect of XCD concentration on hydrate forming / inhibiting characteristics of drilling fluid
	8		
	9		
6	1	Polyglycol	To see the effect of Poly. glycol concentration on hydrate forming / inhibiting characteristics of drilling fluid
	10		
	11		

As was described in Chapter 4 (Experimental set up and procedure) data from thermocouples and pressure transducers is recorded every 5 seconds. Therefore, pressure and temperature data with respect to time for every conducted experiment is

available. On the basis of this data it is possible to plot diagrams, in order to make the analysis more comprehensible and easier to understand.

It is necessary to emphasize that experiments were conducted in static conditions, so if check the same experiments in dynamics, the data obtained for kinetic analysis would strikingly change

A typical plot of pressure, temperature vs time diagram (raw data) is presented on Figure 5.1.

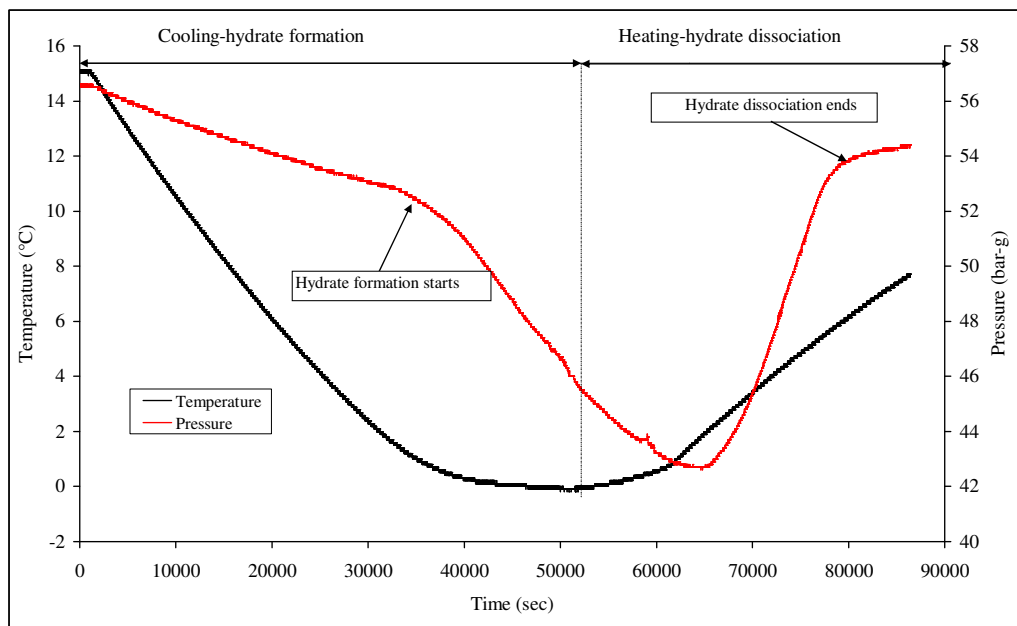


Figure 5.1. Temperature and pressure vs. time diagram (Experiment-1)

The cooling process, by means of refrigerator and then heating of system are the two main processes which are applied to the system. It was mentioned in the previous parts and also shown on Figure 5.1 that the initial conditions of all experiments are always the same, that is 57 bar-g in pressure and 15 °C in temperature. As can be noticed from Figure 5.1, with the decrease in temperature, pressure also gradually

decreases owing to the increase in solubility of gas in water as well as the result of real gas law. But at the point indicated as “Hydrate formation starts” on Figure 5.1, there exists a change (an increase) in pressure decline rate which is actually the result of hydrate formation. The gas molecules in free state pass to the crystalline form and start to form the solid hydrates. This part of the diagram is used to indicate the conditions at which gas hydrates are formed. After the hydrate formation process ends, and the heating starts, again the drastic increase of pressure indicates the dissociation process. Methane molecules captured in hydrate structure leave the crystalline structure and start to contribute the system pressure. The point indicated as “Hydrate dissociation ends” in Figure 5.1 is called Hydrate Equilibrium Point. This point is reported as the **hydrate equilibrium pressure and temperature** of the given system. After hydrate equilibrium point, increase in temperature cause a gradual increase in pressure. The pressure-temperature vs. time plots of all conducted experiments are represented in Appendix B.

When starting the detailed analysis of hydrate formation /dissociation data, researches usually deal with two types of plots obtained on the basis of data presented in Figure 5.1. They are: hydrate hysteresis curves and number of moles vs. time diagrams, that corresponds to thermodynamic and kinetic analysis respectively.

5.1 Thermodynamic Analysis – Hydrate Hysteresis Curves

A plot of pressure vs. temperature data of a hydrate formation/dissociation experiment is known as Hydrate Hysteresis Curve - HHC (Figure 5.2).

Analysis of HHC (pressure-temperature diagram) gives information on beginning of hydrate formation as well as hydrate equilibrium point. Both points for Experiment-1 are listed in table 5.3.

Table 5.3. Data obtained from hydrate hysteresis curve of Experiment-1

Beginning of hydrate formation, (°C)	Hydrate Equilibrium Point, (°C)
1.39	6.43

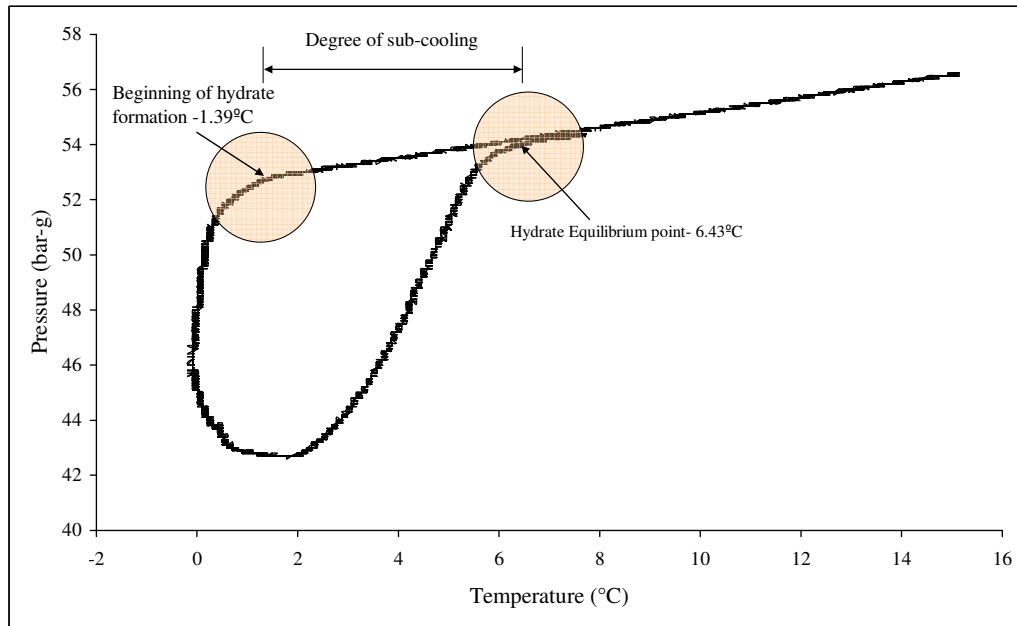


Figure 5.2. Hydrate hysteresis curve (Experiment -1).

As can be noticed from Figure 5.2 that the hydrate formation and hydrate dissociation parts construct a complete cycle and the point of their intersection is referred to “Hydrate Equilibrium Point”. The decline in pressure with temperature shows a linear trend during the early stages of cooling process (due to real gas law and increase in solubility of gas in water), but at a certain point this linearity is broken and pressure starts to decline rapidly. This point is indicated as the “beginning of hydrate formation”.

Beginning of hydrate formation is not only the thermodynamic property of system studied. It is affected by several other parameters, such as so-called “water memory”, small impurities in the system as hydrate seeding points, cooling rate etc. Therefore it is not common to report this point. On the other hand, the Hydrate Equilibrium Point is the thermodynamic property of the system investigated. It is actually the point at which all hydrates are dissociated.

The temperature difference between Hydrate Equilibrium Point and beginning of hydrate formation is known as “Degree of Sub-cooling”, the temperature difference from Hydrate Equilibrium Point, required to initiate bulk hydrate formation.

The hydrate hysteresis curves of all experiments are reported in Appendix C except Experiment-2 and Experiment-7 where no hydrates were formed, and therefore it was impossible to see the hydrate formation-dissociation process.

5.2 Kinetic Analysis – Number of Moles of Free Gas vs. Time

The type of diagram that is used to interpret the data obtained during the experiments from the kinetic point of view is represented in Figure 5.3, and called Number of moles versus time diagram.

Number of moles of free gas is derived from pressure and temperature data obtained from experiments, by means of the computer program (Parlaktuna, Doğan 2002). The principal of this program is based on real gas law expressed in Equation 5.1.

$$P V = z n R T \quad (5.1)$$

where

P - Cell pressure, psia

V - Volume of free gas in the cell, cuft

z - Gas compressibility factor

n - Number of moles of free gas in the cell, lb-mole

R - Universal gas constant, (10.73 psia cuft/ lb-mole °R)

T - Cell temperature, °R

Two parameters of Equation 5.1, pressure and temperature, are recorded at every 5 seconds during the experiments, therefore they are known. The computer program by Parlaktuna (1991) firstly determines the gas compressibility factor (Z), since it is the function of pressure, temperature and gas composition (pure methane). The volume of free gas in the cell is taken to be a constant value of 300 cm³. Therefore the only remaining unknown of Equation 5.1 is the number of moles of free gas (n) in the cell.

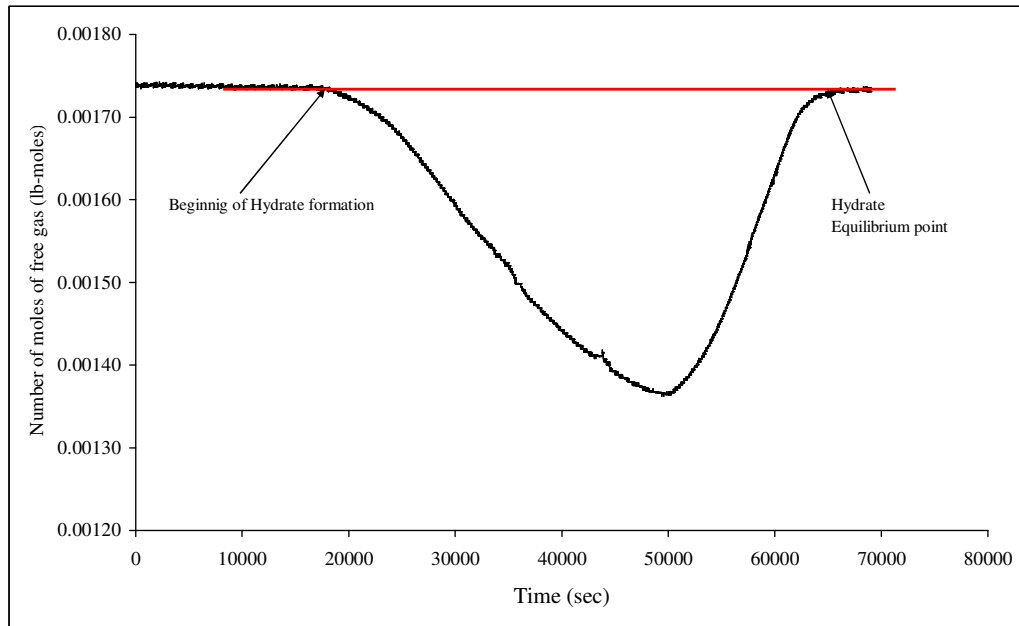


Figure 5.3. Number of moles versus time diagram (Experiment 1)

As can be seen from Figure 5.3, during the hydrate formation the number of moles of free gas in the cell is constant during the cooling process prior to hydrate formation. There exists a sharp decrease in number of moles of free gas after the beginning of hydrate formation. On the other hand, at the end of dissociation process the number of moles of free gas returns to its initial value, which means that experiment went on correctly and number of moles of free gas is the same at the beginning and at the end of experiment and consequently no leakage happened. By putting red line over the curve it is seen clearly. The kinetic analysis is based on the Number of moles of free gas decrease on the curve. It means that the rate of decrease of number of moles of free gas corresponds to the kinetic rate of hydrate formation process. To be more accurate, in this study, we divided the hydrate formation part of the curve into equal one hour time portions (Figure 5.4).

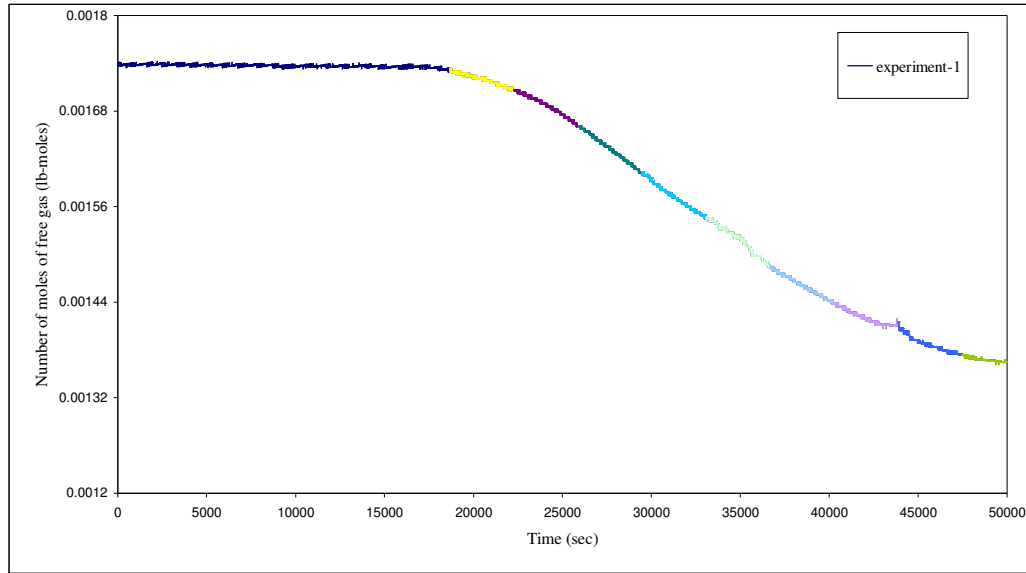


Figure-5.4 Detailed plot of Number of mole of free gas vs time diagram.
(Experiment-1, 9 hours from the start of hydrate formation)

The linear behavior of 1-hour period of the change in number of free gas moles with time gives the rate of change of number of free gas moles during hydrate formation, in other words, it can be taken as hydrate formation rate. Methane hydrate formation rates for Experiment-1 are listed in Table 5.4.

Table 5.4 Data obtained from Number of moles vs time diagram for Experiment-1

Linear equation	Rate of hydrate formation (lb-moles/sec)
$y = -6.68328E-09x + 1.85645E-03$	6.68×10^{-9}
$y = -1.24225E-08x + 1.98563E-03$	1.24×10^{-8}
$y = -1.66685E-08x + 2.09372E-03$	1.67×10^{-8}
$y = -1.58073E-08x + 2.06722E-03$	1.58×10^{-8}
$y = -1.74450E-08x + 2.12651E-03$	1.74×10^{-8}
$y = -1.25884E-08x + 1.94556E-03$	1.26×10^{-8}
$y = -8.36519E-09x + 1.77298E-03$	8.36×10^{-9}
$y = -9.15416E-09x + 1.80535E-03$	9.15×10^{-9}
$y = -3.31737E-09x + 1.52949E-03$	3.32×10^{-9}

The number of moles versus time diagrams for all experiments are represented in Appendix D.

The graphical representation of data from Table 5.4 is shown in Figure 5.5 which can be used to track the hydrate formation rates hour by hour.

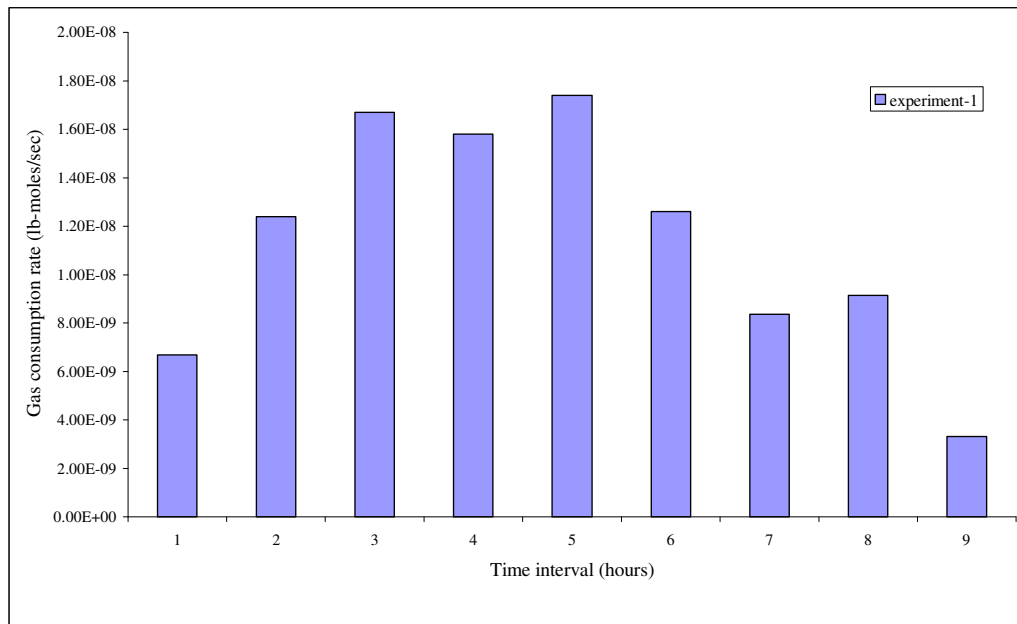


Figure 5.5. Gas consumption rate for Experiment-1.

Analysis of Figure 5.5 shows that:

- At the beginning (first 1 hour) of hydrate formation the gas consumption rate (i.e. the rate at which hydrates were formed) is slow. Only few molecules of methane undergo hydration process.

- The central part of the histogram corresponds to the maximum rate at which hydrates are formed. Most of the hydrate produced during the test is formed during this period and consequently the highest portion gas consumption occurred. This period lasts for 5 hours (2-6).

- At the later stage of hydrate formation process the rate of gas consumption slows down. It can be physically explained by the following fact: as far as hydrates form on the interface of gas and liquid only, the hydrates which were formed during the earlier, high productive rate hours could cover the gas/water contact area, and consequently influence on the following amounts of gas hydrates produced.

It is necessary to emphasize that experiments were conducted in static conditions, so if check the same experiments in dynamics, the data obtained for kinetic analysis would strikingly change as for thermodynamic analysis, the results that are presented here would not change so dramatically.

5.3 Group-1 Experiments: Comparison with Overall Increase In Concentration.

As was mentioned before the experiments conducted in Group-1 had increase in concentration of all components. Table 5.5 represents the compositions of drilling fluids used during these experiments.

Table 5.5 Components concentration for Group-1 experiments

Component	Experiment-1	Experiment-2	Experiment-3
KCl, (weight %)	7	12	9
PHPA, (lb/bbl)	0.75	1.25	1.00
Pac-LV, (lb/bbl)	2	4	3
Starch, (lb/bbl)	4	6	5
XCD, (lb/bbl)	0.50	1.00	0.75
Poly. glycol, (volume %)	3	5	4

Thermodynamic analysis of Group-1 experiments is done by using hydrate hysteresis curves of those experiments (Figure 5.6).

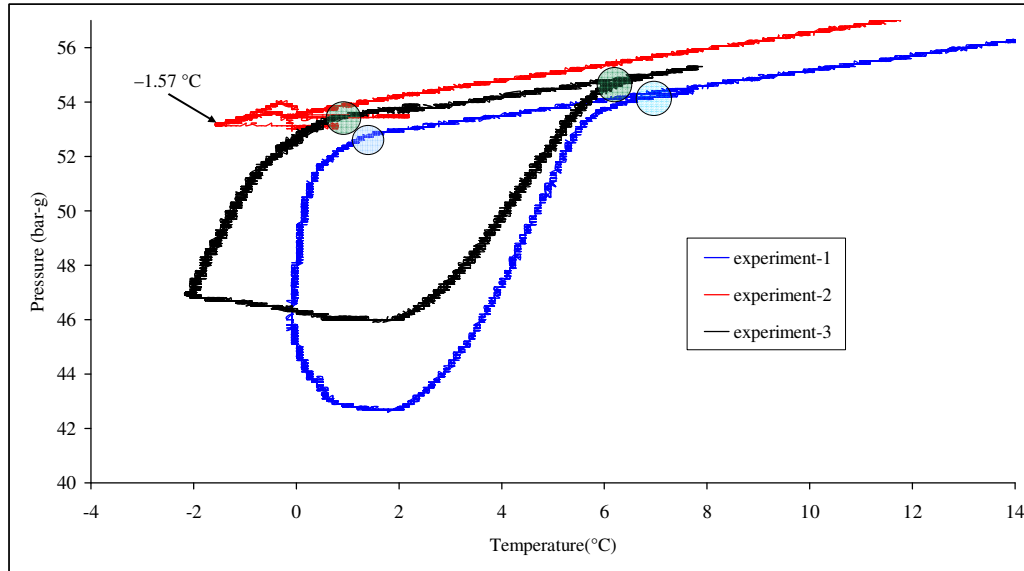


Figure 5.6. Hydrate hysteresis curves for experiments-1, 2 and 3.

As can be seen from Figure 5.6 that, with the increase in concentration of all components of drilling fluid both equilibrium point and hydrate initiation points are shifting towards lower temperature for a given pressure. Beginning of hydrate formation and equilibrium points are reported in Table 5.6. In case of experiment-2 in which the maximum concentrations of all components were used it was not possible to form hydrate. The recorded minimum temperature was $-1.57\text{ }^{\circ}\text{C}$ for that experiment and there was no indication of pressure decrease corresponding to hydrate formation. It is not clear at this point which component has the highest contribution of this observation since all components were used with their maximum concentrations.

Table 5.6 .Data obtained from hydrate hysteresis curves for Experiments 1, 2 and 3.

	Beginning of hydrate formation, °C	Hydrate equilibrium point, °C
Experiment-1	1.39	6.43
Experiment-2	–	–
Experiment-3	0.7	5.94

Analysis of Figure 5.6 show that hydrate formation / dissociation process was complete for Group-1 experiments since the number of moles of free gas in the cell before hydrate formation and after hydrate dissociation are the same.

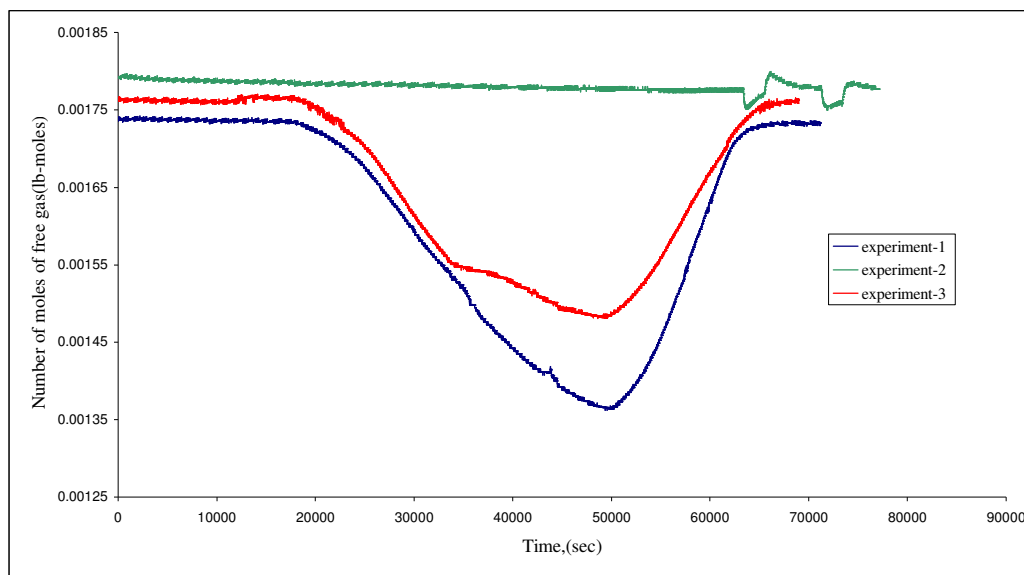


Figure 5.7. Number of moles of free gas vs time diagrams of Group-1 experiments

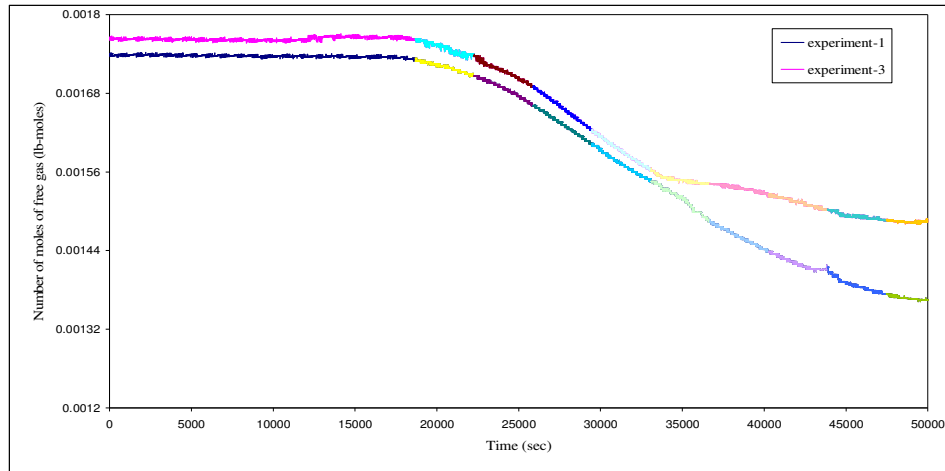


Figure 5.8. Detailed plot of Number of mole of free gas vs time for Group-1

Rate of gas consumption data for 1 hour interval of hydrate formation periods of Group-1 experiments are given in Table 5.7 and plotted in Figure 5.9.

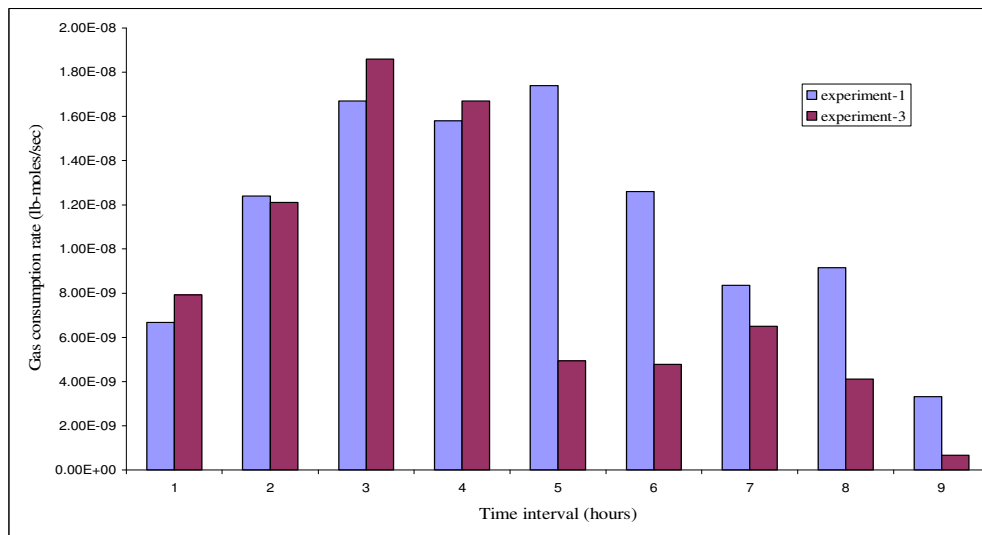


Figure 5.9. Gas consumption rate vs time diagram for Group-1 experiments

Table 5.7. Data for kinetic analysis for Group-1 experiments

Time Interval (hours)	Best line equation		Reaction rate (lb-moles/sec)	
	Experiment-1	Experiment-3	Experiment-1	Experiment-3
0-1	$y = -6.68328E-09x + 1.85645E-03$	$y = -7.92712E-09x + 1.91084E-03$	6.68×10^{-9}	7.93×10^{-9}
1-2	$y = -1.24225E-08x + 1.98563E-03$	$y = -1.21352E-08x + 2.00552E-03$	1.24×10^{-8}	1.21×10^{-8}
2-3	$y = -1.66685E-08x + 2.09372E-03$	$y = -1.85608E-08x + 2.17096E-03$	1.67×10^{-8}	1.86×10^{-8}
3-4	$y = -1.58073E-08x + 2.06722E-03$	$y = -1.67201E-08x + 2.11511E-03$	1.58×10^{-8}	1.67×10^{-8}
4-5	$y = -1.74450E-08x + 2.12651E-03$	$y = -4.94216E-09x + 1.72057E-03$	1.74×10^{-8}	4.94×10^{-9}
5-6	$y = -1.25884E-08x + 1.94556E-03$	$y = -4.78021E-09x + 1.71888E-03$	1.26×10^{-8}	4.78×10^{-9}
6-7	$y = -8.36519E-09x + 1.77298E-03$	$y = -6.51262E-09x + 1.78772E-03$	8.36×10^{-9}	6.51×10^{-9}
7-8	$y = -9.15416E-09x + 1.80535E-03$	$y = -4.11245E-09x + 1.68045E-03$	9.15×10^{-9}	4.11×10^{-9}
8-9	$y = -3.31737E-09x + 1.52949E-03$	$y = -6.59617E-10x + 1.51643E-03$	3.32×10^{-9}	6.6×10^{-10}

Analysis of Figure 5.9 indicate that the overall increase in the concentration of all components of drilling fluid did not cause a significant change in the gas consumption rate in the first four hours. On the other hand, the gas consumption rate with higher concentrations (Experiment-3) slowed down after 5th hour. The reason for this change could be the slightly higher hydrate production rates in the 3rd and 4th hours during Experiment-3 which may cause a considerable reduction in drilling fluid-gas interface to sustain the hydrate production. If the drilling fluid-gas phase interface is covered by hydrate the mass transfer between gas and drilling fluid is reduced which is the driving force of hydrate formation.

The first few hours actually should be taken the representative period of a hydrate formation process in a flowing condition. In a flowing environment, the stream can traverse the portion of pipeline having hydrate forming conditions in few hours. Therefore the discussion for hydrate formation rate in a batch experiment (a closed

cell with constant composition) should be limited to first few hours. The late stages of experiment is affected by some other factors which are not the part of a flowing system. The most important factor among these is the renewal of gas-liquid interface and removal of heat during hydrate formation (hydrate formation is an exothermic process).

5.4 Group -2: Experiments on Repeatability

After the experiments of Group-1, one of the experiments of this group (Experiment-1) was repeated with the same chemical composition under the same pressure-temperature conditions. Half of the drilling was stored in a glass jar for a week before the repeatability test.

The results of these two experiments are shown on the Figures 5.10 and 5.11 representing hydrate hysteresis curves and number of moles of free gas vs time diagrams, respectively. Hydrate equilibrium points and beginning point for hydrate formations reported in Table 5.8

Table 5.8. Data obtained from hydrate hysteresis curves from repeatability tests

	Beginning of hydrate formation, °C	Hydrate equilibrium point, °C
Experiment-1	1.39	6.43
Exp-1 repeat	1.39	6.23

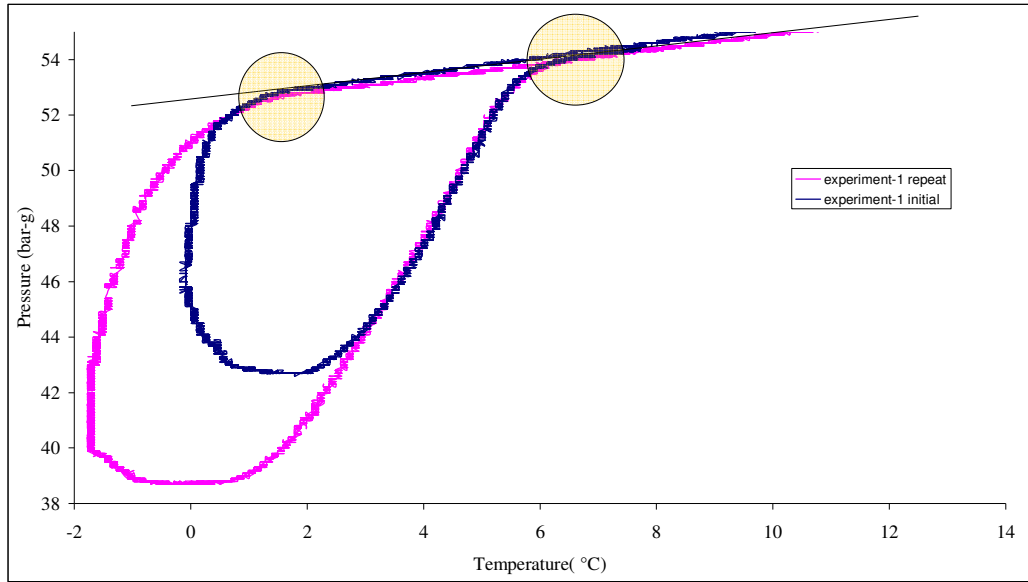


Figure 5.10. Hydrate hysteresis curves from repeatability tests

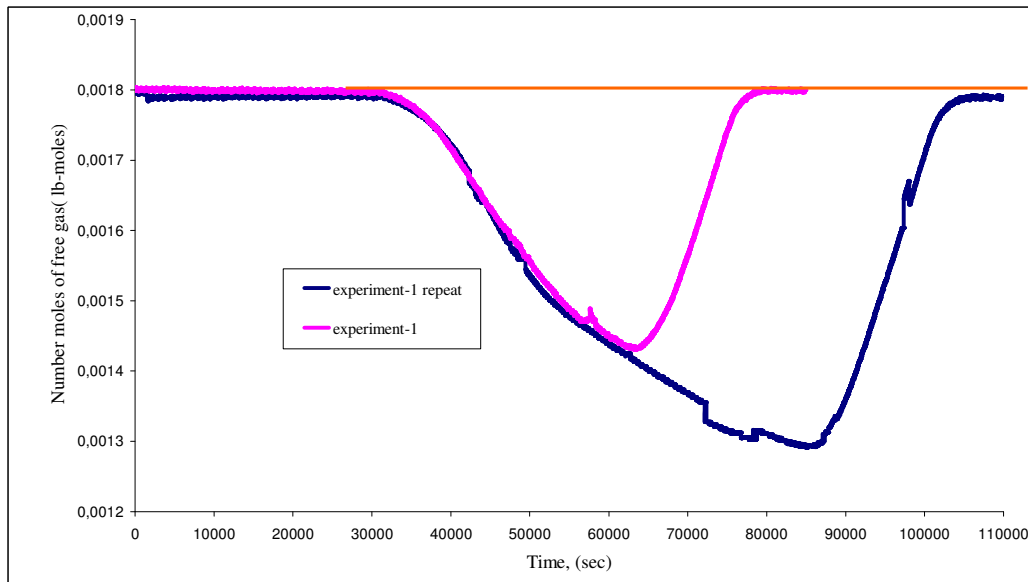


Figure 5.11. Number of moles of free gas comparison for repeatability tests

Analysis of Table 5.8, Figures 5.10 and Figure 5.11 show that the hydrate formation / dissociation experiments are repeatable under the same experimental conditions. From hydrate formation / dissociation thermodynamics points of view both hydrate formation beginning and hydrate equilibrium points are reasonably close each other. In addition, hydrate formation kinetics data from both experiments follow almost the same path except the longer formation period of repeat test. It was decided not to make quantitative analysis since both experiments follow the same path during hydrate formation.

It can be concluded from the results of these test and subsequent thermodynamic and kinetic analysis that drilling fluid preserves its hydrate formation / dissociation characteristics during short term storage.

After completing the repeatability study, the next stage was to study the influence of different components on the thermodynamics and kinetics of hydrate formation. Series of experiments were made with varying concentration of only one component and keeping the rest of components at their minimum concentrations.

5.5 Group-3: Effect of PHPA

PHPA is a readily dispersible product designed to provide cuttings encapsulation and shale stabilization. As was mentioned before, in the 3rd group of experiments only PHPA concentration was changed whereas concentrations of the other components were kept on their minimum values. The data on the components concentration of the Group-3 experiments are presented in Table 5.9. The thermodynamic analysis for Group-3 experiments is represented in Figure 5.12

Table 5.9 Components concentration for Group-3 experiments

Component	Experiment-1	Experiment-4	Experiment-5
KCl, (weight %)	7	7	7
PHPA, (lb/bbl)	0.75	1.00	1.25

Pac-LV, (lb/bbl)	2	2	2
Starch, (lb/bbl)	4	4	4
XCD, (lb/bbl)	0.5	0.5	0.5
Poly. glycol, (volume %)	3	3	3

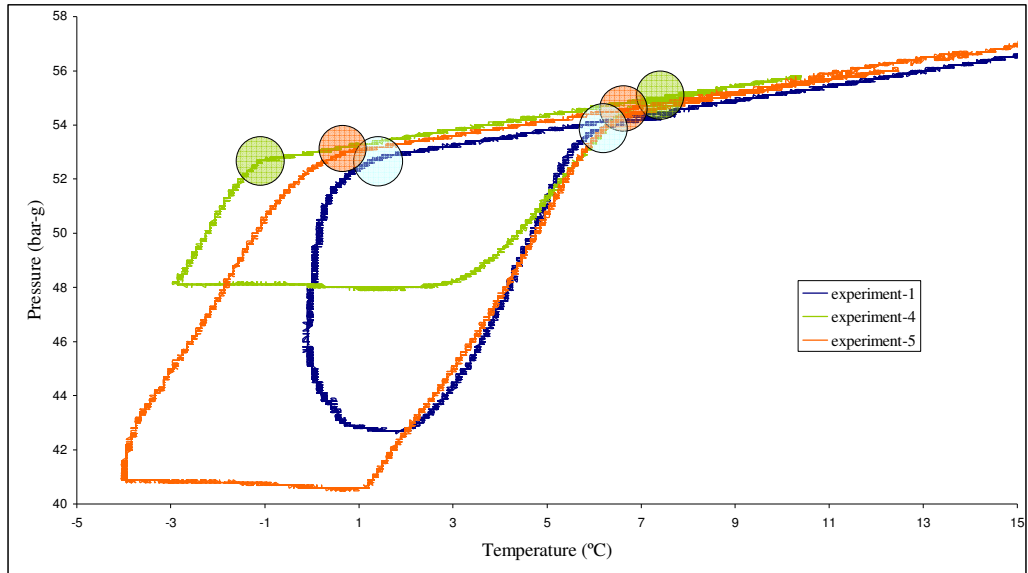


Figure 5.12. Hydrate hysteresis curves for Group-3 experiments.

The point of beginning of hydrate formation and hydrate equilibrium points are listed in Table 5.10.

Table 5.10 Data obtained from Hydrate hysteresis curves for Group-3 experiments

	Beginning of hydrate formation, °C	Hydrate equilibrium point, °C
Experiment-1	1.39	6.43
Experiment-4	-1.18	6.92
Experiment-5	0.8	6.83

In the previous studies it was already reported that PHPA usually acts as a slight thermodynamic promoter. As can be noticed from Figure 5.12 and Table 5.8, it shifts the equilibrium point to the higher temperature with the increase in concentration, nevertheless on the beginning of hydrate formation PHPA's impact is positive (that is beginning point is shifting to the lower temperature), probably it can be explained by the water memory effect or the effect of other components of drilling fluid, as far as previously the similar result were also reported once by Kotkoskie et.al. (1992) when they tested the effect of PHPA on NaCl drilling fluid, probably the presence of salts surpasses the PHPA effect.

Kinetics of the hydrate formation for Group-3 experiments can be checked on Figure 5.13. Straight lines on the curves show that all three experiments went correctly, no gas leakage occurred, and all formed hydrates dissociated to the free state as system underwent heating process. In order to analyze the kinetics or hydrate formation process, let's take only that part of curves which refers to hydrate formation (Figure 5.14).

Tables 5.11 and 5.12 respectively represent the linear equations of 1 hour periods and rates of hydrate formation for these periods for Group-3 experiments.

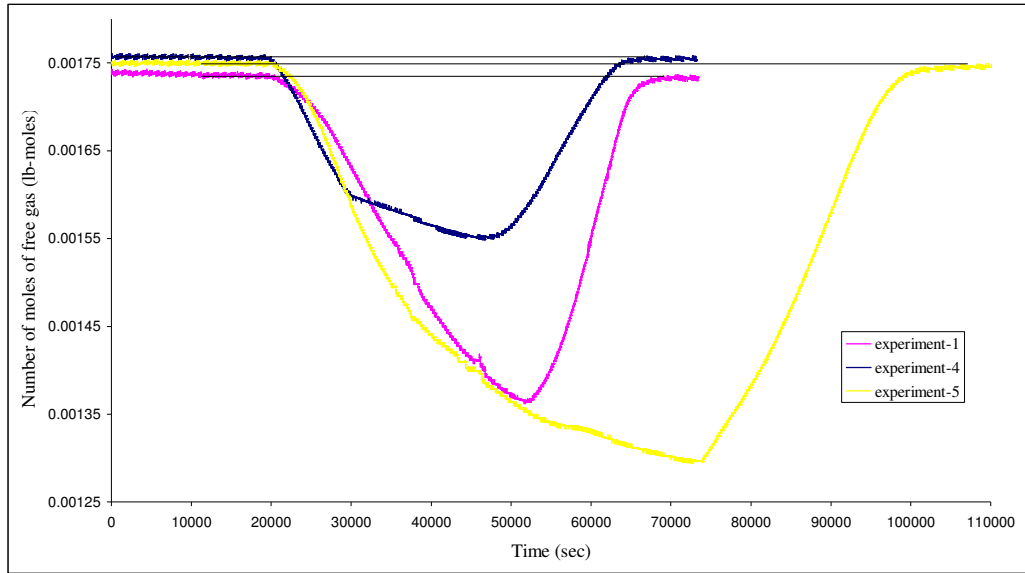


Figure 5.13. Number of moles of free gas vs. time diagram for Group-3 experiments

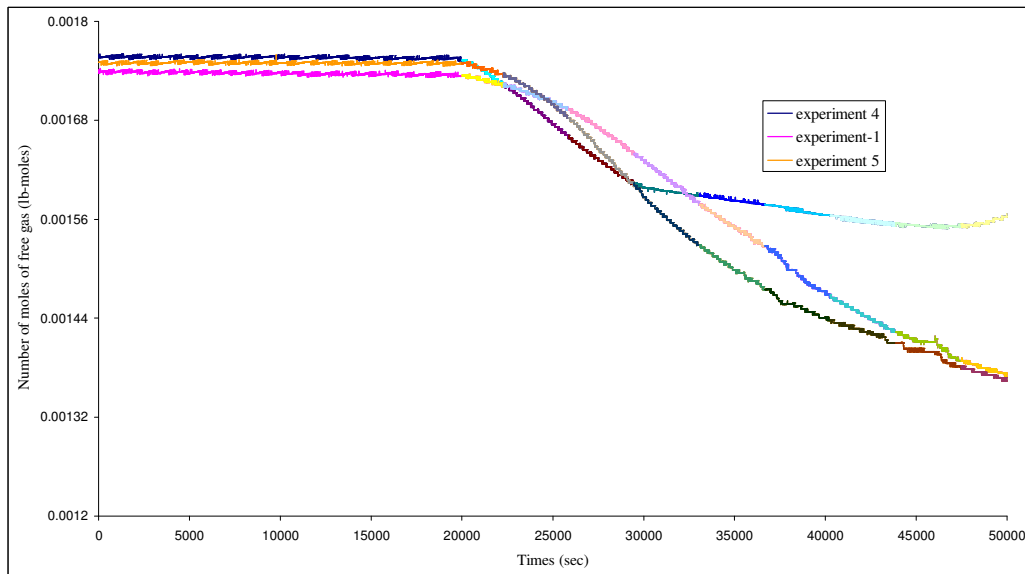


Figure 5.14. Detailed number of moles of free gas vs. time diagram for Group-3 experiments.

Table 5.11 Equations of straight line for each 1hour period for Group-3 experiments

Time Interval (hours)	Best line equation		
	Experiment-1	Experiment-4	Experiment-5
0-1	$y = -6.68328E-09x + 1.85645E-03$	$y = -1.32739E-08x + 2.02064E-03$	$y = -6.26976E-09x + 1.87544E-03$
1-2	$y = -1.24225E-08x + 1.98563E-03$	$y = -1.80555E-08x + 2.12737E-03$	$y = -1.46975E-08x + 2.06626E-03$
2-3	$y = -1.66685E-08x + 2.09372E-03$	$y = -1.56973E-08x + 2.06464E-03$	$y = -2.31016E-08x + 2.28185E-03$
3-4	$y = -1.58073E-08x + 2.06722E-03$	$y = -3.72057E-09x + 1.71100E-03$	$y = -2.01781E-08x + 2.19318E-03$
4-5	$y = -1.74450E-08x + 2.12651E-03$	$y = -3.01692E-09x + 1.68843E-03$	$y = -1.43446E-08x + 2.00161E-03$
5-6	$y = -1.25884E-08x + 1.94556E-03$	$y = -4.09641E-09x + 1.72836E-03$	$y = -1.00989E-08x + 1.84300E-03$
6-7	$y = -8.36519E-09x + 1.77298E-03$	$y = -2.74904E-09x + 1.67466E-03$	$y = -7.60185E-09x + 1.74407E-03$
7-8	$y = -9.15416E-09x + 1.80535E-03$	$y = -9.91774E-10x + 1.59748E-03$	$y = -8.05647E-09x + 1.76458E-03$
8-9	$y = -3.31737E-09x + 1.52949E-03$	$y = 4.62218E-09x + 1.33123E-03$	$y = -6.26350E-09x + 1.67817E-03$

Table 5.12 Reaction rates of Group-3 experiments

Time Interval (hours)	Reaction rate (lb-moles/sec)		
	Experiment-1	Experiment-4	Experiment-5
0-1	6.68×10^{-9}	1.33×10^{-8}	6.27×10^{-9}
1-2	1.24×10^{-8}	1.81×10^{-8}	1.47×10^{-8}
2-3	1.67×10^{-8}	1.57×10^{-8}	2.31×10^{-8}
3-4	1.58×10^{-8}	3.72×10^{-9}	2.02×10^{-8}
4-5	1.74×10^{-8}	3.02×10^{-9}	1.43×10^{-8}
5-6	1.26×10^{-8}	4.10×10^{-9}	1.01×10^{-8}
6-7	8.36×10^{-9}	2.75×10^{-9}	7.60×10^{-9}
7-8	9.15×10^{-9}	9.92×10^{-10}	8.06×10^{-9}
8-9	3.32×10^{-9}	4.62×10^{-9}	6.26×10^{-9}

The histograms of change in kinetic rates is shown on Figure 5.15

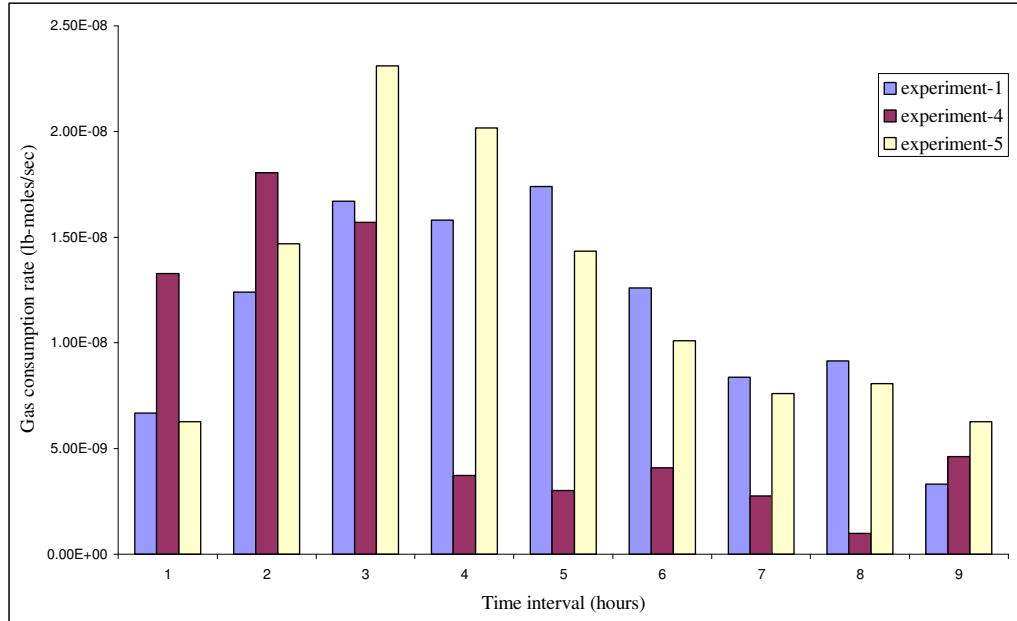


Figure 5.15 Gas consumption rate vs. time histograms for Group-3 experiments

The kinetic influence of PHPA is represented by Figures 5.13-5.14 and Tables 5.9-5.10. Besides The analysis of last histograms gives us clear information about the effect of PHPA on the kinetics of hydrate formation.

Increase in concentration of PHPA promotes the hydrate formation rate. In spite the fact that acceleration of the hydrate formation rate does not go accordingly with the increase in concentration, it can be explained as follows:

- With the medium concentration of PHPA (Experiment-4, 1 lb/bbl) the hydrate formation rate from the very first hour is almost twice higher than the experiments-1 rate (minimum concentration), but during the time interval of 3 – 4 hours, it dramatically slows down, probably as a result of decrease in interfacial gas/liquid area of hydrate formation.

- The maximum concentration experiment (Experiment-5) on the contrary begins with almost the same rate as Experiment -1, but starting with 2nd hour the rate of hydrate formation is constantly higher than both Experiment-1 and Experiment-4 till almost 6th hour.

These observations suggest that PHPA can be considered as a kinetic promoter of gas hydrate formation.

Kotkoskie et. al., (1992) had also tested PHPA effect on hydrate inhibition. The study, consist of 2 experiments, with PHPA and removing it. They used water based drilling mud, and after removing PHPA the hydrate equilibria slightly decreased, proving the previous assumptions of PHPA’s promoting effect on hydrate formation. Hebeltoft (2001), again mentioned PHPA as the thermodynamic promoter of hydrate formation in his studies, our results are consistent with the previous works in this direction

5.6 Group-4: Effect of KCl

The concentrations of experiments referred to Group-4 are listed in the Table-5.13

Table 5.13 Components concentration for Group-4 experiments

Component	Experiment-1	Experiment-6	Experiment-7
KCl, (weight %)	7	9	12
PHPA, (lb/bbl)	0.75	0.75	0.75
Pac-LV, (lb/bbl)	2	2	2
Starch, (lb/bbl)	4	4	4
XCD, (lb/bbl)	0.5	0.5	0.5
Poly. glycol, (volume %)	3	3	3

For the thermodynamic analysis, plots of pressure - temperature diagrams (hydrate hysteresis curves) are presented in Figure 5.16. The numerical values of points indicated on the Figure 5.16 are listed in Table 5.12.

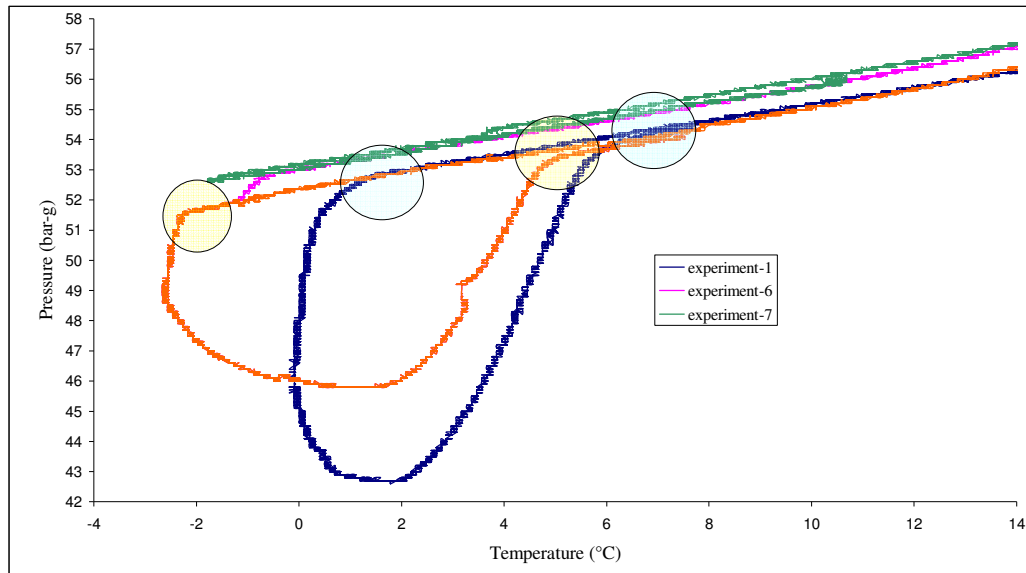


Figure 5.16 Hydrate hysteresis curves for Group-4 experiments.

Table 5.14 Data obtained from Hydrate hysteresis curves for Group-4 experiments

	Beginning of hydrate formation, °C	Hydrate equilibrium point, °C
Experiment-1	1.39	6.43
Experiment-6	-2.26	5.34
Experiment-7	–	–

Salts are known as thermodynamic inhibitors, they are widely utilized instead of methanol and when using with poly. glycols, present almost identical inhibiting capacities. So in this study KCl is used as main thermodynamic inhibitor, it showed the significant results and decreased both equilibrium point and hydrate formation beginning point (Figure 5.16, Table 5.14). Unfortunately, it was not possible to form hydrate with the maximum concentration of KCl (Experiment-7). No hydrates were formed even the temperature decreased to -2.5 °C, which was the limit of the cooler after adding anti-freezing agent into cooling water.

As obvious from Figure 5.17 that it was not possible to form hydrate during Experiment-7 since there is no decline in number of moles curve and this experiment

was excluded from further consideration. In Table 5.15 linear equations and kinetic rates only for Experiment -1 and Experiment-6 are given.

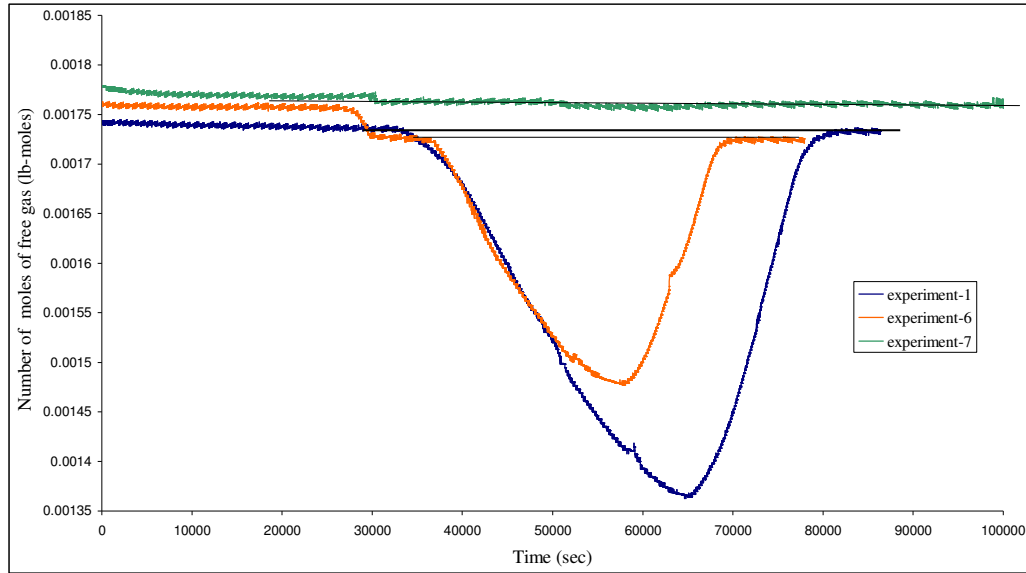


Figure 5.17 Number of moles of free gas vs. time diagram for Group-4 experiments

For the clear view let's consider only the hydrate formation part of the previous curves (Figure-5.18)

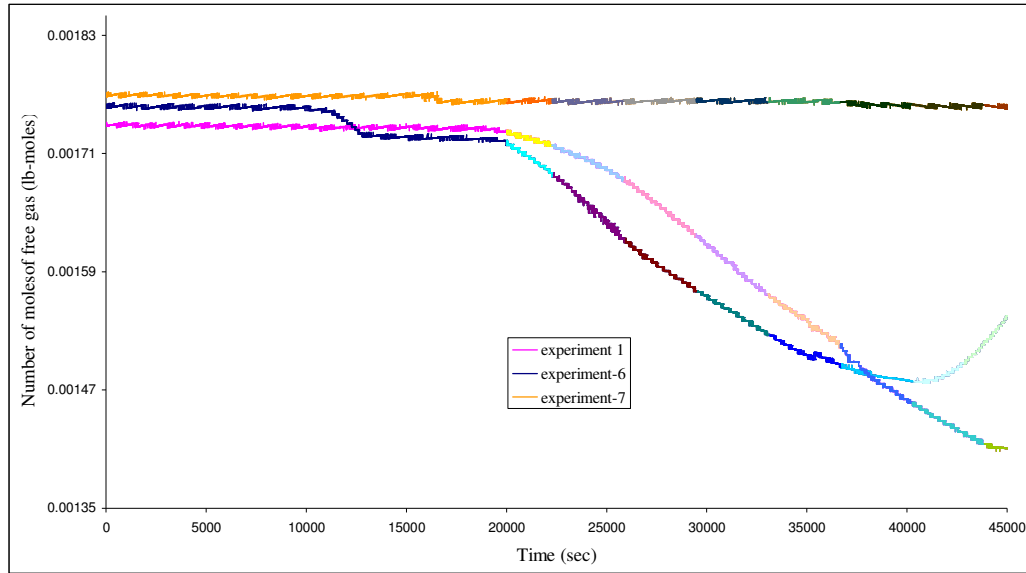


Figure 5.18 Detailed number of moles of free gas vs. time diagrams for Group-4 experiments

Table 5.15 Data for kinetic analysis of Group-4 experiments

Time Interval (hours)	Best line equation		Reaction rate (lb-moles/sec)	
	Experiment-1	Experiment-6	Experiment-1	Experiment-6
0-1	$y = -6.68328E-09x + 1.85645E-03$	$y = -1.36687E-08x + 1.99482E-03$	6.68×10^{-9}	1.37×10^{-8}
1-2	$y = -1.24225E-08x + 1.98563E-03$	$y = -1.87197E-08x + 2.10808E-03$	1.24×10^{-8}	1.87×10^{-8}
2-3	$y = -1.66685E-08x + 2.09372E-03$	$y = -1.38786E-08x + 1.97967E-03$	1.67×10^{-8}	1.39×10^{-8}
3-4	$y = -1.58073E-08x + 2.06722E-03$	$y = -1.23899E-08x + 1.93657E-03$	1.58×10^{-8}	1.24×10^{-8}
4-5	$y = -1.74450E-08x + 2.12651E-03$	$y = -8.14059E-09x + 1.79297E-03$	1.74×10^{-8}	8.14×10^{-9}
5-6	$y = -1.25884E-08x + 1.94556E-03$	$y = -4.31647E-09x + 1.65134E-03$	1.26×10^{-8}	4.32×10^{-9}
6-7	$y = -8.36519E-09x + 1.77298E-03$	$y = 7.09145E-09x + 1.18896E-03$	8.36×10^{-9}	7.09×10^{-9}

The data presented in Table 5.15 visually represented in histograms of Figure 5.19.

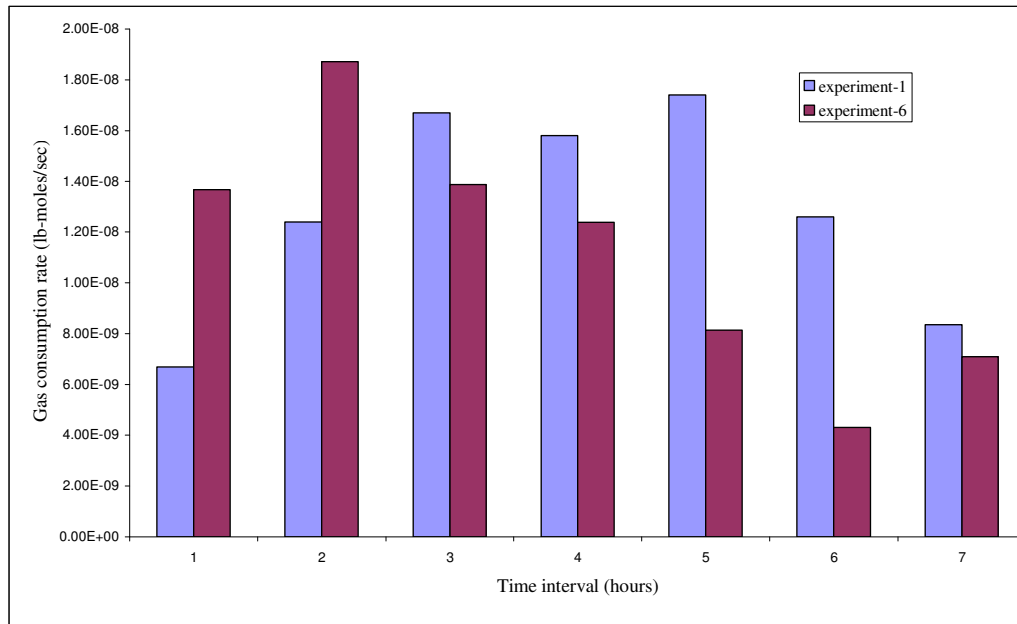


Figure 5.19 Gas consumption rate of Group-4 experiments (except experiment-7)

Although KCl shows an ability of thermodynamic inhibition (reducing the hydrate equilibrium temperature for a given pressure) once hydrate starts to form it promotes hydrate formation kinetically. This observation is based on the initial stage the gas consumption (i.e. gas hydrate formation rate) during higher KCl concentration experiment. It is clear from Figure 5.19 that the hydrate formation rate obtained from the Experiment-6 is almost twice as high as the Experiment-1 values. Nevertheless starting with 3 hour its effect vanishes or and hydration rate slows down which could be the result the covering the gas-liquid interface as a result of very high hydrate formation. It was already mentioned previously that it was not possible to form hydrates in the Experiment-7 so that no discussion was made on this experiment.

5.7 Group-5: Effect of XCD

Group-5 experiments were carried out to study the effect of XCD by changing its concentration as 0.50, 0.75 and 1.00 lb/bbl while keeping the concentration of other components at their minimum (Table 5.16).

Hydrate hysteresis curves of Group-5 experiments are presented in Figure 5.20 and the hydrate formation points obtained from hysteresis curves are given in Table 5.17.

Table 5.16 Components concentration for Group-5 experiments

Component	Experiment-1	Experiment-8	Experiment-9
KCl, (weight %)	7	7	7
PHPA, (lb/bbl)	0.75	0.75	0.75
Pac-LV, (lb/bbl)	2	2	2
Starch, (lb/bbl)	4	4	4
XCD, (lb/bbl)	0.50	0.75	1.00
Poly. glycol, (volume %)	3	3	3

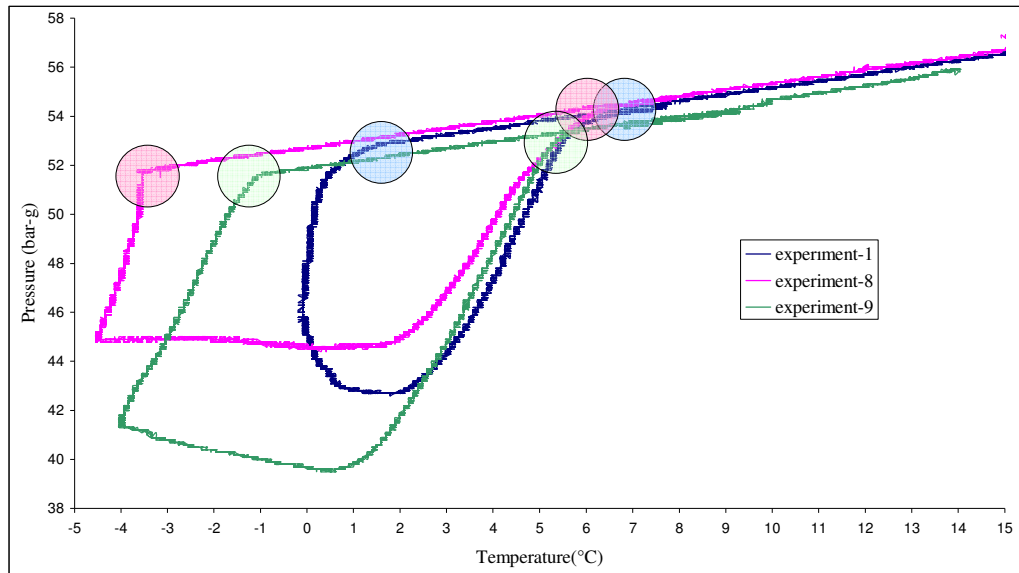


Figure 5.20 Hydrate hysteresis curves for Group-5 experiments

Table 5.17 Data obtained from Hydrate hysteresis curves for Group-5 experiments

	Beginning of hydrate formation, °C	Hydrate equilibrium point, °C
Experiment-1	1.39	6.43
Experiment-8	-3.55	6.13
Experiment-9	0.98	5.54

In the literature XCD is reported as a slight thermodynamic inhibitor, and it is also confirmed by the experimental results of this study. As clearly shown on Figure 5.20 and Table 5.15 that hydrate equilibrium point tends to decrease with increasing concentration of XCD.

Figures 5.21-5.22 and Tables 5.18-5.19 represent the graphical and numerical values in terms of kinetic analysis. Details of the hydrate formation kinetics are represented in Figure 5.22

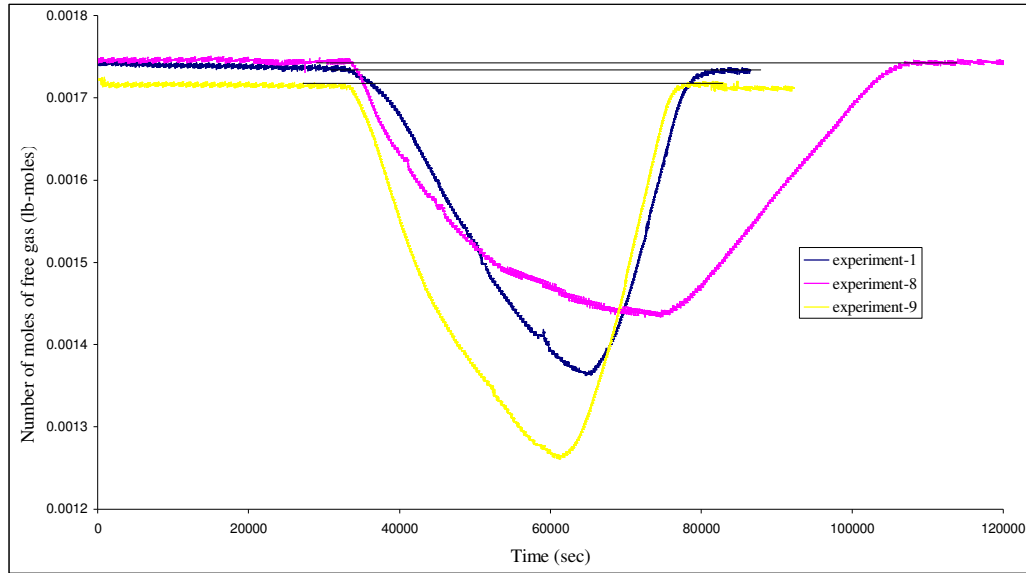


Figure 5.21 Number of moles of free gas vs. time diagrams for Group-5 experiments

Table 5.18 Equations of straight line for each 1hour period for Group-5 Experiments

Time Interval (hours)	Best line equation		
	Experiment-1	Experiment-8	Experiment-9
0-1	$y = -6.68328E-09x + 1.85645E-03$	$y = -1.89910E-08x + 2.12219E-03$	$y = -2.01044E-08x + 2.11140E-03$
1-2	$y = -1.24225E-08x + 1.98563E-03$	$y = -1.71197E-08x + 2.07526E-03$	$y = -2.88821E-08x + 2.30767E-03$
2-3	$y = -1.66685E-08x + 2.09372E-03$	$y = -1.42127E-08x + 2.00443E-03$	$y = -2.42124E-08x + 2.18385E-03$
3-4	$y = -1.58073E-08x + 2.06722E-03$	$y = -1.11650E-08x + 1.91740E-03$	$y = -1.63314E-08x + 1.95094E-03$
4-5	$y = -1.74450E-08x + 2.12651E-03$	$y = -9.14945E-09x + 1.84936E-03$	$y = -1.27435E-08x + 1.83246E-03$
5-6	$y = -1.25884E-08x + 1.94556E-03$	$y = -7.11804E-09x + 1.77521E-03$	$y = -1.26976E-08x + 1.83285E-03$
6-7	$y = -8.36519E-09x + 1.77298E-03$	$y = -2.79759E-09x + 1.60251E-03$	$y = -1.11387E-08x + 1.76903E-03$
7-8	$y = -9.15416E-09x + 1.80535E-03$	$y = -4.07695E-09x + 1.65833E-03$	$y = -5.40247E-09x + 1.51858E-03$

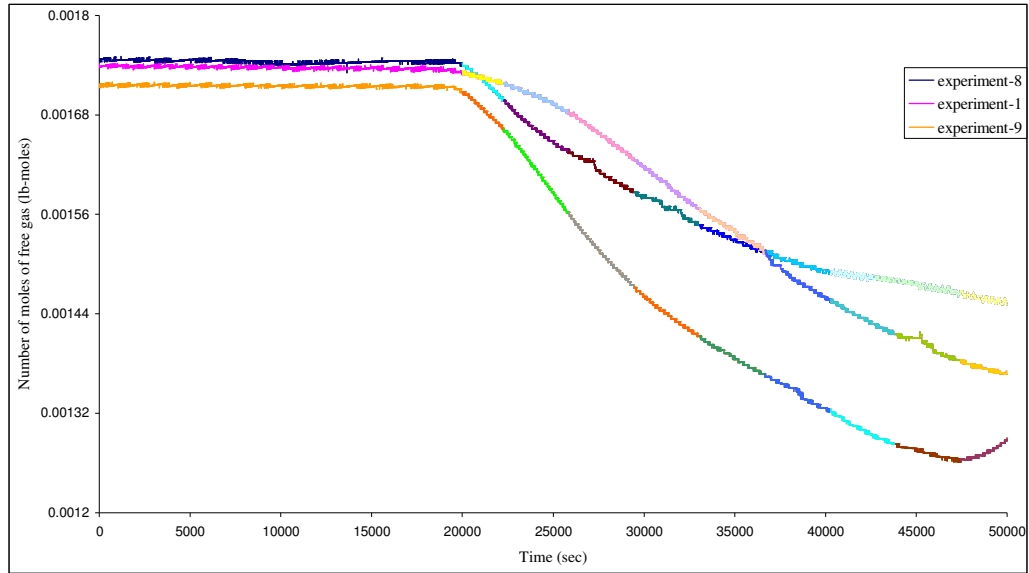


Figure 5.22 Detailed number of moles of free gas vs. time diagram for Group-5 experiments

Table 5.19 Reaction rates for Group-5 Experiments

Time Interval (hours)	Reaction rate (lb-moles/sec)		
	Experiment-1	Experiment-8	Experiment-9
0-1	6.68×10^{-9}	1.90×10^{-8}	2.01×10^{-8}
1-2	1.24×10^{-8}	1.71×10^{-8}	2.89×10^{-8}
2-3	1.67×10^{-8}	1.42×10^{-8}	2.42×10^{-8}
3-4	1.58×10^{-8}	1.12×10^{-8}	1.63×10^{-8}
4-5	1.74×10^{-8}	9.15×10^{-9}	1.27×10^{-8}
5-6	1.26×10^{-8}	7.12×10^{-9}	1.27×10^{-8}
6-7	8.36×10^{-9}	2.80×10^{-9}	1.11×10^{-8}
7-8	9.15×10^{-9}	4.08×10^{-9}	5.40×10^{-9}

Data from Table 5.19 are shown graphically on the histograms on Figure 5.23.

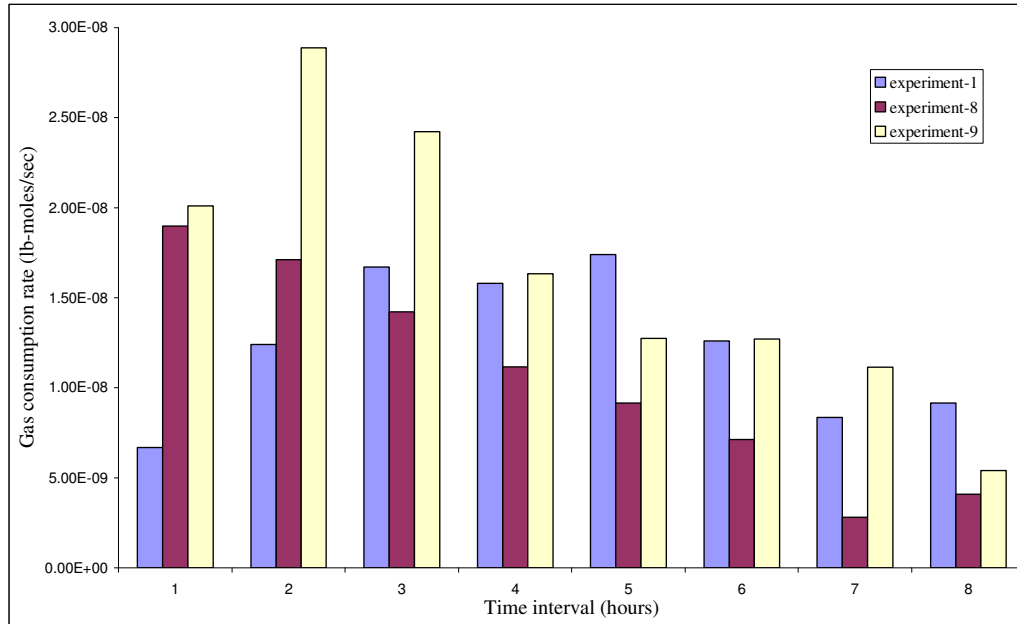


Figure 5.23 Gas consumption rates for Group-5 experiments

Analysis of Figure 5.23 show that XCD acts as a hydrate promoter as its concentration increases.

Starting with the first hour of hydrate formation the rates of experiments with higher XCD concentrations are almost 3 times higher than the base case. This effect continues till the 3rd hour in case of Experiment-8 and 4th hour for Experiment-9. After the 4th hour the hydration rate of Experiment-9 (maximum concentration of XCD) is almost the same as base case. And regarding the fact that for the base case medium period (2-6 hours) corresponds to the maximum rates of gas consumption it means that even after 3 hours of very high hydrate formation, XCD's promoting effect continues. In case of medium concentration of XCD (Experiment-8) the effect of promoting does not last for so long, but with maximum concentration it holds almost till the end.

Other studies involving XCD were performed by Kotkoskie et.al., (1992), water based drilling fluid was tested in the presence of XCD and after removing it totally from the system. As was reported in the paper, the XCD had slight thermodynamic

promoting effect on hydrate formation, besides they emphasized that results were surprising as far as in preliminary works to this study the XCD has shown inhibitive thermodynamic effect on hydrate formation. According to explanation given in the paper, the inhibition capacities of XCD components were suppressed by the other components of drilling fluid, since the preliminary studies were carried out with pure XCD component. The result of our experimental work in spite the fact that we tested the multi-component drilling fluid as well, has shown that with increase in concentration the XCD still acts as the thermodynamic inhibitor, hence its effect is less impressive than KCL.

5.8 Group-6: Effect of Poly. glycol

As all the other components of drilling fluid the effect of poly. glycol on hydrate formation / dissociation was studied by changing its concentration while keeping the others concentrations constant (Table 5.20).

It can be expected for poly. glycol, as any other polymer, to be a kinetic inhibitor and not to be effective in terms of thermodynamic inhibition. In fact, it was found that it actually acts as slight thermodynamic promoter (Figure 5.24 and Table 5.21).

Table 5.20 Components concentration for Group-6 experiments

Component	Experiment-1	Experiment-10	Experiment-11
KCl, (weight %)	7	7	7
PHPA, (lb/bbl)	0.75	0.75	0.75
Pac-LV, (lb/bbl)	2	2	2
Starch, (lb/bbl)	4	4	4
XCD, (lb/bbl)	0.5	0.5	0.5
Poly. glycol, (volume %)	3	4	5

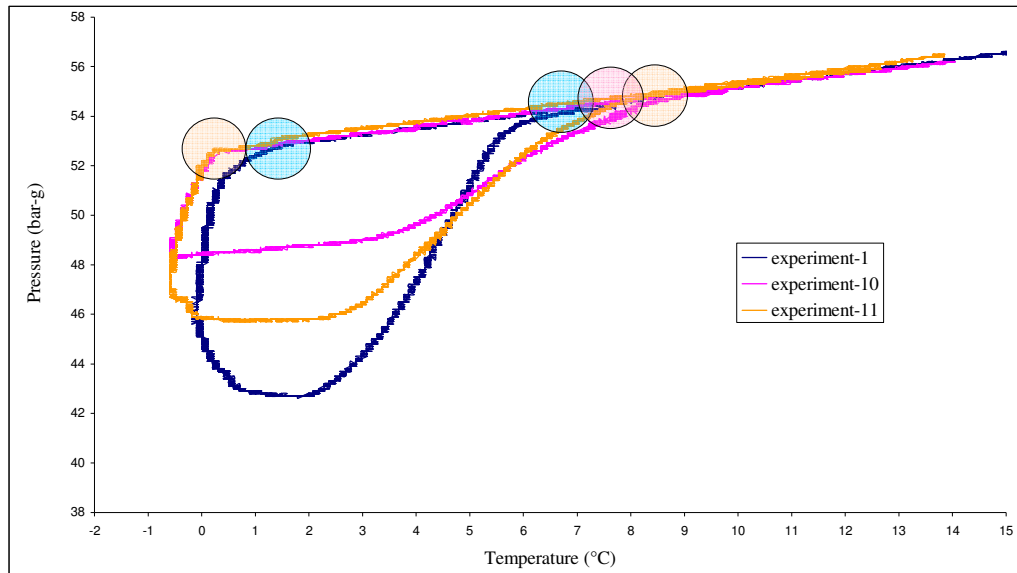


Figure 5.24 Hydrate hysteresis curves for Group-6 experiments

Table-5.21 Data obtained from Hydrate hysteresis curves for Group-6 experiments

	Beginning of hydrate formation, °C	Hydrate equilibrium point, °C
Experiment-1	1.39	6.43
Experiment-10	0.21	8.80
Experiment-11	0.31	8.21

The kinetic analysis for the effect of poly. glycol is presented by Figures 5.25-5.27 and Tables 5.22 - 5.23. The graphical analysis of the data from Table 5.23 is shown in Figure 5.27.

The analysis of Figure 5.27 should be done carefully since the observations do not follow a systematic change with the increase in poly. glycol concentration. Although it was postulated that poly. glycol could be a kinetic inhibitor it exhibits almost 3 times higher hydrate formation rate when its concentration was increased from 3 volume % to 4 volume %. This is somewhat unexpected and could be easily explained. On the other hand, with the highest poly. glycol concentration (5 volume %), there was no big difference in the hydrate formation rate at the initial stage of hydrate formation, but starting with 2nd hour it strongly affected the reaction rate. As

can be noticed from the histograms, its inhibitive effect holds on till the end of hydrate formation.

Previously, Tahir (2001) had already tested effect of poly.glycol on hydrate formation, he made a series of experiments with increasing concentration of poly.glycol in aqueous solution, and polyglycol +KCl . Both groups of experiments were positive in terms of kinetic inhibiting of hydrate formation, besides the pure polyglycol group increased the equilibrium point of hydrate formation, which mean that pure poly.glycol acted as the thermodynamic inhibitor. Our results are consistent in this term with previous study, in terms of kinetic analysis it tend to inhibit only with maximum concentration. That could possible be explained by the effect of other components of drilling fluids and some impurities in drilling fluid used in Experiment-10.

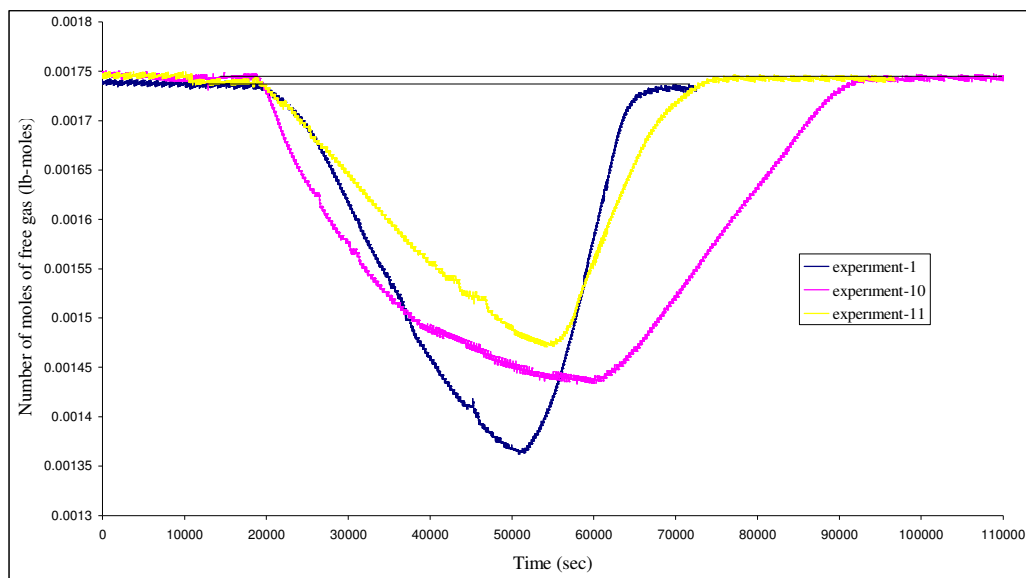


Figure 5.25 Number of moles of free gas vs. time diagram for Group-6 experiments

Table 5.22 Equations of straight line for each 1hour period for Group-6 experiments

Time Interval (hours)	Best line equation		
	Experiment-1	Experiment-10	Experiment-11
0-1	$y = -6.68328E-09x + 1.85645E-03$	$y = -2.16356E-08x + 2.16286E-03$	$y = -8.21040E-09x + 1.89695E-03$
1-2	$y = -1.24225E-08x + 1.98563E-03$	$y = -1.50855E-08x + 2.01408E-03$	$y = -9.86618E-09x + 1.93800E-03$
2-3	$y = -1.66685E-08x + 2.09372E-03$	$y = -1.37380E-08x + 1.98126E-03$	$y = -8.41350E-09x + 1.89962E-03$
3-4	$y = -1.58073E-08x + 2.06722E-03$	$y = -1.18257E-08x + 1.92979E-03$	$y = -9.77319E-09x + 1.93889E-03$
4-5	$y = -1.74450E-08x + 2.12651E-03$	$y = -8.66363E-09x + 1.82581E-03$	$y = -9.23525E-09x + 1.92144E-03$
5-6	$y = -1.25884E-08x + 1.94556E-03$	$y = -6.15941E-09x + 1.73342E-03$	$y = -7.66772E-09x + 1.86294E-03$
6-7	$y = -8.36519E-09x + 1.77298E-03$	$y = -2.99512E-09x + 1.60868E-03$	$y = -6.13600E-09x + 1.80109E-03$
7-8	$y = -9.15416E-09x + 1.80535E-03$	$y = -4.36303E-09x + 1.66814E-03$	$y = -4.58743E-09x + 1.72916E-03$
8-9	$y = -3.31737E-09x + 1.52949E-03$	$y = -3.31028E-09x + 1.61676E-03$	$y = -6.27181E-09x + 1.80223E-03$

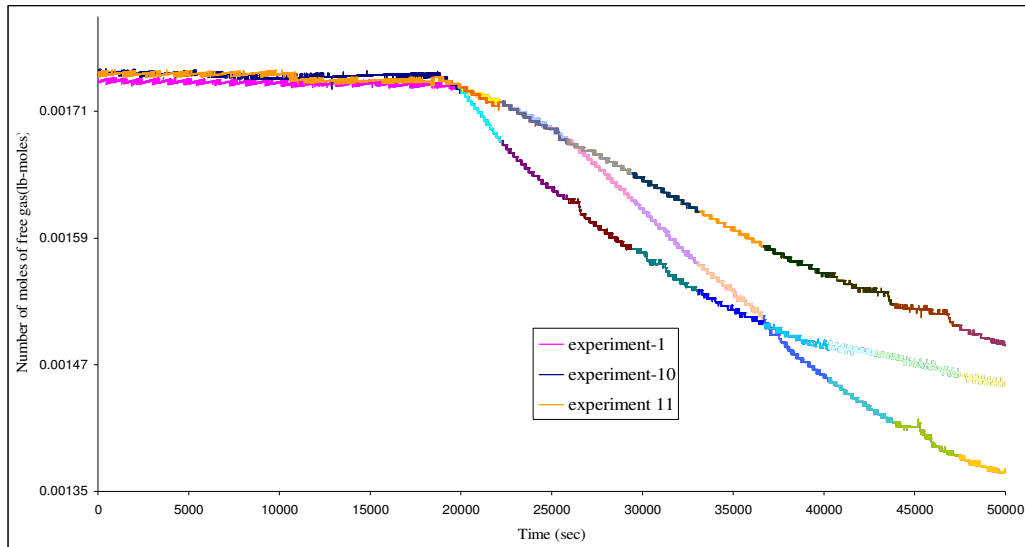


Figure 5.26 Detailed number of moles of free gas vs. time diagram for Group-6 Experiments

Table 5.23 Reaction rate of Group-6 experiments

Time Interval (hours)	Rate of hydrate formation (lb-moles/sec)		
	Experiment-1	Experiment-10	Experiment-11
0-1	6.68×10^{-9}	2.16×10^{-8}	8.21×10^{-9}
1-2	1.24×10^{-8}	1.51×10^{-8}	9.87×10^{-9}
2-3	1.67×10^{-8}	1.37×10^{-8}	8.41×10^{-9}
3-4	1.58×10^{-8}	1.18×10^{-8}	9.77×10^{-9}
4-5	1.74×10^{-8}	8.66×10^{-9}	9.24×10^{-9}
5-6	1.26×10^{-8}	6.16×10^{-9}	7.67×10^{-9}
6-7	8.36×10^{-9}	3.00×10^{-9}	6.14×10^{-9}
7-8	9.15×10^{-9}	4.36×10^{-9}	4.59×10^{-9}
8-9	3.32×10^{-9}	3.31×10^{-9}	6.27×10^{-9}

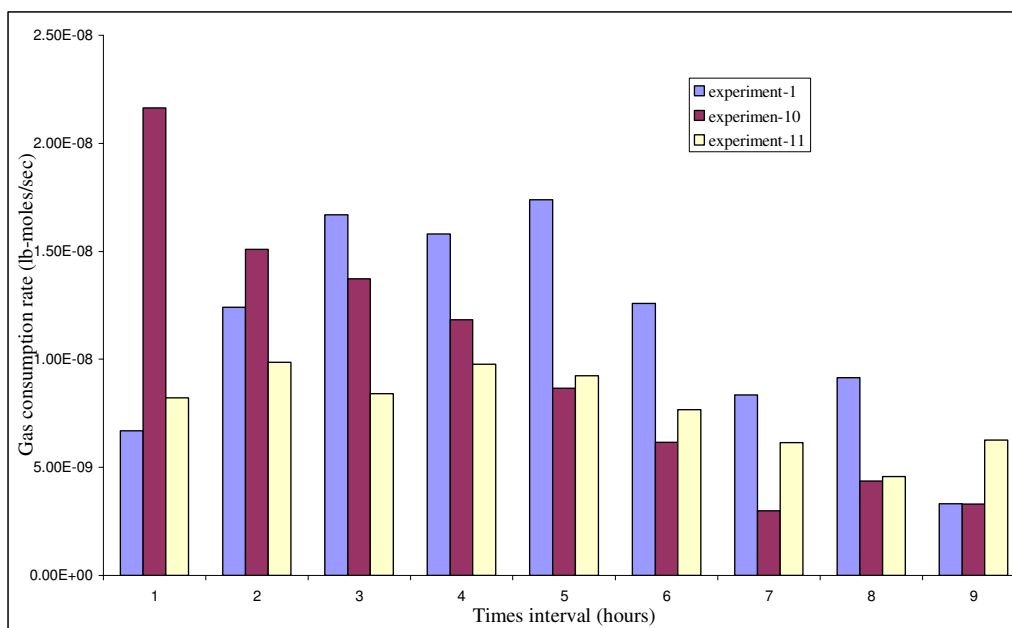


Figure 5.27 Gas consumption rates for Group-6 experiments

CHAPTER 6

CONCLUSIONS

The following conclusions can be drawn from the experimental results of this study:

- Among the all components of drilling fluid, tested for their hydrate inhibiting potentials, poly. glycol and PHPA do not exhibit any thermodynamic inhibition capacity while KCl and XCD has an ability of hydrate inhibition thermodynamically.
- XCD has weaker thermodynamic inhibition characteristics than KCl, it slightly changes the thermodynamic equilibria, while at increasing concentrations of KCl the hydrate equilibrium point shift significantly.
- On the contrary all the PHPA and poly. glycol tend to promote hydrate formation thermodynamically.
- The temperature conditions of hydrate formation in the increasing concentrations of Poly. glycol higher than PHPA, which means that poly. glycol is stronger thermodynamic promoter of hydrate formation than PHPA.
- Poly. glycol which should inhibit methane hydrate formation kinetically, have shown negative results with medium concentration, however with the highest poly. glycol concentration in drilling fluid the rate of hydrate formation slows down.

CHAPTER 7

RECOMMENDATIONS

Under the light of the results of current study, the followings are recommended for further studies:

- Performance of poly. glycol with more samples of varying concentration can be studied.
- Other components of drilling fluids (bentonite, barite, etc.), should be studied on the purpose of determination their influence on hydrate formation conditions and new experiments should be carried out.
- Methyl-ethyl glycol, a known hydrate inhibitor, can be tested to compare the effectiveness of poly. glycol-KCl system as hydrate inhibitor.
- The drilling fluids of the same chemical composition could be tested in dynamic conditions, that are more close to the real case.

REFERENCES

Barker J.W., Gomez R.K., (1987): "Formation of Hydrates During Deepwater Drilling Operations", paper SPE/IADC 16130, SPE/IADC Drilling Conference, New Orleans, March 15-18.

Baker Petrolite, 2006: "About HI-M-PACT: Thermodynamic Hydrate Inhibitors". Available from: <http://www.bakerhughes.com/bakerpetrolite/oilgas/him pact.htm> (accessed on 13 June 2007)

Carroll J. J., (2003) Natural Gas Hydrates: A Guide for Engineers Gulf Professional Publishing, Amsterdam, The Netherlands

Cha S.B. (1988): "A Third Surface Effect on Hydrate Formation" J. Phys. Chem., 92 #23, 6492-94

Dickens, GR; Paull CK, Wallace P (1997). "Direct measurement of in situ methane quantities in a large gas-hydrate reservoir". *Nature* 385 (6615): 426-428.

Ebeltoft H., Yousif M., Soergaard E., (1997): "Hydrate Control during Deep Water Drilling: Overview and New Drilling Fluids Formulations", paper SPE 38567, SPE Annual Technical Conference and Exhibition, Texas, 5-8 October.

Fadnes, F.H., Jakobsen, T., Bylov, M., Holset, A., Downs, J.D. (1998): "Studies on the Prevention of Gas Hydrate Formation in Pipelines Using Potassium Formate as a Thermodynamic Inhibitor", paper SPE 50688, Proc. of the 1998 SPE European Petroleum Conference, The Hague, The Netherlands, 22-22 October, pp. 497-506.

Fu B., Neff S., Mathur A., Bakeev K., (2001): "Novel Low Dosage Hydrate Inhibitors for Deepwater Operations", paper SPE 71472, SPE Annual Technical Conference and Exhibition, New Orleans, 30 September-3 October.

Frostman L.M., (2000): "Anti- Agglomerate Hydrate Inhibitors for Prevention of Hydrate Plugs in Deepwater Systems", paper SPE 63122, Proc. of the SPE Annual Technical Conference and Exhibition, Dallas, Texas, 1-4 October, pp. 1-7.

Frostman L.M., (2003): "Low- Dosage Hydrate Inhibitors (LDHIs): Reducing Costs in Existing System and Designing for the Future", paper SPE 80269, Proc. of the SPE International Symposium on Oilfield Chemistry, Houston, Texas, 5-8 February, pp. 1-7. Problems in Hydrates: Mechanisms and Elimination Methods

Hale A.H., Dewan A.K.R., (1990): "Inhibition of Gas Hydrates in Deep water Drilling", SPEDE June-1990, pp.109-55

- Halliday, W., Dennis, K., Clapper, Smalling, M., (1998): “ New Gas Hydrate Inhibitors for Deepwater Drilling Fluids”, paper SPE 39316, Proc. of the 1998 IADC/SPE Drilling Conference, Dallas, Texas 3-6 March, pp. 201-211.
- Hammerschmidt, E.G. (1934): “Formation of Gas Hydrates in Natural Gas Transmission Lines”, *Ind. & Eng. Chem.* (1934) 26, 851.
- Howard, S. K., (1995): “Formate Brine for Drilling and Completion State of the Art”, paper SPE 30498, Proc. of the SPE Annual Technical Conference and Exhibition, Dallas, U.S.A. 22-25 October, pp.483-496.
- Istomi V.A., Kvon V.G. (2004) *Gas Production: Prevention and Elimination of Gas Hydrates*, Irte. Gas. Prom.: Moscow.
- Kelland M.A., Svartaas T.M. and Dybvik L., (1995) “Studies on New Gas Hydrate Inhibitors”, paper SPE 30420, Proc. of the SPE Offshore Europe Conference, Aberdeen, 5-8 September, pp.531-539.
- Kotkoskle T.S., Basil Al Ubaldi, Wildeman T.R., Sloan Jr. E.D., (1992): “Inhibition of Gas Hydrates in Water-Based Drilling Muds”, paper SPE 20432, SPE Drilling Engineering.
- Kvenvolden, K. (1995). "A review of the geochemistry of methane in natural gas hydrate". *Organic Geochemistry* 23 (11-12): 997-1008.
- Lai D.T., Dzialowski A.K., (1989): “Investigation of Natural Gas Hydrates in Various Drilling Fluids”, paper SPE/IADC 18637, SPE/IADC Drilling Conference, Orleans, February 28-March 3.
- Lederhos, J.P., (1996).: “Effective Kinetic Inhibitors for Natural Gas Hydrates,” *Chemical Engineering Science*, (1996) v.51, n.8, 1221.
- Makogon Y.F., (1997): *Hydrates of Hydrocarbons*, Penn Well Publishing Company, Tulsa, Oklahoma 74101, Chapters 1-3-4-5. 45
- Makogon Y.F., Makogon T.Y., Holditch S.A. (1999): “Gas Hydrate Formation and Dissociation with Thermodynamic and Kinetic Inhibitors”, paper SPE 56568, SPE Annual Technical Conference and Exhibition held in Houston, 3-6 October.
- Milkov, AV (2004). "Global estimates of hydrate-bound gas in marine sediments: how much is really out there?". *Earth-Sci Rev* 66 (3-4): 183-197.
- Ouar, H. (1992).: “The Formation of Natural Gas Hydrates in Water-Based Drilling Fluids,” *J. Chem. Eng*, January -992 70, Part A.
- Pakulski M. (1997): “High Efficiency Non-Polymeric Gas Hydrate Inhibitors”, paper SPE 37285, SPE International Symposium on Oilfield Chemistry, Houston, 18-21 February.
- Paez J. E., Blok R., Vaziri H., Islam M.R. (2001): “Problems in Hydrates: Mechanisms and Elimination Methods” paper SPE 67322, Proc. of the SPE Production Operations Symposium, Oklahoma City, Oklahoma, 26-28 March 2001. pp. 1-9

- Parlaktuna M. (1991): “Physical Properties of Natural Gases, Computer Program and Subroutines” University of Trondheim, The Norwegian Institute of Technology
- Product Bulletin, (2003): “Glydril®MC”, M-I L.L.C A Smith/Schlumberger Company, Available from <http://www.midf.com>. (accessed 05 May 2007)
- Product Bulletin, (1996): “POLY-PLUS RD”, M-I Drilling Fluids L.L.C. Available from http://www.miswaco.com/Publications/Water-Base_Fluids/index.cfm (accessed 05 May 2007)
- Product Bulletin, (2004) “TRUZAN”, Petrochem Performance Chemicals Limited LLC Available from: <http://www.ppc.ae/english/products/visco08.asp> (accessed 05 May 2007)
- Quigley, M.S. and Hubbard, J.C., (1990), : “Gas Hydrates Formation in Drilling Fluids,” presented at the 1990 Drilling Managers Technical Meeting at Mobil Research and Development Corp., Dallas Research Laboratory (1990).
- Rabinovich V.A., Havin Z.Y. (1977) Brief Handbook of Chemistry, Himiya.: Leningrad.
- Sloan E. D., Jr. (1990) Clathrate hydrates of natural gases. Second edition, Marcel Dekker Inc.:New York.
- Sloan, E. D., (2000) Hydrate Engineering, Richardson, Texas, Society of Petroleum Engineers.
- Swanson T.A., Petrie M., Sifferman T.R., (2005): “the Successful Use of Both Kinetic and Paraffin Inhibitors Together in a Deepwater Pipeline with a High Water Cut in the Gulf of Mexico”, paper SPE-93158, Proc. of the SPE International Symposium on Oilfield Chemistry, Houston, Texas, 2-4 February, pp. 1-10.
- Tahir A.N. (2005): “Effect of Poly. glycols on Hydrate Formation During Drilling Operations”, M.Sc. Thesis, Middle East Technical University.
- Von Stackelberg, M. & Müller, H. M. (1954) *Zeitschrift für Elektrochemie* 58, 1, 16, 83

APPENDIX A

REAGENTS

GLYDRIL MC poly. glycol is a medium-cloud-point additive designed for medium-to-high salinity poly. glycol systems. It can provide improved well bore stability, lubricity, high-temperature filtration control, plus reduce dilution rates and bit balling. While poly. glycols are most effective when used in conjunction with an inhibitive salt, such as KCl, in a non-dispersed polymer system, they can be used as additives in most water-base systems. **GLYDRIL MC** Poly. glycol is acceptable-for most applications specifying low-toxicity additives.

Typical Physical Properties

Physical appearance	Straw yellow to opaque, brown liquid
Specific gravity	1.012
Solubility in water	Variable
Flash point	230°F (110°C)

Applications

GLYDRIL MC Product has application in poly. glycol systems in fresh-to-medium high salinity make-up water and can be used in wells with moderate formation temperatures. When used properly, this medium-cloud-point additive helps to stabilize troublesome shales by plugging shale pores, preventing the equalization of hydrostatic pressure away from the wellbore.

Poly. glycol systems are generally low-to-medium density, non-dispersed polymer systems utilizing an electrolyte to activate the cloud point poly. glycol. They have application where troublesome water-sensitive shales are to be drilled, and can be used in lieu of oil-base systems for certain applications. GLYDRIL MC Poly. glycol can be used in thermally activated mud emulsion (TAME) applications (near the cloud point) or in situations where it is insoluble (above the cloud point). Normal concentrations of GLYDRIL MC Poly. glycol range from 2 to 5% by volume of the liquid phase or 7 to 17.5 lb/bbl (20 to 50 kg/m³) (Product Bulletin, 2003).

POLY-PLUS RD polymer (PHPA) is a readily dispersible product designed to provide cuttings encapsulation and shale stabilization. It is formulated for easy mixing with improved dispersion to eliminate “fish-eyes.” This is beneficial when rapidly mixing either large quantities or high concentrations of polymer or where good mixing equipment is unavailable.

POLY-PLUS RD also acts as a viscosifier, friction reducer, flocculant, and provides some fluid-loss control. POLY-PLUS RD is a specially treated, high-molecular-weight acrylic copolymer (PHPA). It can be used in mud systems ranging from low-solids to weighted muds, utilizing makeup waters from fresh to saltwater.

Physical appearance	White, granular powder
Specific gravity	1.25 – 1.40
PH (1% solution)	7.7

Bulk density	40 – 46 lb/ft ³ (641 – 737 kg/m ³)
Nature of charge	Anionic
Activity	>90%

POLY-PLUS RD provides cuttings encapsulation and improved wellbore stability. Typical concentrations of POLY-PLUS RD are 0.25 to 1 lb/bbl (0.71 to 2.85 kg/m³). It is effective in salt muds such as KCl or NaCl-enhanced fluids, although slightly higher concentrations of POLY-PLUS RD may be required. The polymer also provides cuttings encapsulation and improved wellbore stability. This system is frequently used in slimhole continuous-coring applications. (Product Bulletin, 1996)

TRUZAN (XCD) is a polysaccharide (xanthan gum) used to viscosify water based drilling and completion fluids.

Features and Benefits

TRUZAN provides excellent suspension properties restricting the settlement of weighting agents and drilled cuttings. It is shear thinning and promotes low bit viscosity needed to maximize penetration rates, and high annular viscosity to ensure effective hole cleaning. TRUZAN is stable over a wide pH range and is effective in saturated brines as well as fresh and sea water base drilling fluids.

TRUZAN is non-damaging to formations and can be removed effectively by acids and oxidants.

Application

TRUZAN is used in drilling and completion fluids to enhance their rheology, ensuring efficient hole cleaning and effective suspension properties.

The effective concentration of TRUZAN required will depend upon the base fluid being treated. Treatment levels are normally in the range of 0.25–1.5 lbs/bbl (0.7–4.3 kgs/m³) (Product Bulletin, 2004).

Physical appearance	cream color free flowing powder
pH (1% solution)	6 – 8
Bulk Density	650–800 kg/m ³

POTASSIUM CHLORIDE (KCl)

The chemical compound **potassium chloride** (KCl) is a metal halide composed of potassium and chlorine. In its pure state it is odorless. It has a white or colorless vitreous crystal, with a crystal structure that cleaves easily in three directions. Potassium chloride crystals are either simple cubic or face-centered cubic depending on what atoms are involved. If only potassium or chlorine atoms are considered, then the structure is face-centered cubic. However, both atoms form a crystal with a simple cubic structure: x-ray diffraction analysis will yield a simple cubic structure. Potassium chloride is also commonly known as "Muriate of Potash". KCl is used in medicine, scientific applications, food processing and in judicial execution through lethal injection. It occurs naturally as the mineral sylvite and in combination with sodium chloride as sylvinite. Potassium chloride has a crystalline structure like many other salts. Structure: face-centered cubic. Lattice Constant: roughly 6.3 angstroms. In chemistry and physics it is a very commonly used as a standard, for example as a calibration standard solution in measuring electrical conductivity of (ionic) solutions, since carefully prepared KCl solutions has well-reproducible and well-repeatable measurable properties. Potassium chloride can react as a source of chloride ion. (Rabinovich V., 1997)

APPENDIX B

TEMPERATURE AND PRESSURE VS. TIME DIAGRAM OF ALL EXPERIMENTS

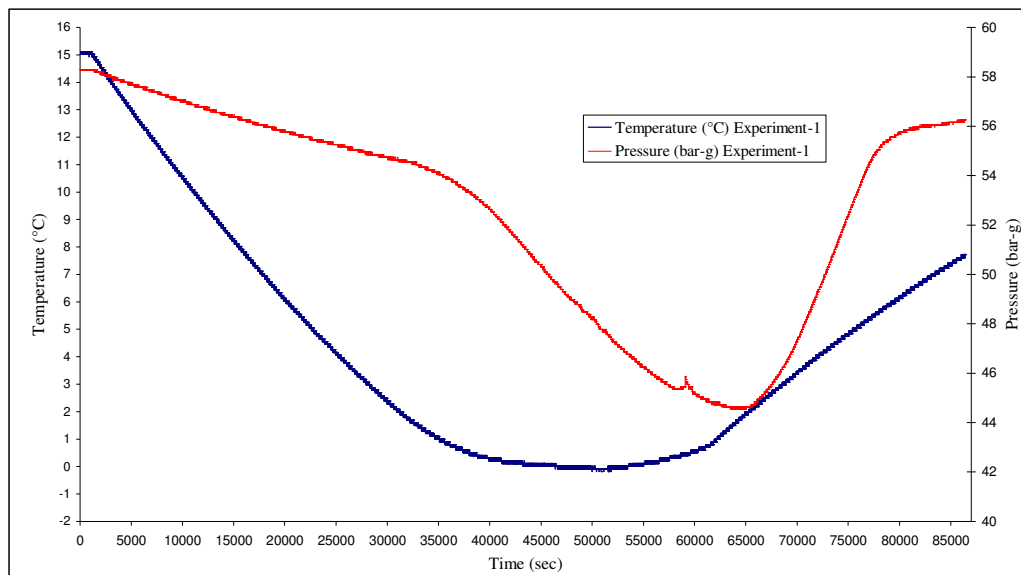


Figure-B.1. Temperature and pressure vs. time diagram (Experiment-1).

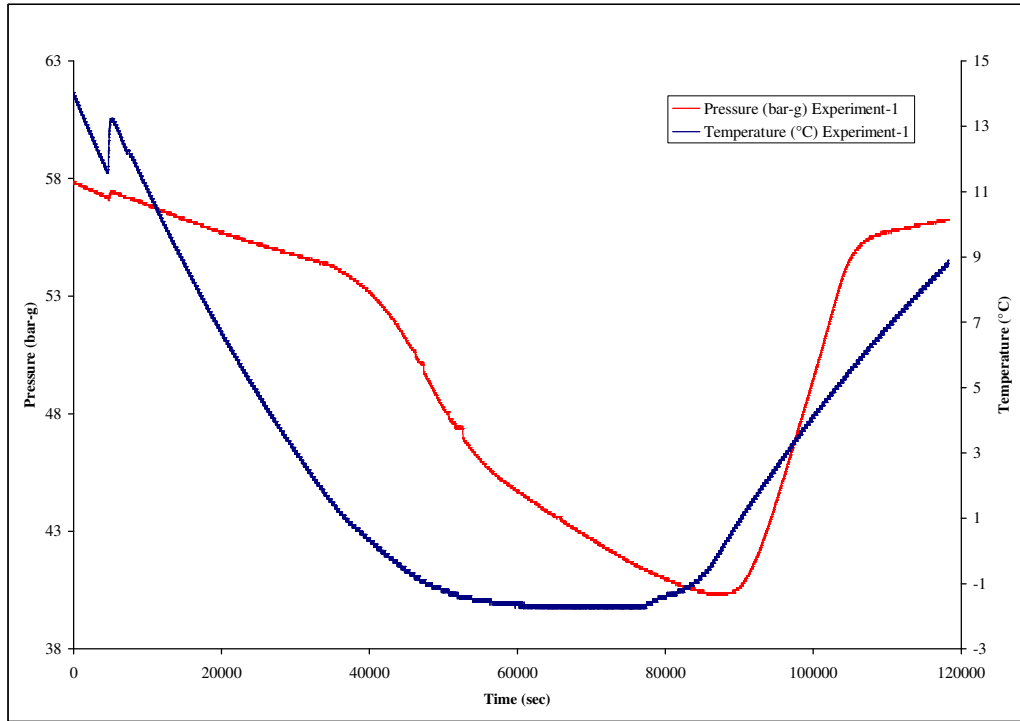


Figure-B.2. Temperature and pressure vs. time diagram (repeatability test).

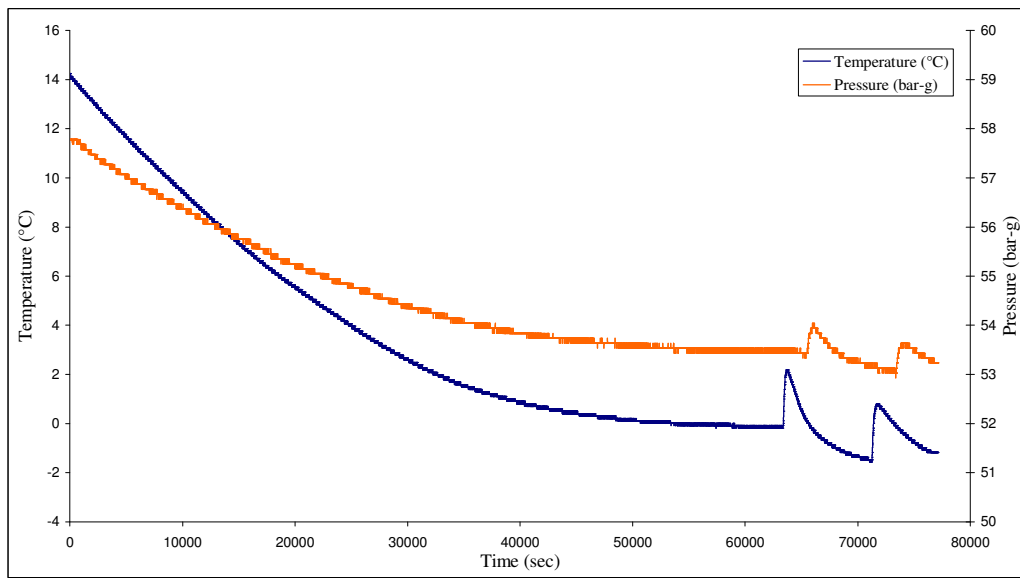


Figure-B.3. Temperature and pressure vs. time diagram (Experiment-2).

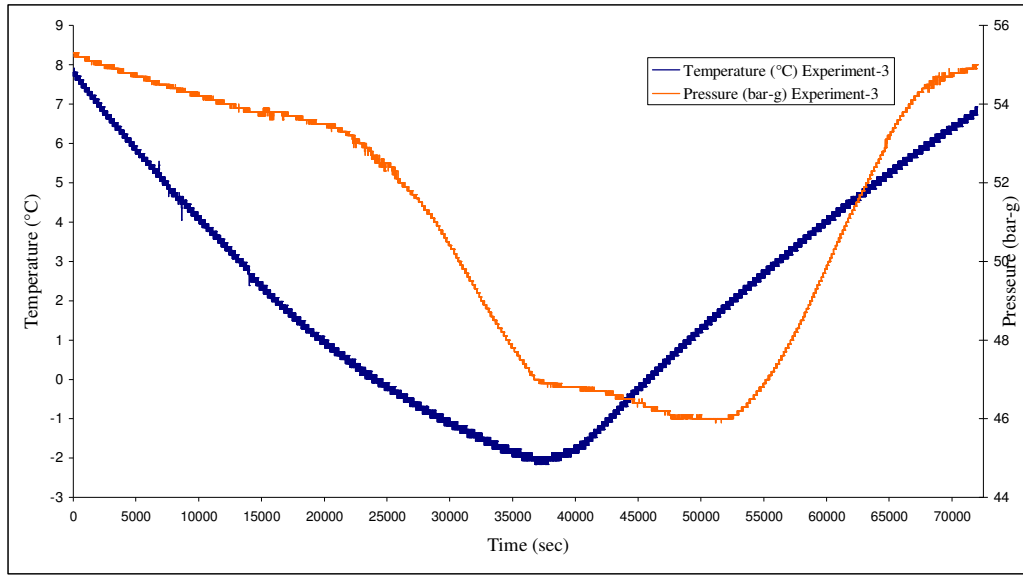


Figure-B.4. Temperature and pressure vs. time diagram (Experiment-3).

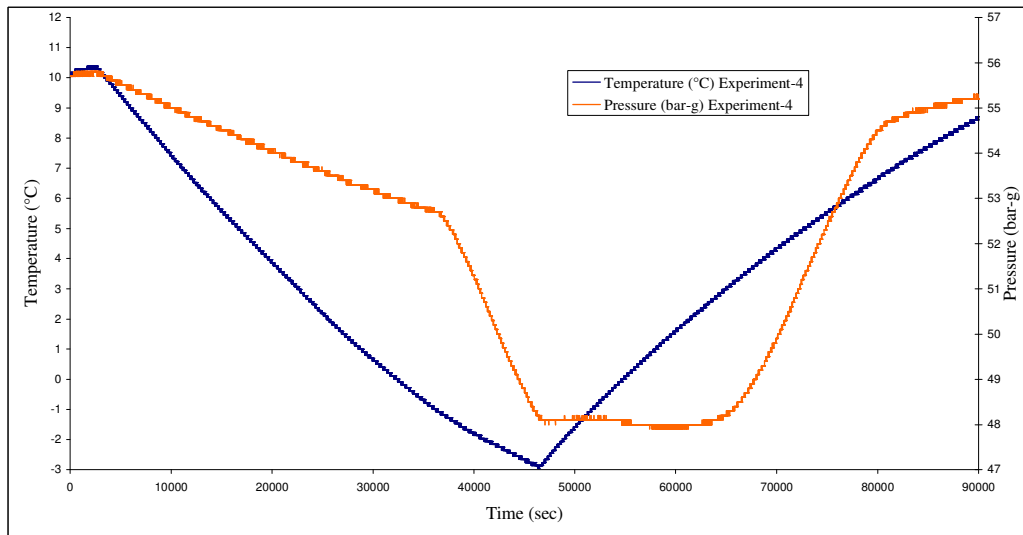


Figure-B.5. Temperature and pressure vs. time diagram (Experiment-4).

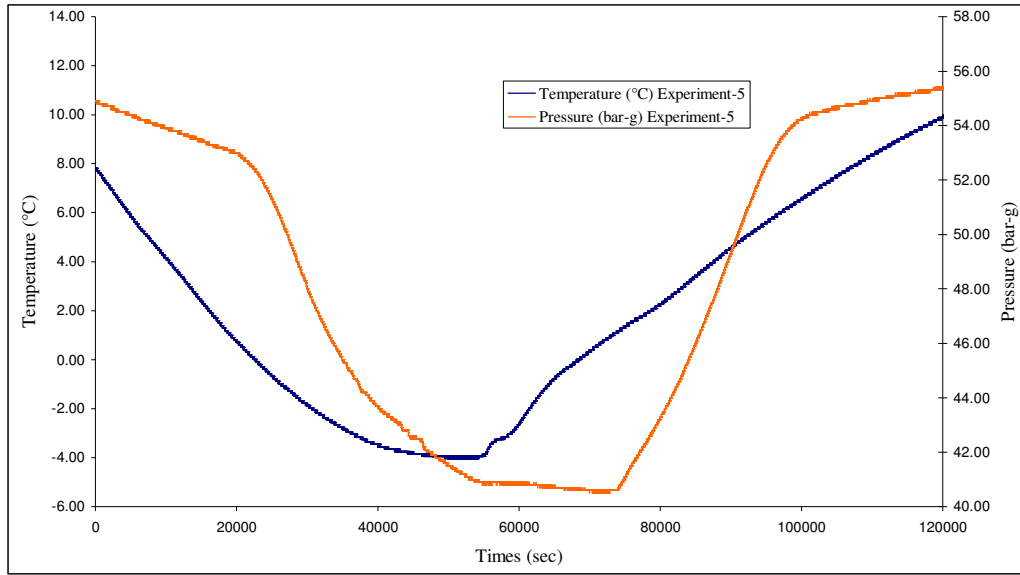


Figure-B.6. Temperature and pressure vs. time diagram (Experiment-5).

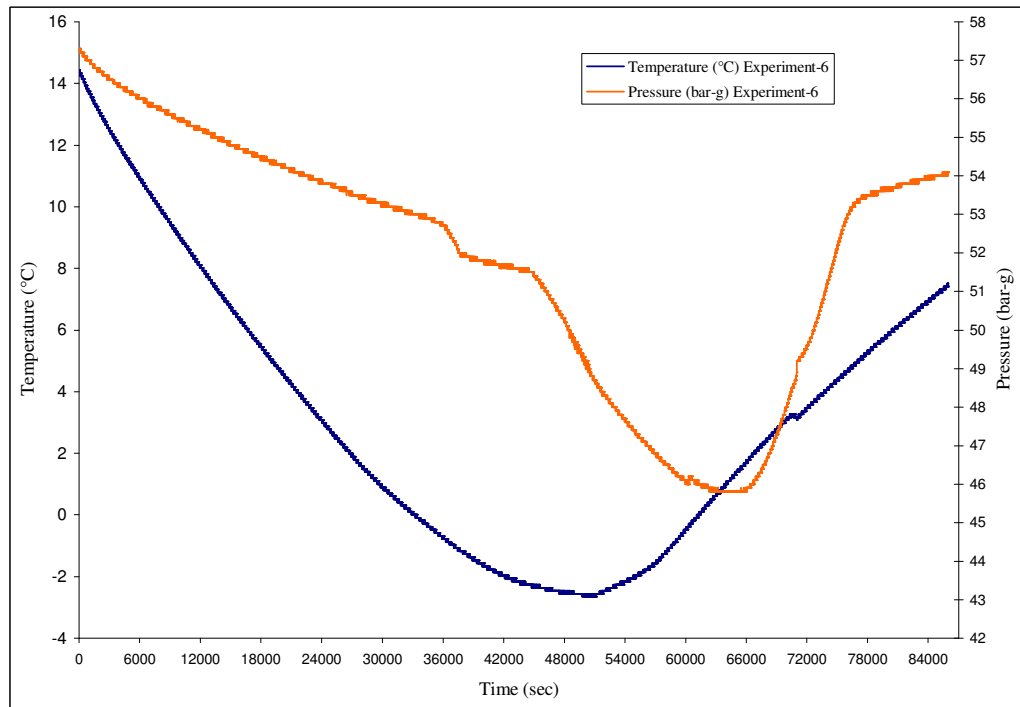


Figure-B.7. Temperature and pressure vs. time diagram (Experiment-6).

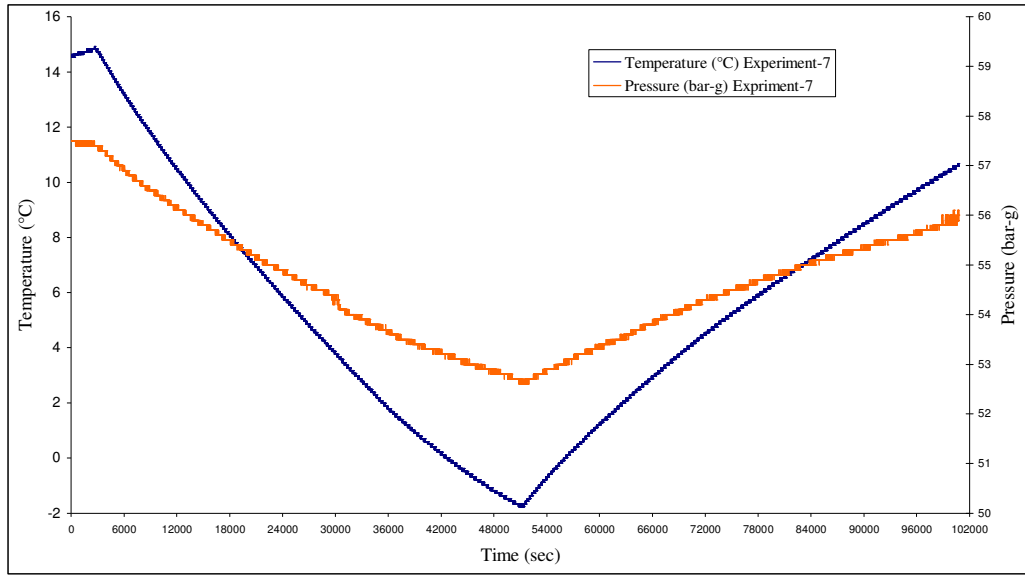


Figure-B.8. Temperature and pressure vs. time diagram (Experiment-7).

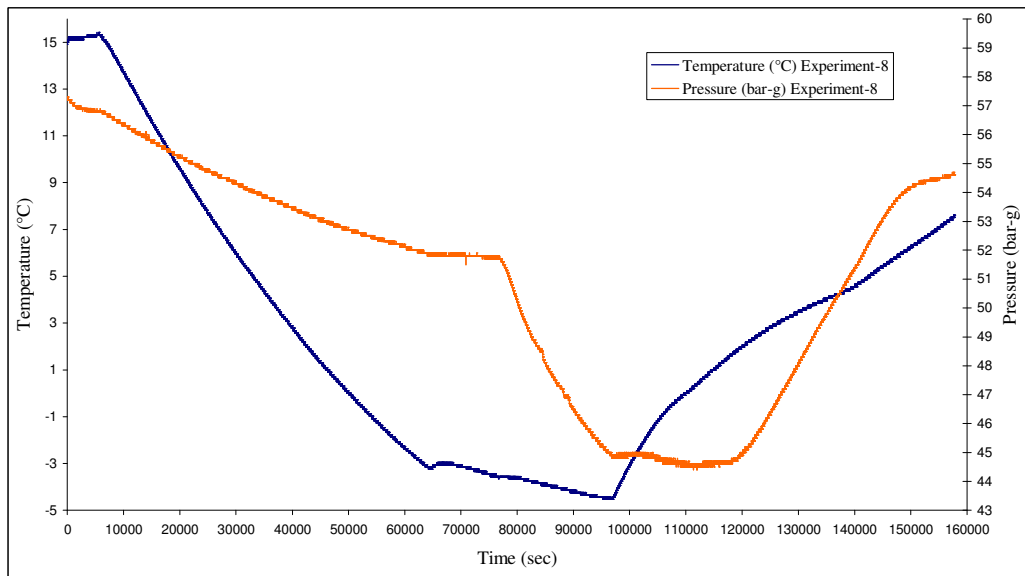


Figure-B.9. Temperature and pressure vs. time diagram (Experiment-8).

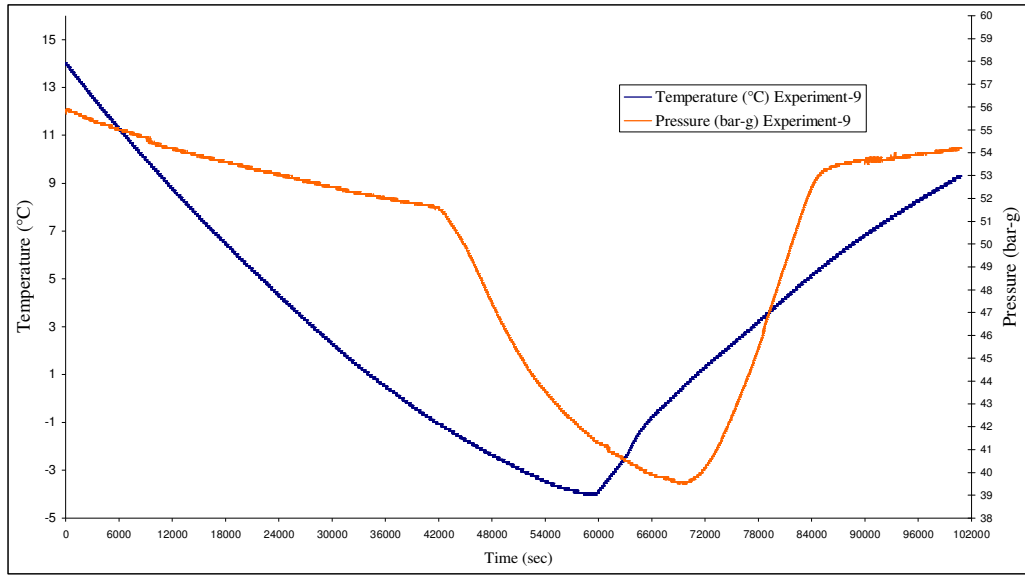


Figure-B.10 Temperature and pressure vs. time diagram (Experiment-9).

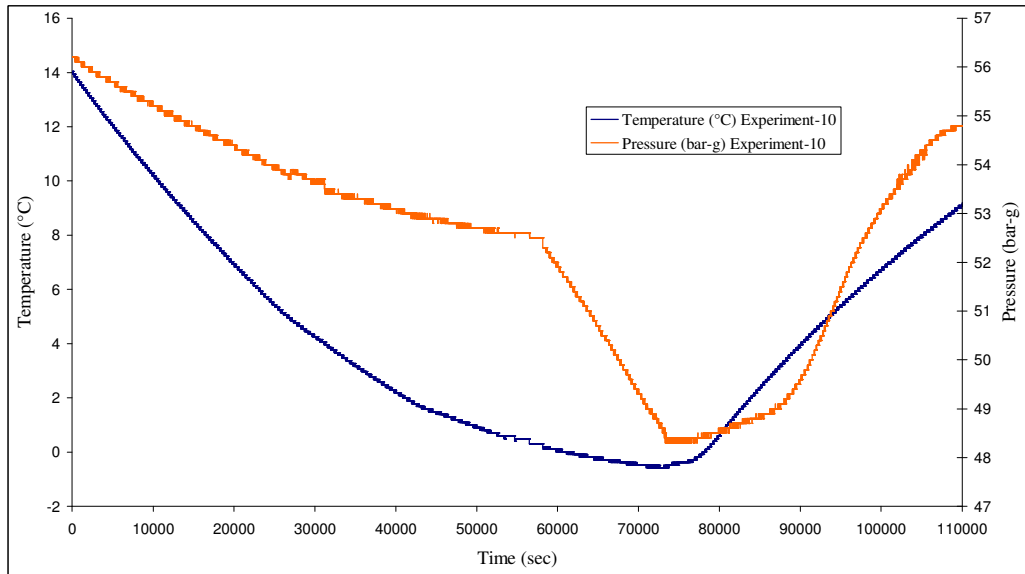


Figure-B.11 Temperature and pressure vs. time diagram (Experiment-10).

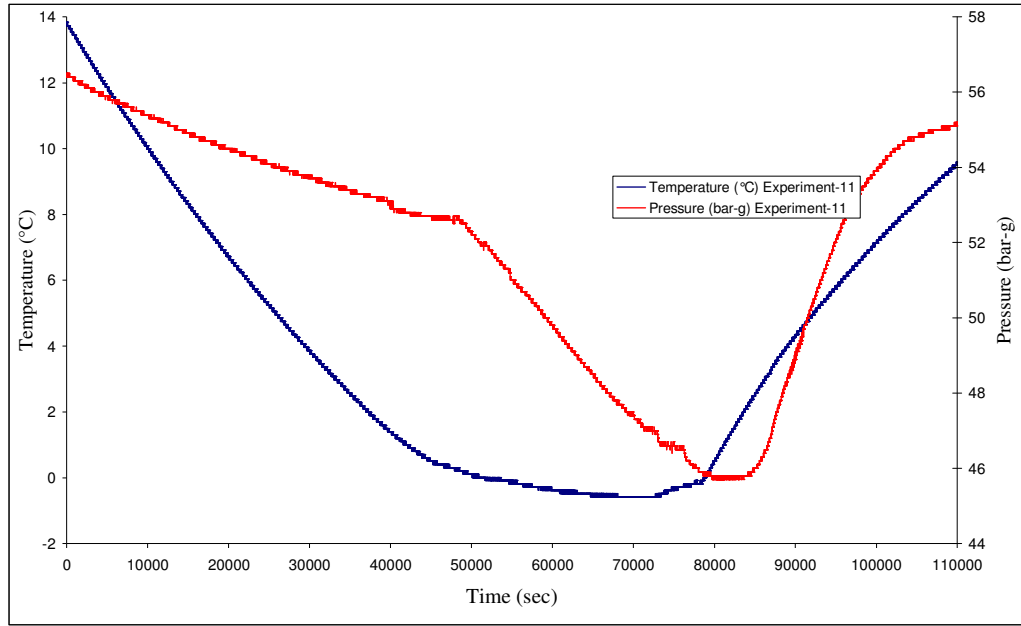


Figure-B.12 Temperature and pressure vs. time diagram (Experiment-11).

APPENDIX C

HYDRATE HYSTERESIS CURVES OF ALL EXPERIMENTS

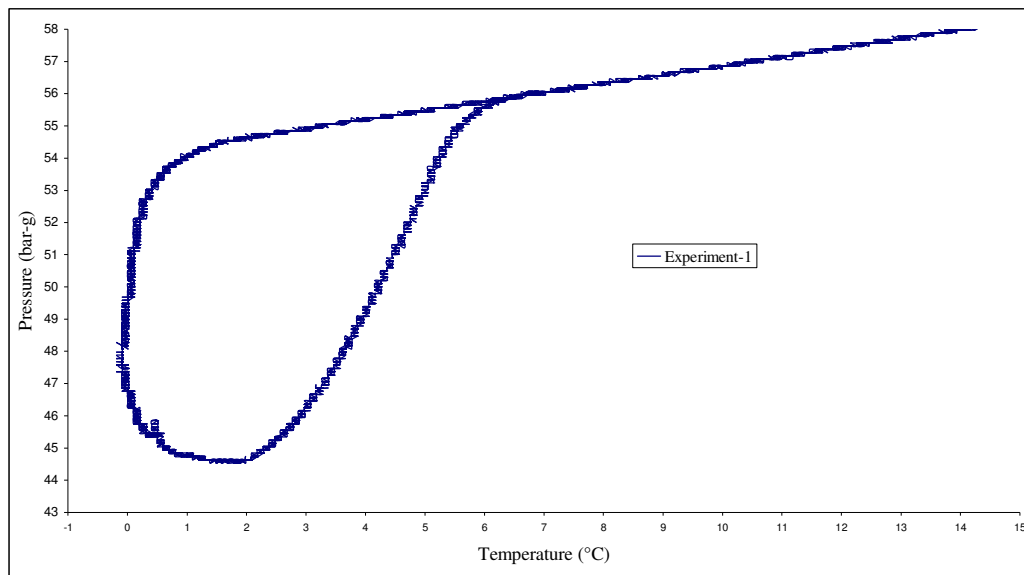


Figure-C.1. Hydrate hysteresis curve (Experiment -1).

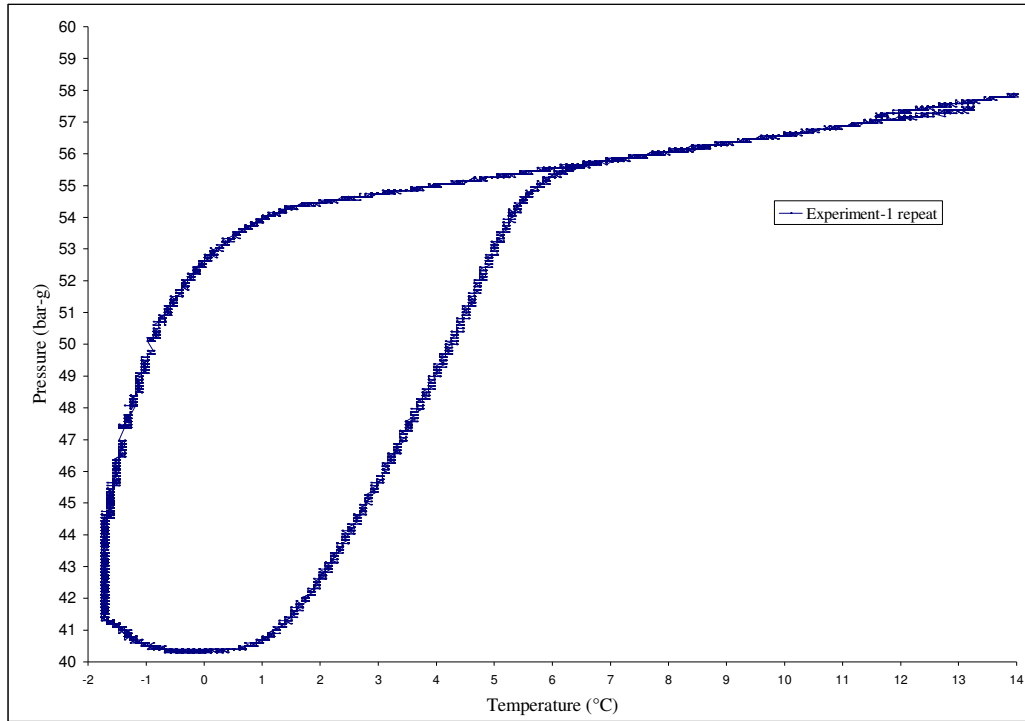


Figure-C.2. Hydrate hysteresis curve (Experiment -1 repeatability test).

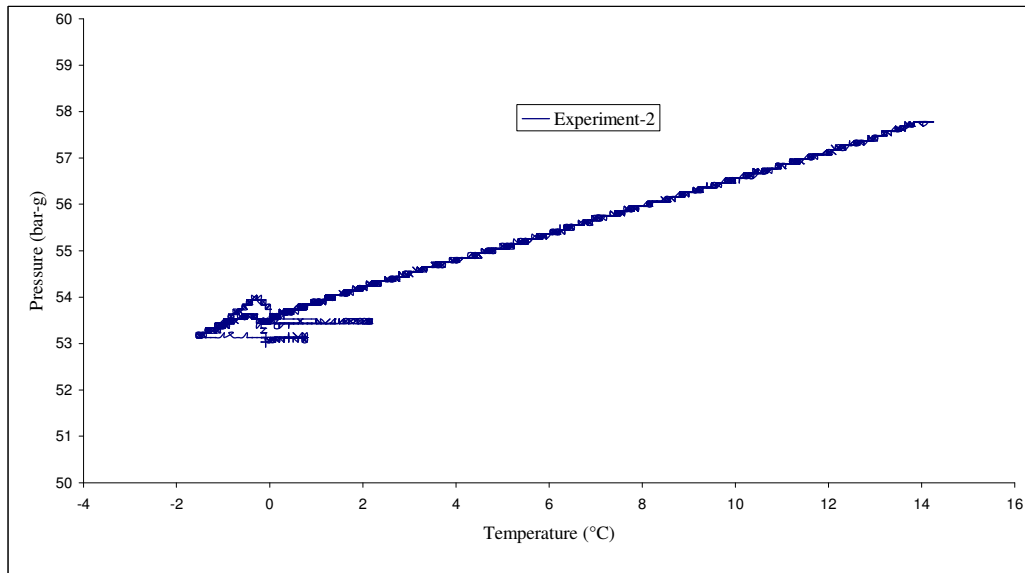


Figure-C.3. Pressure vs. Temperature diagram (Experiment -2).

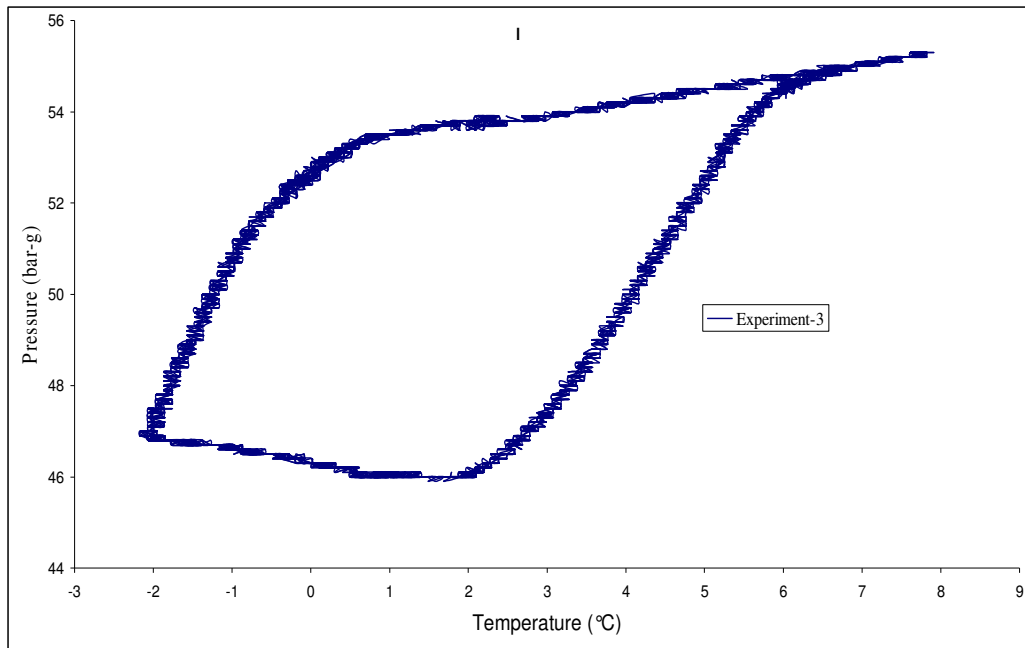


Figure-C.4. Hydrate hysteresis curve (Experiment -3).

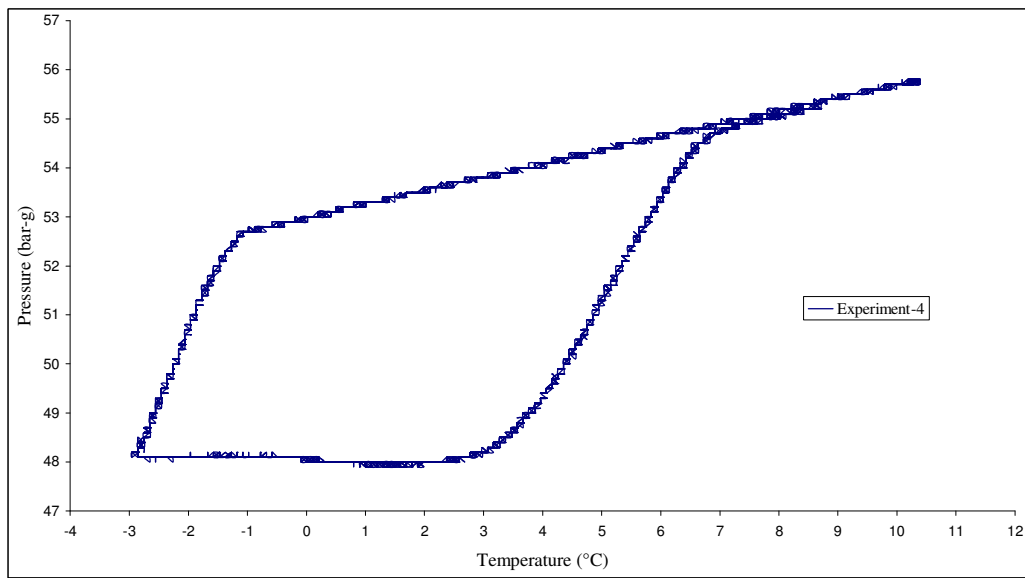


Figure-C.5. Hydrate hysteresis curve (Experiment -4).

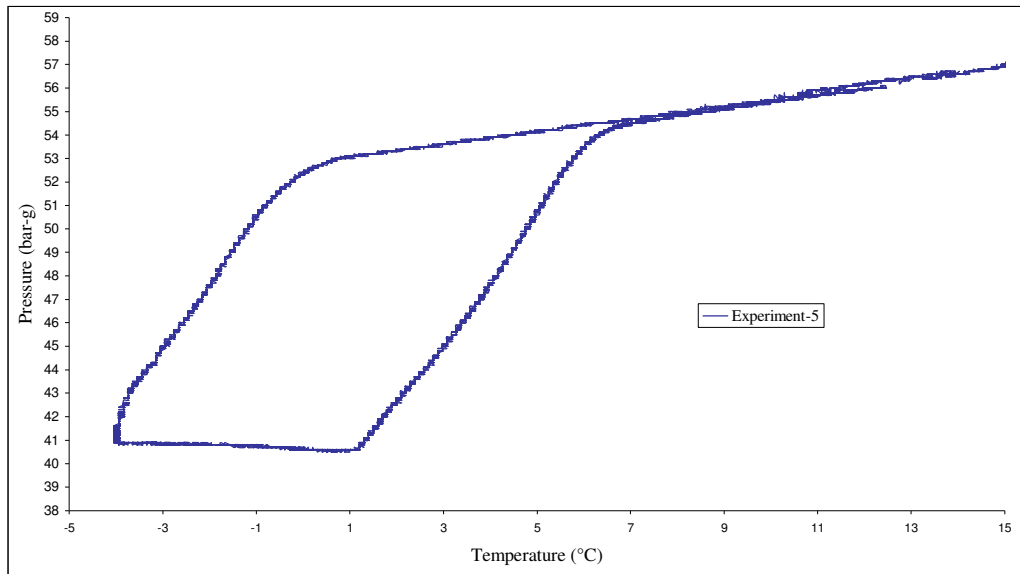


Figure-C.6. Hydrate hysteresis curve (Experiment -5).

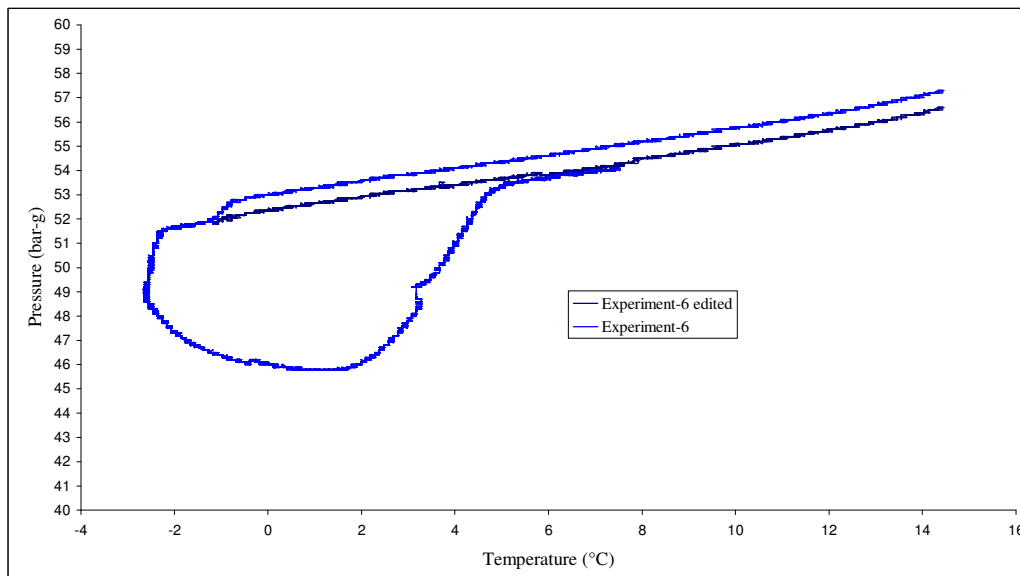


Figure-C.7. Hydrate hysteresis curve (Experiment -6).

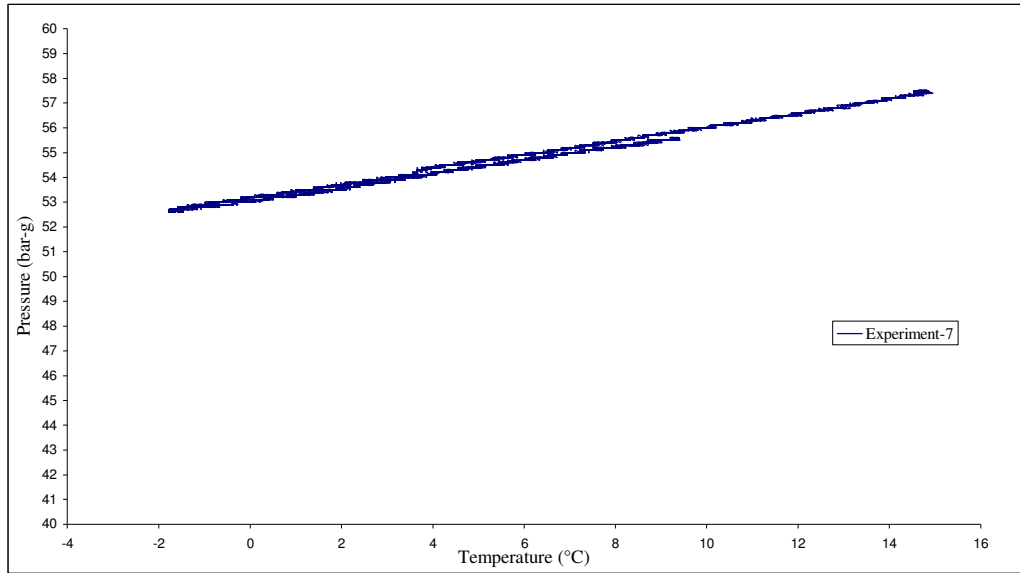


Figure-C.8. Pressure vs. Temperature diagram (Experiment -7).

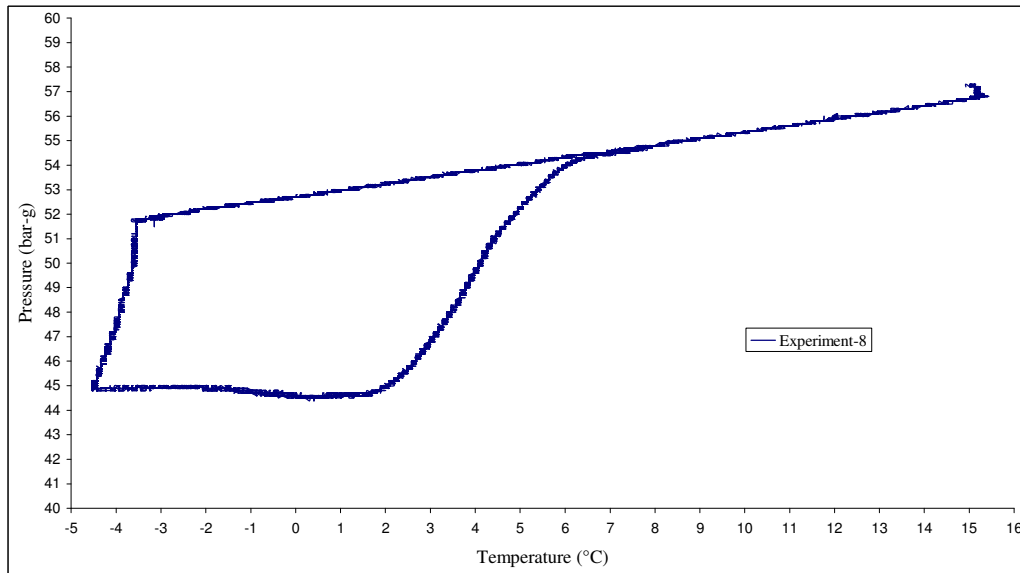


Figure-C.9. Hydrate hysteresis curve (Experiment -8).

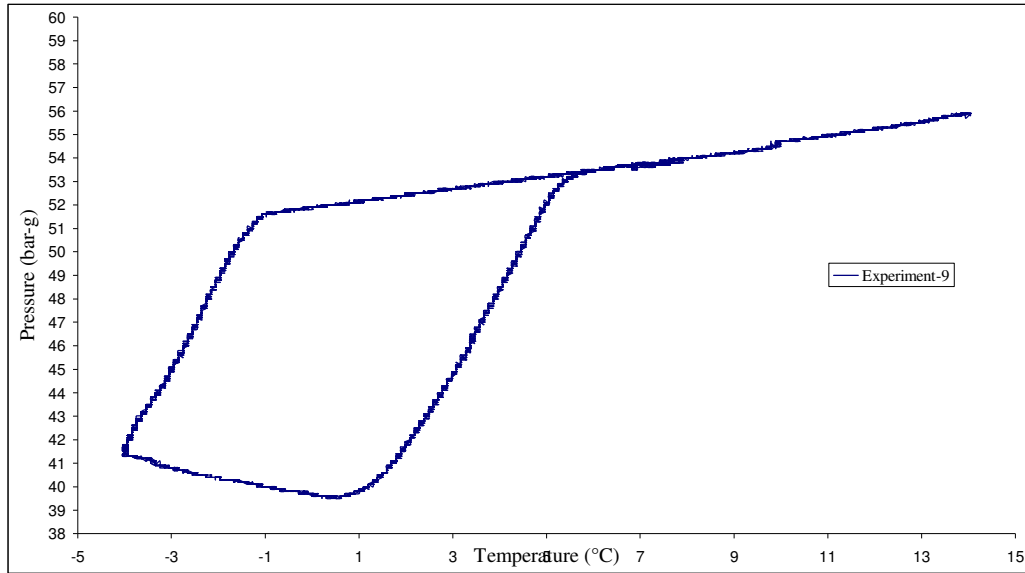


Figure-C.10. Hydrate hysteresis curve (Experiment -9).

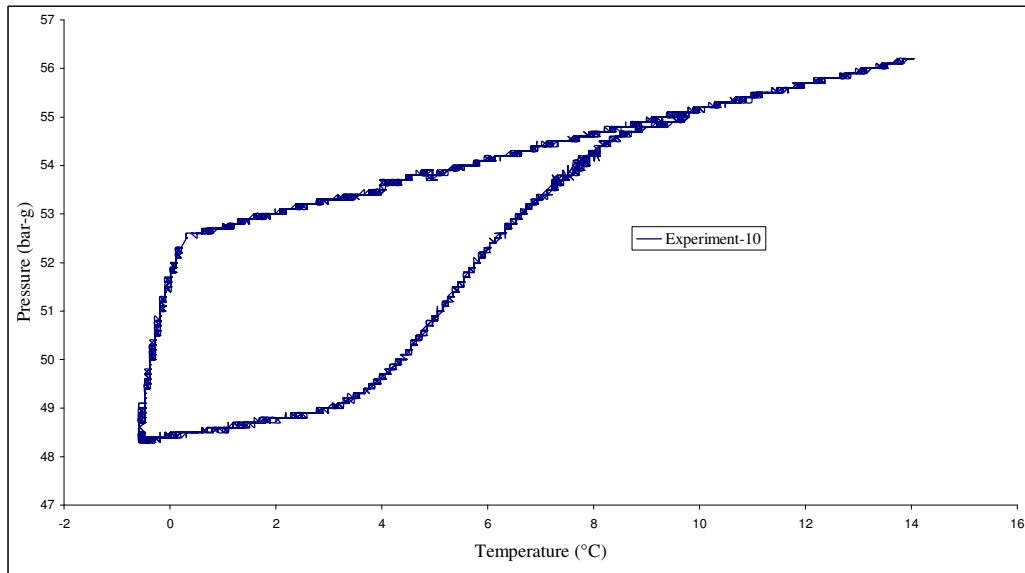


Figure-C.11. Hydrate hysteresis curve (Experiment -10).

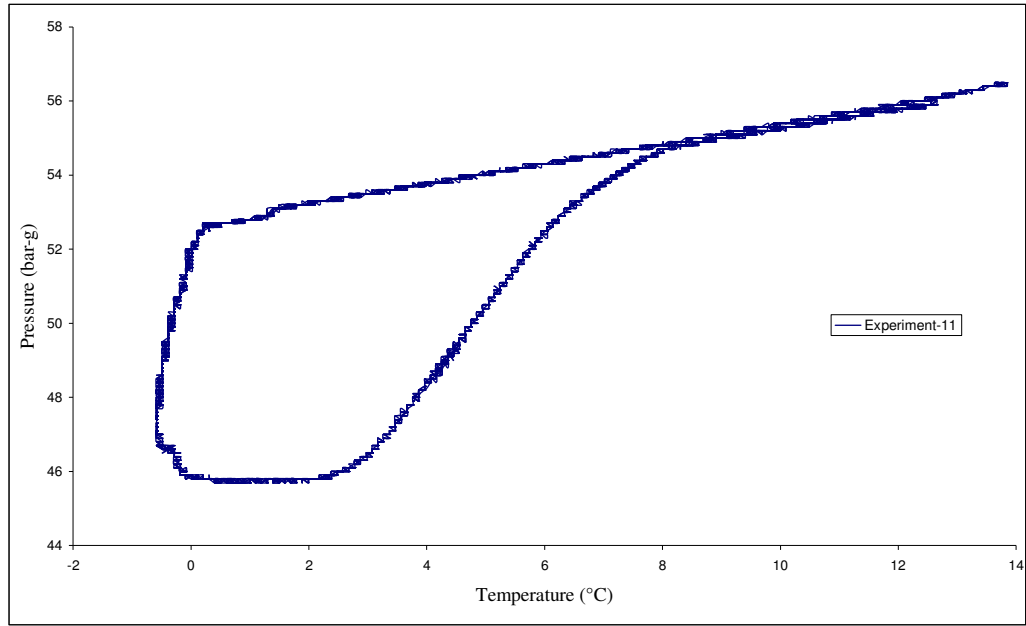


Figure-C.12. Hydrate hysteresis curve (Experiment -11).

APPENDIX D

NUMBER OF MOLES OF FREE GAS VERSUS TIME DIAGRAM

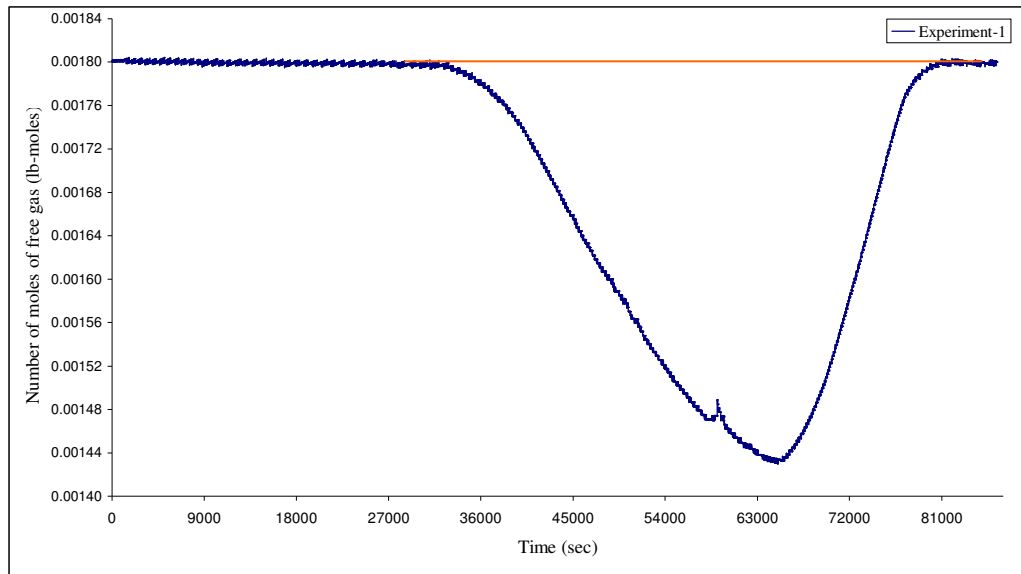


Figure-D.1 Number of moles of free gas vs. time diagram (Experiment-1)

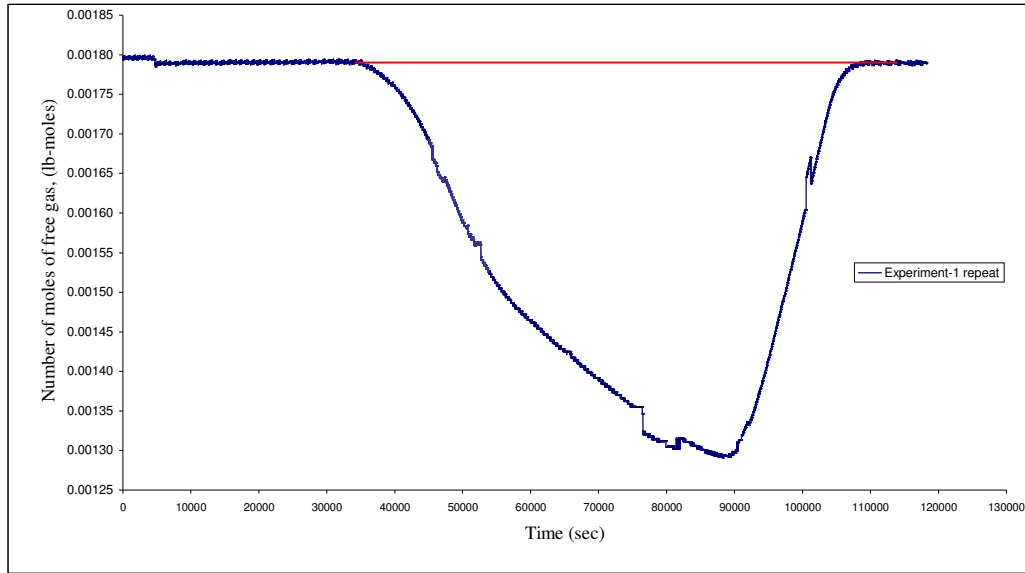


Figure-D.2 Number of moles of free gas vs. time diagram (Experiment-1 repeatability test)

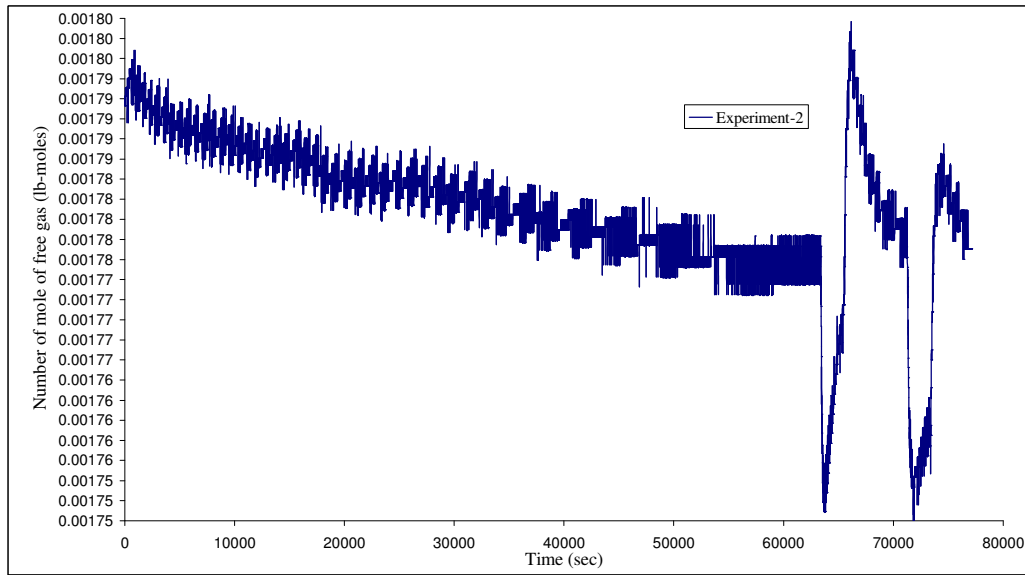


Figure-D.3 Number of moles of free gas vs. time diagram (Experiment-2 failed)

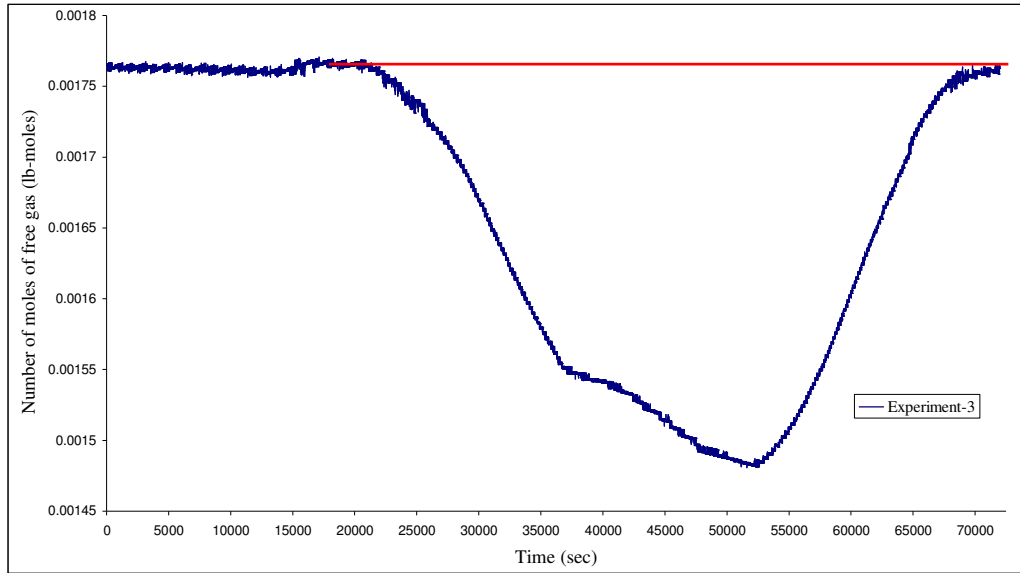


Figure-D.4 Number of moles of free gas vs. time diagram (Experiment-3)

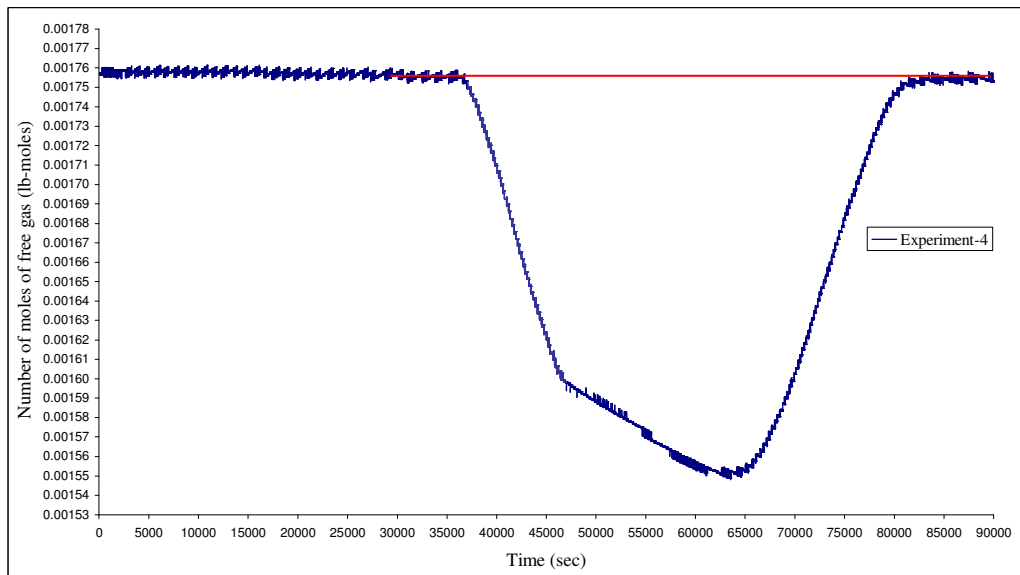


Figure-D.5 Number of moles of free gas vs. time diagram (Experiment-4)

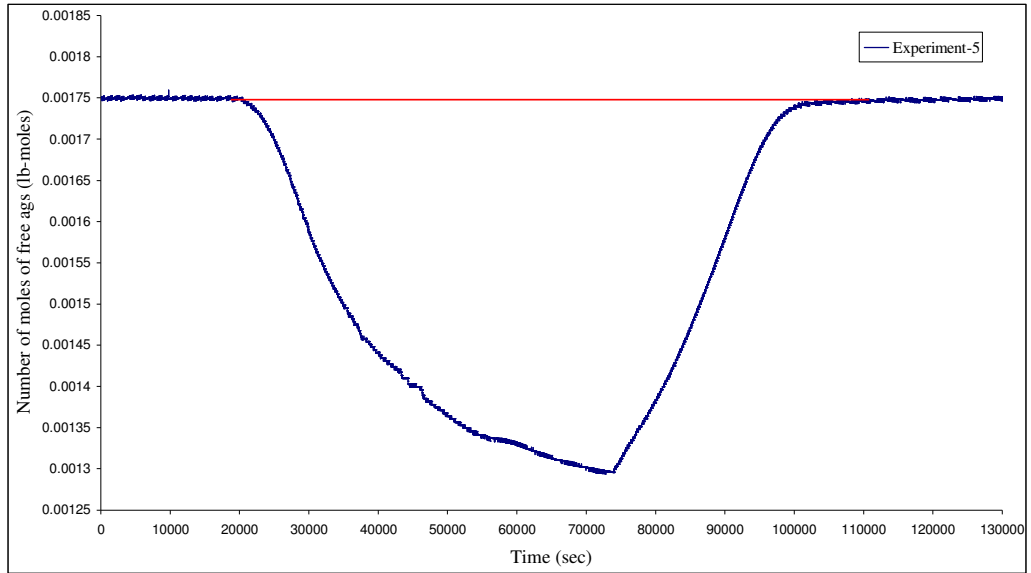


Figure-D.6 Number of moles of free gas vs. time diagram (Experiment-5)

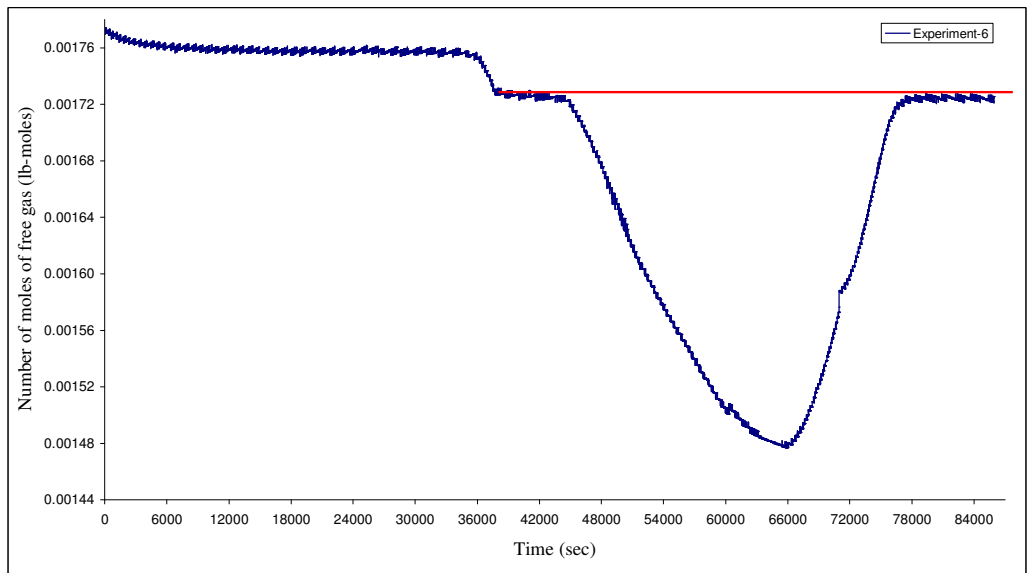


Figure-D.7 Number of moles of free gas vs. time diagram (Experiment-6)

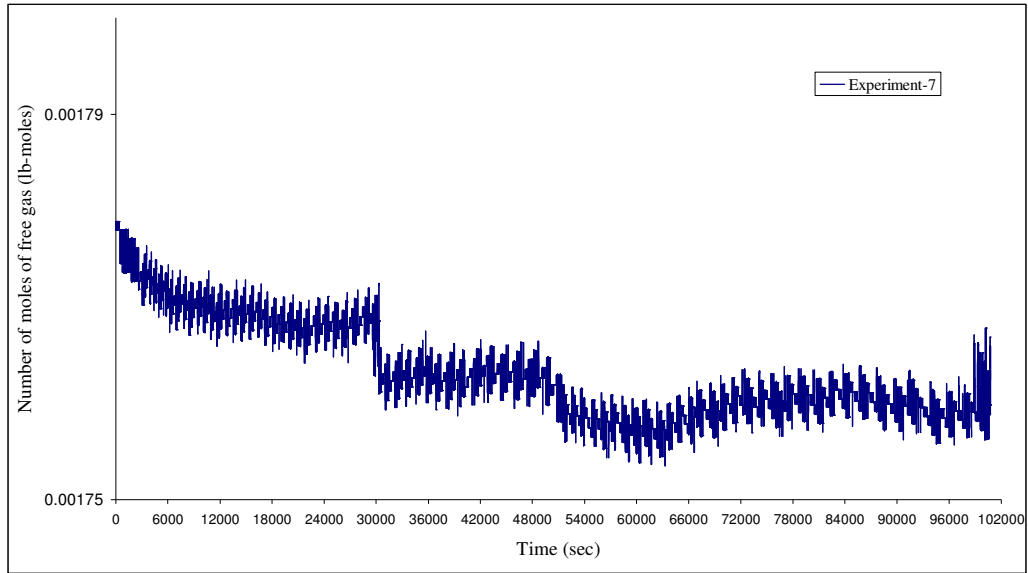


Figure-D.8 Number of moles of free gas vs. time diagram (Experiment-7)

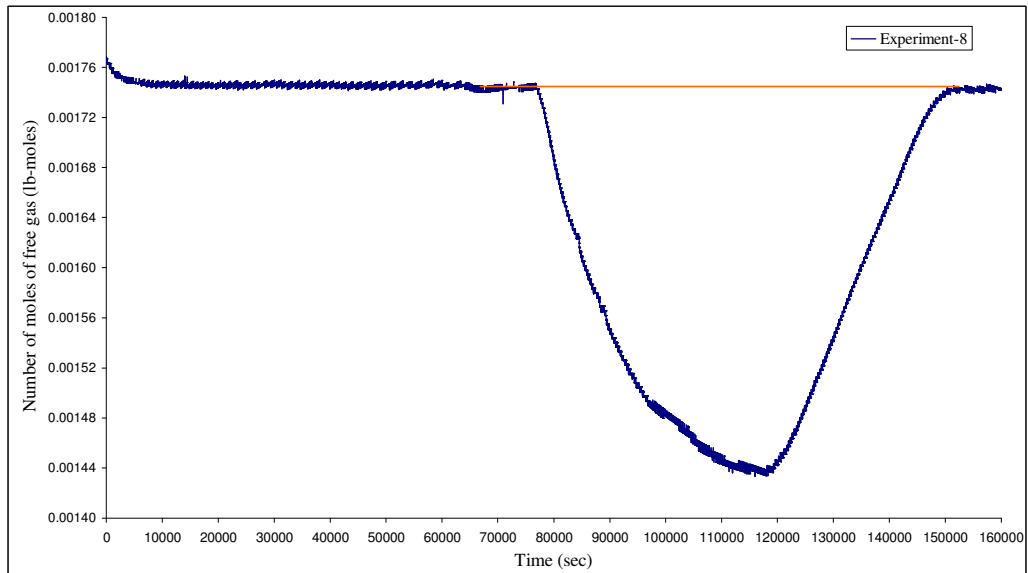


Figure-D.9 Number of moles of free gas vs. time diagram (Experiment-8)

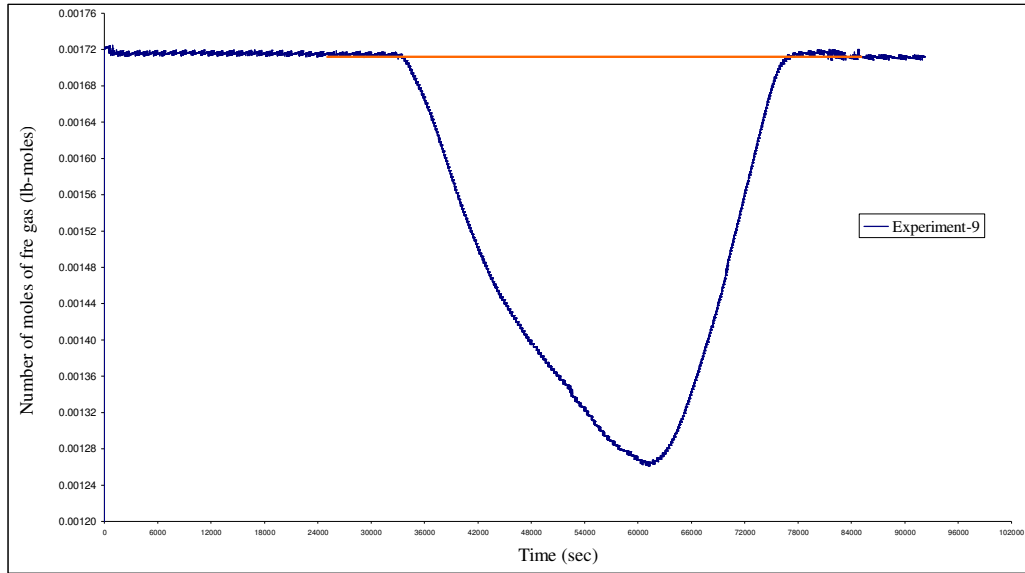


Figure-D.10 Number of moles of free gas vs. time diagram (Experiment-9)

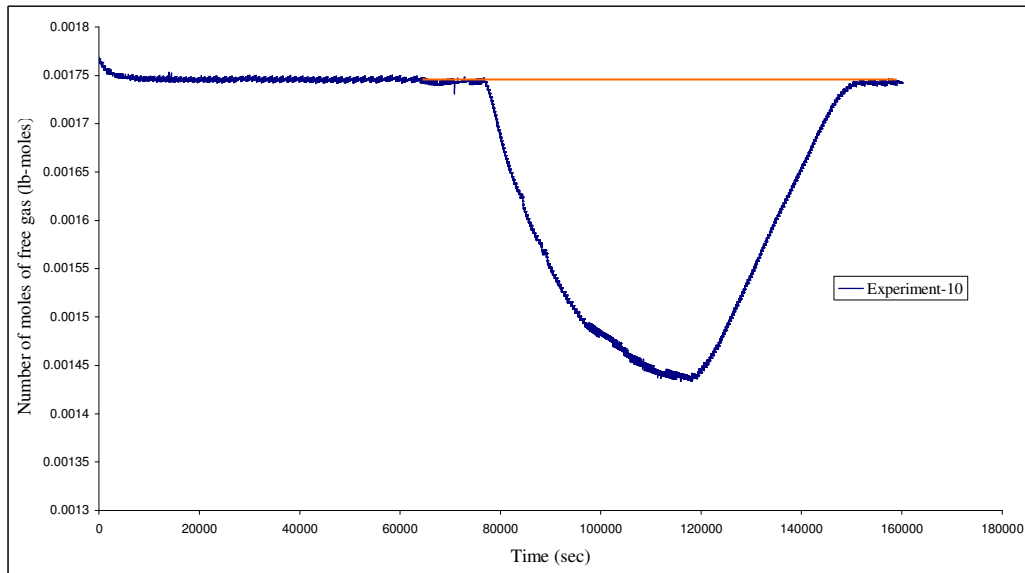


Figure-D.11 Number of moles of free gas vs. time diagram (Experiment-10)

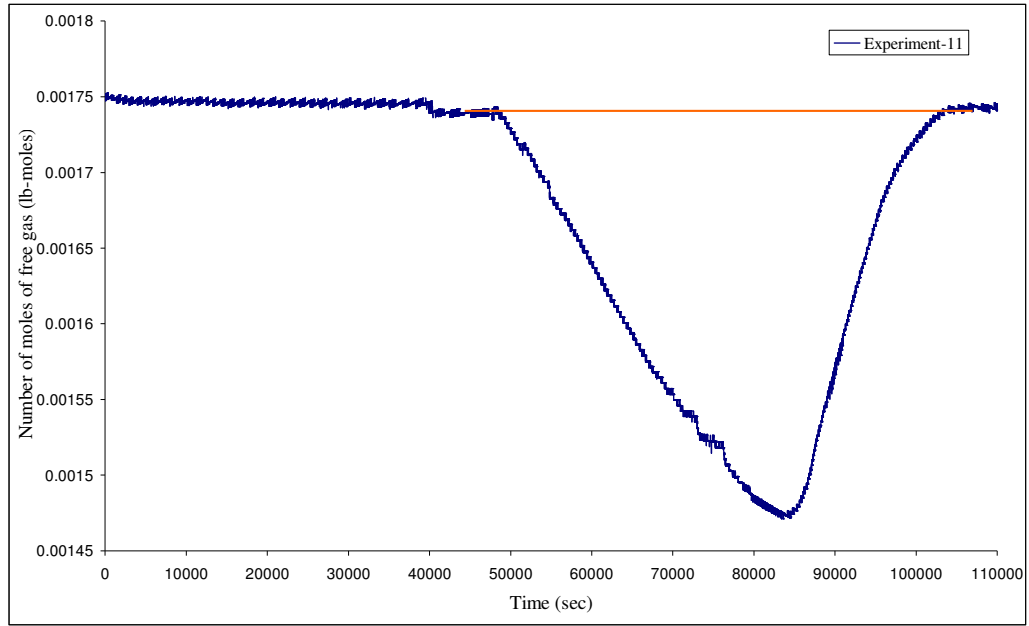


Figure-D.12 Number of moles of free gas vs. time diagram (Experiment-11)